UNIVERSITY OF CALIFORNIA SAN DIEGO

Deregulation of Protein Kinase C alpha Signaling in Neurodegenerative Disease

A dissertation submitted in partial satisfaction of the
requirements for the degree Doctor of Philosophy

in

Biomedical Sciences

by

Julia Ann Callender

Committee in charge:

Professor Alexandra C. Newton, Chair
Professor Joan Heller Brown
Professor Jack E. Dixon
Professor William J. Joiner
Professor Edward H. Koo
Professor Susan S. Taylor

2019

The Dissertation of Julia Ann Callender is approved,
and it is acceptable in quality and form for publication
on microfilm and electronically:

_____

_____

_____

_____

_____

_____
Chair

University of California San Diego

2019

DEDICATION

This work is dedicated to scientists past and present on whose shoulders I stand, and to my family, whose unwavering love and support provided me with a leg up to climb those shoulders.

EPIGRAPH

The difference between science and the arts is not that they are different sides of the same coin…or even different parts of the same continuum, but rather, they are manifestations of the same thing. The arts and sciences are avatars of human creativity. It's our attempt as humans to build an understanding of the universe, of the world around us…science provides an understanding of a universal experience, and art provides a universal understanding of a personal experience.

- Mae Jemison

LIST OF ABBREVIATIONS

Aβ: Amyloid-beta

AD: Alzheimer's Disease;

AMPAR: α-amino-3-hydroxy-5-methyl-5-isoxazolepropionic acid receptor;

APP: Amyloid Precursor Protein;

CHO: Chinese hamster ovary;

DAG: diacylglycerol;

GABA: gamma-aminobutyric acid;

GAP43: Growth Associated Protein 43;

GSK-3β: Glycogen synthase kinase-3 beta;

GWAS: genome-wide association study;

IP_3: inositol trisphosphate;

LTD: long-term depression;

LTP: long-term potentiation;

MARCKS: Myristoylated alanine-rich C-kinase substrate;

NMDAR: N-methyl-D-aspartate receptor;

PICK1: Protein Interacting with C Kinase 1;

PIP_2: phosphatidylinositol-4,5-bisphosphate;

PKC: Protein Kinase C;

PLC: phospholipase C;

PS: phosphatidylserine.

TABLE OF CONTENTS

LIST OF FIGURES

LIST OF TABLES

ACKNOWLEDGEMENTS

I would first and foremost like to thank my advisor Alexandra Newton. Her exceptional mentorship throughout the years has shaped me into the scientist I am today, and she has been a model for how to pursue scientific research thoroughly, thoughtfully, and most importantly, joyfully. Her advice has not only been invaluable in the development of my thesis research, it will also serve as a guiding light as I continue my future scientific career. I would also like to thank my other committee members, Dr. Jack Dixon, Dr. Bill Joiner, Dr. Joan Heller Brown, Dr. Eddie Koo, and Dr. Susan Taylor, for their regular feedback and advice throughout the years. Thank you to everyone in the Newton Lab, past and present, with whom I've worked over the years, particularly Maya Kunkel, who has been an invaluable source of mentorship and humor. The lab environment is a reflection of its people, and I will always appreciate how lively, collaborative, and supportive an environment the Newton lab has been. I thank my collaborators for their scientific contributions, especially Dr. Rudy Tanzi, Dr. Roberto Malinow, Dr. Susan Taylor, Dr. Alexandr Kornev, Dr. Ronit Ilouz, and Dr. John Brognard.

Last, but certainly not least, I would like to thank my family for all their love and support throughout my life. From a young age, my parents taught me to view the natural world with curiosity, wonder, and appreciation, and I attribute my deep-seated love for the act of discovery to their influence. They have always encouraged me to pursue what makes me happy, and everything I have achieved can be traced back to this unending

support they have provided me. I would also like to thank my husband for being a necessary source of love, humor, and understanding throughout my graduate experience.

Chapter 1, in part, is an adaptation of material that appears in "Conventional protein kinase C in the brain: 40 years later", as published in Neuronal Signaling 2016, by Julia A. Callender and Alexandra C. Newton. The dissertation author was the primary author of this work.

Chapter 2 is in large part published online as "Gain-of-function mutations in protein kinase Cα (PKCα) may promote synaptic defects in Alzheimer's disease." Alfonso SI*, Callender JA*, Hooli B*, Antal CE, Mullin K, Sherman MA, Lesné SE, Leitges M, Newton AC, Tanzi RE, Malinow R. in Science Signaling, 2016 May 10;9(427). The dissertation author was one of the primary investigators and authors of this work (*, co-first authors).

Chapter 3 in its entirety is published online as "Protein Kinase Cα gain-of-function variant in Alzheimer's disease displays enhanced catalysis by a mechanism that evades down-regulation." Callender JA, Yang Y, Lordén G, Stephenson NL, Jones AC, Brognard J, Newton AC in Proc Natl Acad Sci U S A. 2018 Jun 12;115(24). The dissertation author was the primary investigator and author of this work.

Chapter 4 is in part unpublished material generated in collaboration with Tatyana Igumenova, Alexandr Kornev, Susan Taylor, and Ronit Ilouz. We acknowledge Tatyana Igumenova for fitting of translocation data and calculation of rate constants for Figure 4.2. We also thank Alexandr Kornev for modeling and docking the C2 domain of PKCα onto the catalytic domain, which is depicted in Figure 4.1C.

VITA

Education

2019 Ph.D., Biomedical Sciences
University of California, San Diego

2013 B.S., Biochemistry-Molecular Biology
University of California, Santa Barbara

Publications

Antal CE, **Callender JA**, Kornev AP, Taylor SS, Newton AC. Intramolecular C2 Domain-Mediated Autoinhibition of Protein Kinase C βII. *Cell Reports* 2015, Aug 25;12(8):1252-60.

Dowling CM, Phelan J, **Callender JA**, Cathcart MC, Mehigan B, McCormick P, Dalton T, Coffey JC, Newton AC, O'Sullivan J, Kiely PA. Protein Kinase C beta II suppresses colorectal cancer by regulating IGF-1 mediated cell survival. *Oncotarget* 2016, Mar 12;DOI:10.18632/oncotarget.8062.

Woodruff G, Reyna SM, Dunlap M, Van Der Kant R, **Callender JA**, Young JE, Roberts EA, Goldstein LS. Defective Transcytosis of APP and Lipoproteins in Human iPSC-Derived Neurons with Familial Alzheimer's Disease Mutations. *Cell Reports* 2016, Oct 11;17(3):759-773.

*Alfonso S, ***Callender JA**, *Hooli B, Antal CE, Mullin K, Sherman MA, Lesne SE, Leitges M, Newton AC, Tanzi RE, Malinow R. Protein Kinase C alpha required for synaptic defects and has gain of function mutations in Alzheimer's Disease. *Science Signaling* 2016, May 10;9(427)
***co-first authors**

Callender JA and Newton AC. Conventional protein kinase C in the brain: 40 years later. *Neuronal Signaling* 2017, Apr 10;1(2):NS20160005.

Callender JA, Yang Y, Lordén G, Stephenson NL, Jones AC, Brognard J, Newton AC. Protein Kinase Cα Gain-of-Function Variant in Alzheimer's Disease Displays Enhanced Catalysis by Mechanism that Evades Down-Regulation. *PNAS* 2018, June 12;115(24):E5497-E5505.

Phosphorylation of Conserved Tyrosine in Protein Kinase C C2 Domain Promotes Activation. (in preparation).

Oral Presentations at Meetings

2018: ASBMB annual meeting, Experimental Biology
Gain-of Function Variant in Alzheimer's Disease Displays Enhanced Catalysis by a Mechanism that Evades Down-Regulation

Poster Presentations at Meetings

2015: ASBMB Symposium: Kinases and Pseudokinases
Intramolecular C2-Kinase Domain Interactions Autoinhibit Conventional Protein Kinase C

2016: Experimental Biology, ASBMB annual meeting
Intramolecular C2-Kinase Domain Interactions Autoinhibit Conventional Protein Kinase C

2016: FASEB: Cell Signaling in Cancer
Deregulation of PKC alpha signaling in Alzheimer's Disease

2016: Salk Institute for Biological Studies: Post-translational Regulation of Cell Signaling
Deregulation of PKC alpha signaling in Alzheimer's Disease

2018: FASEB: Cell Signaling in Cancer
Protein Kinase Cα (PKCα) Gain-of Function Variant in Alzheimer's Disease Displays Enhanced Catalysis by a Mechanism that Evades Down-Regulation

2018: Salk Institute for Biological Studies: Post-translational Regulation of Cell Signaling
Protein Kinase Cα (PKCα) Gain-of Function Variant in Alzheimer's Disease Displays Enhanced Catalysis by a Mechanism that Evades Down-Regulation

2018: ASBMB Special Symposium: The Many Faces of Kinases and Pseudokinases
Phosphorylation of Conserved Tyrosine in Protein Kinase C C2 Domain Promotes Activation

ABSTRACT OF THE DISSERTATION

Deregulation of Protein Kinase C alpha Signaling in Neurodegenerative Disease

by

Julia Ann Callender

Doctor of Philosophy in Biomedical Sciences

University of California San Diego, 2019

Professor Alexandra C. Newton, Chair

The focus of this thesis is to study the mechanisms that control the activity of Protein Kinase C α and how deregulation of these mechanisms leads to neurodegenerative pathology. Protein kinase C (PKC) is a family of enzymes whose members transduce a large variety of cellular signals instigated by the receptor-mediated hydrolysis of membrane phospholipids. Conventional protein kinase C (PKC) family

members are reversibly activated by binding to the second messengers Ca^{2+} and diacylglycerol, events that break autoinhibitory constraints to allow the enzyme to adopt an active, but degradation-sensitive, conformation. Perturbing these autoinhibitory constraints, resulting in protein destabilization, is one of many mechanisms by which PKC function is lost in cancer. Here we show that PKCα signaling contributes to the pathology of Alzheimer's disease (AD), a neurodegenerative disease that remains incurable. We observe changes in electrophysiology in hippocampal brain slices to show that PKCα is necessary for Amyloid beta (Aβ)-mediated synaptic depression. We use FRET-based PKC activity reporters to show that PKCα is activated as a result of exposing primary astrocytes to Aβ and that AD-associated mutations in PKCα increase its signaling output in cells. We use a combination of biochemical, *in silico*, and *in vivo* approaches to conduct an in-depth characterization of one of these variants (PKCα-M489V), thus establishing the mechanism through which it confers enhanced PKCα activity without compromising stability. We also use live cell imaging assays to study in more detail the mechanism of PKCα signaling, showing that it is regulated by intramolecular interactions between its N-terminal and C-terminal domains. We investigate a previously unstudied tyrosine phosphorylation site in the C2 domain of PKCα and establish that phosphorylation at this site—as well as tyrosine phosphorylation in general—promotes PKCα activity. Taken together, the work presented within this thesis serves the ultimate goal of understanding the mechanisms that regulate PKCα signaling in order to effectively target PKCα in the treatment of neurodegenerative diseases.

CHAPTER 1

INTRODUCTION

1.1 HISTORY OF PROTEIN KINASE C

Protein kinase C (PKC) was discovered in the late 1970s by Nishizuka and colleagues as the pro-enzyme of a constitutively-active kinase they had purified from bovine brain (1, 2). The originally-purified enzyme was termed protein kinase M (PKM), as the only cofactor required for activity was Mg^{2+} (2). Subsequent studies revealed that PKM was a proteolytic product of a parent pro-enzyme whose activity was stimulated by Ca^{2+} and the particulate fraction of brain extracts; they named the pro-enzyme protein kinase C (PKC) for its activation by the second messenger Ca^{2+} (3). In a series of classic biochemical studies involving adding back components of brain extracts, the "activators" of the pro-enzyme were identified as phospholipids, notably phosphatidylserine (3), and a "trace impurity" later identified as diacylglycerol (4). The discovery that PKC (whose official name was now Ca^{2+}-activated, phospholipid-dependent kinase) was directly activated by diacylglycerol provided the long-sought effector for the phospholipid hydrolysis that earlier studies by Hokin and Hokin had shown was provoked by cholinergic stimulation (5).

The discovery that catapulted PKC to the forefront of signaling was its identification as a receptor for the tumor promoting phorbol esters (6), a finding made possible by the synthesis of relatively water soluble phorbol esters, notably phorbol dibutyrate (PDBu) by Blumberg and colleagues (7). This diverted studies of PKC from the brain to understanding its role in cancer (8). Yet 30+ years of clinical trials for cancer using PKC inhibitors not only failed (9), but in some cases worsened patient outcome (10). It took analysis of cancer-associated mutations in PKC to reveal that the multiple

isozymes in this family generally function to suppress survival signaling (11), so therapies for cancer should focus on restoring rather than inhibiting activity. Mounting evidence suggests that PKC opposes oncogenic survival signaling by its phosphorylation and inactivation of oncogenes such as K-Ras (12, 13), growth factor receptors (14-16) and phosphatidylinositol-3 kinase (17-19), among others. The key role of PKC in suppressing proliferative and survival pathways poise it to play a role not only in cancer via its loss-of-function, but also in degenerative diseases via gain-of-function. The investigation of the role played by PKC signaling in neurodegenerative disease has been the primary focus of this dissertation work.

1.2 REGULATION OF PKC ACTIVITY

The PKC family is encoded by nine genes whose protein products are organized into three subfamilies based on their cofactor dependence: conventional PKC isozymes (α, the alternatively spliced βI and βII, and γ) are activated by diacylglycerol and Ca^{2+}, novel PKC isozymes (δ, ε, θ, and η), are activated by diacylglycerol, and atypical PKC isozymes (ζ, ι) are regulated by protein scaffolds (20, 21) (Figure 1.1). In addition, a splice variant of PKCζ lacking the regulatory moiety is expressed in the brain; it is named PKMζ in reference to the constitutively-active kinase moiety PKM described above (22). Biochemical analyses by Nishizuka's group originally showed that PKC activity is higher in brain than in any other tissue examined, with particular enrichment in synaptosomal membrane fractions (23). Subsequent immunohistochemical studies revealed strong expression of PKC in both neuronal and glial cells in different regions of

the brain (24-28). Isozyme-specific differences were later unveiled with the generation of isozyme-specific antibodies. For example, while the conventional PKCα is expressed in both glial and neuronal cells in multiple brain regions including the cerebral cortex and the basal ganglia, it is most highly expressed in the hippocampus. PKCβ expression is more limited to neurons, in a wide range of brain regions. The expression of PKCγ is restricted to neurons and is not normally found outside the brain (29). All of the novel PKC isozymes are also enriched in brain tissues, and in addition to the PKCζ splice variant PKMζ whose expression is restricted to brain, the full-length atypical PKC isozymes are themselves highly expressed in the brain, although they are mostly found in neurons and not in glia.

All PKC isozymes are processed by a series of ordered phosphorylations and ordered conformational transitions to yield a signaling-competent enzyme that is maintained in an autoinhibited conformation until the correct second messengers are present (30-32). Specifically, binding of a pseudosubstrate segment in the substrate-binding cavity of the kinase domain prevents activation in the absence of agonist. Agonist binding to the diacylglycerol-sensing C1 domain and Ca^{2+}-sensing C2 domain breaks intramolecular contacts to "open" PKC and permit substrate phosphorylation. PKCα is the only diacylglycerol-dependent isozyme with an identified C-terminal PDZ ligand, which it uses to engage in interactions with PDZ domain-containing scaffold proteins such as Protein Interacting with C Kinase 1 (PICK1), PSD95 and SAP97 (33, 34). For extensive reviews of PKC structure, function, regulation, and pharmacology, the reader is referred to (8, 30, 35-37).

Conventional and novel PKC isozymes move through a tightly-regulated life cycle of signaling (Figure 1.2). Newly-synthesized isozymes are in an open and degradation-sensitive conformation; they undergo a series of stabilizing phosphorylations at sites termed the activation loop, turn motif, and hydrophobic motif that lock the enzyme in an autoinhibited and stable conformation (Figure 1.2, species (i)) (20, 21). These phosphorylations—unlike those found in many other kinases—are constitutive and not agonist-evoked. The "matured" PKC remains in the cytosol in its inactive, auto-inhibited form (31, 38), a state which is discussed below in more detail. Agonist-triggered, receptor-mediated activation of phospholipase C, typically via coupling to the G protein Gq, results in the generation of diacylglycerol, the key allosteric activator of PKC (39). Typically the lipid hydrolyzed is phosphatidylinositol-4,5-bisphosphate (PIP_2) resulting in release of the headgroup inositol trisphosphate (IP_3) and Ca^{2+} mobilization (40). Phosphoinositide signaling is particularly robust in neurons, with recent kinetic analysis revealing that PIP_2 is resynthesized significantly more rapidly in these cells compared with electrically non-excitable cells (41). Conventional PKC isozymes respond to both of these second messengers produced from PIP_2 hydrolysis: first, Ca^{2+} binds the C2 domain to recruit PKC to the plasma membrane via [1] bridging of the C2-bound Ca^{2+} to anionic phospholipids, such as phosphatidylserine, and [2] PIP_2 binding at a distal site that serves as a plasma membrane sensor (Figure 1.2, species (ii)). Once at the membrane, the enzyme binds its membrane-embedded ligand, diacylglycerol, primarily by the C1B domain, which also specifically recognizes PS. Engagement of the C1B domain to the membrane provides the energy to release the autoinhibitory

pseudosubstrate, yielding an open and active enzyme that can propagate downstream signaling (Figure 1.2, species (iii)). This membrane translocation is a hallmark of PKC activation, and movement to the membrane serves as a marker for the activation of the enzyme (42, 43). Binding to protein scaffolds, such as Receptors for Activated C Kinase (RACKS) identified by Mochly-Rosen and coworkers in the early 1990s (44) or PDZ domain proteins, also play roles in localizing PKC and positioning it near substrates (45). While a closed, auto-inhibited PKC is resistant to dephosphorylation and degradation, an open PKC protein is now sensitive to phosphatases (46, 47). Consequently, prolonged activation of PKC results in its dephosphorylation and degradation by a PHLPP-mediated quality control pathway (48) (Figure 1.2, species (iv)), as is seen during chronic treatment with potent PKC activators such as phorbol esters and bryostatins, which cause the downregulation of PKC (42, 49). Indeed, overnight treatment with phorbol esters was a common way to deplete cells of PKC before the advent of siRNA and gene editing technologies. The precise regulation of each step of this pathway must be maintained for cellular homeostasis.

1.3 PKC STRUCTURE AND AUTOINHIBITION

With regards to the crystal structure of PKC, until recently only the crystal structures of the individual domains had been resolved. The kinase domain alone has been crystallized for PKC α, βII, θ, and ι (50-54). The C2 domain has been crystallized for PKC α, βII, δ, η, and ε (55-60). The C1 domains of PKC α, γ, and δ have been crystallized as well (61-63). The structure of full-length PKC was not solved until 2011,

when Hurley and colleagues successfully crystallized full-length rat PKCβII and resolved the C1B, C2, and kinase domain (64). Using the crystal packing data from this study, we proposed a model in which the C2 domain clamps against the kinase domain and autoinhibits PKCβII's signaling, a state that persists until Ca^{2+} binds the C2 domain and facilitates translocation to the plasma membrane (38). Subsequently, Igumenova and colleagues proposed that the C2 domain of another conventional PKC (PKCα) autoinhibits the inactive state of the enzyme, thus supporting that autoinhibition by the N-terminal regulatory domains is a shared mechanism among the conventional PKC isozymes (65). Given the importance of maintaining a tight regulation of PKC signaling for avoiding disease states, understanding the details of how PKCα's N-terminal domains (primarily, the C2 domain) regulate its signaling has been an ongoing goal of this thesis work.

1.4 PKC SUBSTRATES IN THE BRAIN

PKC phosphorylates a large variety of substrates and plays a role in many different signaling cascades. Here, we discuss some illustrative examples of both presynaptic and postsynaptic PKC substrates in the brain, which are summarized in Figure 1.3.

Regulation of the cytoskeleton: MARCKS, GAP43, and Tau

The Myristoylated Alanine-rich C-Kinase Substrate (MARCKS) was identified by Greengard and colleagues in 1982 as a protein highly enriched in brain that is heavily phosphorylated by PKC (66, 67). It has since become one of the most robust and well

characterized read-outs of conventional and novel PKC signaling (68). Its deletion in mice has revealed that it is required for mouse brain development and postnatal survival (69). MARCKS binds to the plasma membrane via a myristoyl electrostatic switch, whereby the coordinated association of a hydrophobic N-terminal myristic acid with the bilayer and an adjacent basic segment with anionic phospholipid headgroups drives membrane association (70). At the membrane, MARCKS facilitates the cross-linking of actin filaments (71). Phosphorylation at multiple residues within the basic segment by PKC causes MARCKS to be released from the plasma membrane to the cytosol, thus promoting actin depolarization (70, 72-76). Growth Associated Protein 43 (GAP43), required for neuronal development (77), is another conventional and novel PKC substrate that, similarly to MARCKS, normally localizes to the plasma membrane. Phosphorylation by PKC causes GAP43 to move away from the membrane (78), which promotes the disassociation of long actin filaments (79). This phosphorylation also breaks GAP43's interaction with calmodulin (80, 81). In addition to their roles in regulating the cytoskeleton, both MARCKS and GAP43 interact with and sequester PIP_2 while at the plasma membrane. Release of these proteins from the membrane as a result of phosphorylation by PKC therefore leads to an increase in available PIP_2 levels for other cellular processes such as endocytosis (82, 83).

PKC also regulates microtubule dynamics through its effects on tau, a microtubule-associated protein that is highly enriched in neurons (84). First, PKC directly phosphorylates tau in a non-pathological setting both *in vitro* and *in vivo* (85, 86). Second, PKC has been implicated in tau phosphorylation indirectly through its ability to

phosphorylate and inactivate Glycogen synthase kinase-3 beta (GSK-3β), thereby reducing tau phosphorylation catalyzed by this kinase (87). PKC has also been linked to N-methyl-D-aspartate receptor (NMDAR)-mediated reduction in tau phosphorylation (88). Overall, PKC's regulation of cytoskeleton dynamics in the brain plays a critical role not only in synapse formation and maintenance, but also in the functions of non-neuronal cells such as endothelial and glial cells (68).

Regulation of Neurotransmission Proteins

PKC has long been implicated in the regulation of neurotransmission and synaptic plasticity by phosphorylating transporters, ion channels, and G protein-coupled receptors. For example, PKC phosphorylates and regulates the dopamine transporter, AMPA-type glutamate receptors (AMPARs), NMDA-type glutamate receptors (NMDARs), gamma-aminobutyric acid (GABA) receptors, mu opioid receptor, and mGluR5 receptors, to name a few (89-97). It is PKC's role in postsynaptic signaling that places it in a key position to regulate synaptic plasticity; PKC phosphorylation of GluA2 subunits of AMPARs is required for AMPAR internalization from the post-synaptic membrane, thus promoting long-term depression (LTD) (98, 99). The PDZ-domain containing scaffold PICK1 mediates this internalization (99, 100). On the other hand, PKC phosphorylation of GluA1 has been implicated in the synaptic incorporation of AMPAR, thus promoting long-term potentiation (LTP) (98). It is noteworthy that the regulation of surface receptors is a general mechanism by which PKC suppresses signaling in non-neuronal systems and is one of the mechanisms by which it functions as a tumor suppressor (see (11)). Given the importance of the dynamic regulation of receptor levels and functioning

in the context of learning and memory, this function of conventional and novel PKC isozymes is critical for further study, especially in the context of brain pathologies.

1.5 PKC IN THE PATHOLOGY OF NEURODEGENERATION

The balance between phosphorylation and dephosphorylation finely tunes the signaling output in the cell, and any changes in the normal activity of a phosphatase or a kinase can have pathological consequences. PKC isozymes play roles in a variety of brain pathophysiologies, including alcoholism, opiate addiction, epilepsy, stroke, and glioblastoma (101-105). Perhaps one of the most pressing neurological diseases of our time is the neurodegenerative Alzheimer's Disease (AD), especially given the progressive aging of our population and the current lack of therapies for AD (106).

PKC, Amyloid beta (Aβ), and Tau

Mounting evidence points to a key role of PKC signaling in the pathology of Alzheimer's Disease, a degenerative disease characterized by loss of synapses and plasticity mechanisms in the brain. The disease is associated with the appearance of extracellular amyloid plaques caused by the mis-cleavage of Amyloid Precursor Protein (APP) and intracellular neurofibrillary tangles composed of hyperphosphorylated tau protein (107, 108), two pathologies for which PKC involvement has been implicated over the years. But the critical importance of deregulated PKC signaling in AD was recently cemented by the results of a an unbiased and comprehensive phosphoproteomic analysis of both human AD postmortem brains and brains from four AD mouse models (109): PKC substrates accounted for over half of the core molecules that displayed increased

phosphorylation in AD compared to control brains. The most robust increase in phosphorylation in AD compared to control brains occurred on MARCKS but also included PKC substrates such as GAP43. Furthermore, increases in MARCKS phosphorylation relative to other proteins occurred most significantly at early disease stages, leading the authors to propose that increased phosphorylation of this key PKC substrate initiates synapse pathology. Consistent with enhanced PKC output in AD, increased PKC levels have been implicated in Alzheimer's Disease, with early studies reporting increased staining of PKC at neurite plaques from human postmortem AD brains, including increased PKCα in reactive astrocytes associated with plaques (110, 111).

One mechanism by which PKC could promote the pathology of AD is by regulating the processing of amyloid precursor protein (APP) and production of Aβ peptides (112). However conflicting results have been presented as to whether PKC enhances or inhibits Aβ production. (113-116). This could arise from specific PKC isozymes having unique functions, and also the use of phorbol esters to probe PKC involvement; the paradoxical effect of short-term activation followed by long-term down-regulation lead to the confusion in the cancer field as to their function. It is noteworthy that Aβ production requires the dynamic endocytic recycling of APP from the cell surface, and it has been found that enlargement of early endosomes is one of the earliest events in AD (117-119). MARCKS protein, whose phosphorylation is significantly enhanced in AD, connects PKC to both of these processes; PKC phosphorylation of MARCKS causes the liberation of both PIP_2 and filamentous actin at the plasma

membrane, both of which may promote increased endocytosis into early endosomes (120).

Another mechanism by which enhanced PKC signaling promotes the pathology of AD involves the PDZ-scaffolded conventional isozyme, PKCα. Electrophysiological studies have revealed that the biological effects of Aβ at synapses are abolished in brain tissue from mice lacking PKCα or a PDZ domain scaffold it binds, PICK1 (121). Synaptic depression is also prevented by treatment of rat brain slices with a PKC inhibitor (BisIV) that works on PKC bound to protein scaffolds, but not with an inhibitor (Gö6976) that does not inhibit PKC bound to protein scaffolds (122). Aβ-induced synaptic depression can be restored by re-expression of PKCα, but not a construct lacking the PDZ ligand. These results suggest that the activity of PKCα, specifically, bound to a PDZ domain scaffold, transduces the effects of Aβ on synapses. One possible mechanism for the downstream effects of PKC could be by controlling receptor function: exposure of synapses to Aβ peptide *in vitro* causes a decrease in GluA2-containing AMPA receptors facing the synapse, and GluA2 mutants incapable of regulating endocytosis are insensitive to Aβ-induced synaptic depression (123). PKCα and its scaffold PICK1 play a critical role in AMPAR internalization, and both PICK1 (121, 124). Taken together with the finding that both PKCa and PICK1 are required for Aβ-induced synaptic depression, a reasonable hypothesis is that PKCa promotes neurodegeneration by removing AMPA receptors from synapses. It is also noteworthy that PKCa has been shown to be necessary for cerebellar LTD by a mechanism that depends on its intact PDZ ligand (125).

Gain-of-function PKC mutations identified in neurodegenerative diseases

While loss-of-function somatic mutations in PKC isozymes are associated with cancer, germline gain-of-function mutations in PKC have been identified in two neurodegenerative diseases. First, activating mutations in PKCg are causal in spinocerebellar ataxia, a progressive and often fatal degenerative disease (126, 127). Over 20 such mutations have been identified in spinocerebellar ataxia Type 14 (SCA14), many of them occurring in the C1B domain (128). These mutations enhance the "open" and signaling competent conformation of PKC. This is in contrast to PKC mutations identified in cancer, which all either had no effect on PKC activity or were inactivating (11). This is perhaps unsurprising given the long-standing inverse relationship between cancer, a disease of cell proliferation, and neurodegeneration, a disease of cell death (129). Many of the same signaling pathways are deregulated in both diseases (130, 131), and a recent meta analysis of nine independent studies found that AD patients exhibit a 45% decreased risk of cancer compared with the general population (132).

1.6 RESEARCH GOALS

The work presented here both investigates the role played by PKCα in Alzheimer's disease and also provides further insight into how PKCα's N-terminal regulatory domains control its autoinhibition, activation, and signaling output. Specifically, Chapter 2 explores a role for PKCα in pathology mediated by Aβ. We use a combination of electrophysiology, genetics, and biochemistry experiments to establish that [1] PKCα is necessary for Aβ-mediated synaptic depression, [2] PKC in astrocytes is

activated downstream of exposure to Aβ, and [3] AD-associated mutations in PKCα enhance its signaling output. In Chapter 3, we provide an in-depth biochemical characterization of one of these AD-associated mutations (PKCα-M489V), describing the mechanism through which it enhances signaling output without compromising stability of the enzyme. We then use a PKCα-M489V mouse model to show that phosphorylation of a key PKCα substrate known to play a role in AD pathology (MARCKS) is increased in the brains of these mice. In Chapter 4, we explore the ways in which PKCα signaling is regulated by [1] intramolecular interactions between the C2 domain and the catalytic domain, and [2] tyrosine phosphorylation of the C2 domain. These studies all serve the general purpose of understanding the mechanisms of PKCα signaling, and how these mechanisms are deregulated in neurodegenerative pathologies.

Chapter 1, in part, is an adaptation of material that appears in "Conventional protein kinase C in the brain: 40 years later", as published in *Neuronal Signaling* 2016, by Julia A. Callender and Alexandra C. Newton. The dissertation author was the primary author of this literature review.

FIGURES AND TABLES

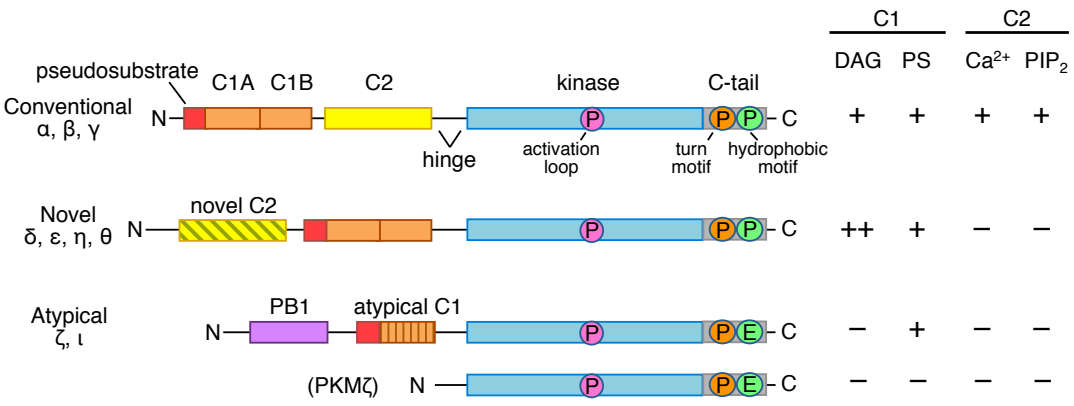

Figure 1.1: Schematic showing domain composition of PKC family members. PKC isozymes are classified into one of three sub-families based on their domain composition (left), which in turn dictates their second messenger and co-factor sensitivity (right). The N-terminal regulatory moiety contains the autoinhibitory pseudosubstrate segment (red), the tandem diacylglycerol-binding C1 domains (orange), and the Ca^{2+}-binding C2 domain (yellow). The C2 domain in novel PKC isozymes and the C1 domain in atypical PKC isozymes are non-ligand binding variants (striped). Novel PKC isozymes are able to respond to increases in diacylglycerol alone because their C1B domain binds this ligand with two orders of magnitude higher affinity than that of conventional PKC isozymes, whose cellular activation depends on signals that elevate both Ca^{2+} and diacylglycerol. Atypical PKC isozymes have a PB1 domain (purple) that mediates binding to protein scaffolds. The C-terminal kinase moiety contains the catalytic domain that has a priming phosphorylation site by PDK-1 (pink) and a C-terminal tail that is phosphorylated at the turn motif (orange) and hydrophobic motif (green); atypical PKC isozymes have a Glu at the phosphoacceptor site of the hydrophobic motif. Also shown is a brain-specific splice variant of the kinase moiety of PKCζ, PKMζ.

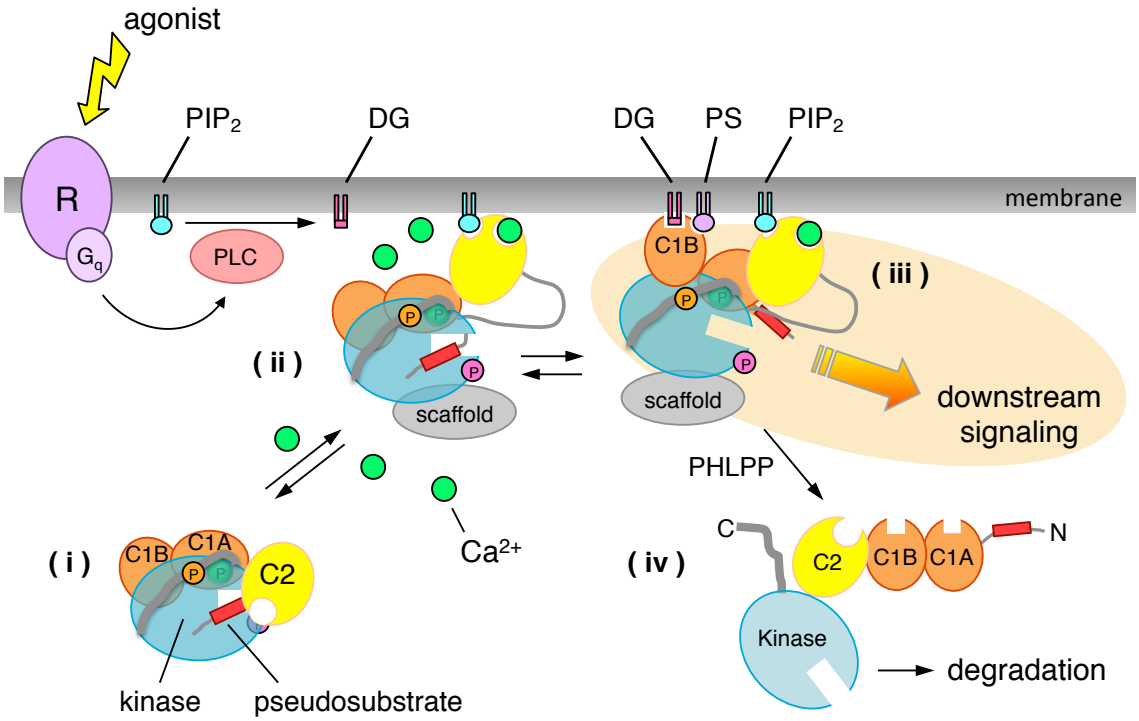

Figure 1.2: The priming, activation, and deactivation life cycle of a conventional PKC. Newly-synthesized PKC is processed via a series of tightly-coupled phosphorylations (circles labeled 'P') to yield a matured species that localizes to the cytosol and is maintained in an autoinhibited conformation by intramolecular contacts between the kinase domain and the regulatory domains (species (i)). Agonist binding to Gq-coupled receptors (R) results in phospholipase C-catalyzed hydrolysis of phosphatidylinositol-4,5-bis phosphate (PIP_2) to generate two second messengers: diacylglycerol (DG) and, indirectly, Ca^{2+} mobilization. Ca^{2+} (green circle) binds the C2 domain, facilitating the bridging of the C2 domain to anionic phospholipids in the plasma membrane; specificity for the plasma membrane is mediated by binding of PIP_2 to a distal surface on the C2 domain that is masked in the autoinhibited conformation of PKC (species (ii)). Subsequent binding of diacylglycerol to the C1B domain, which also specifically binds PS, results in release of the pseudosubstrate from the substrate-binding cavity (species (iii)), allowing substrate phosphorylation and down-stream signaling. Binding to protein scaffolds (grey), such as PSD95 for PKCα, can further constrain PKC signaling to specific intracellular locations. Prolonged membrane binding, as occurs upon treatment of cells with phorbol esters, results in dephosphorylation (species (iv)) and degradation of PKC, a process referred to as down-regulation. Novel PKC isozymes are similarly regulated except they do not have a Ca^{2+}/plasma membrane sensing C2 domain and respond only to diacylglycerol; their C1B domain binds diacylglycerol with two orders of magnitude higher affinity than that of conventional PKC isozymes, so they respond to diacylglycerol alone and localize primarily to diacylglycrol-rich Golgi membranes.

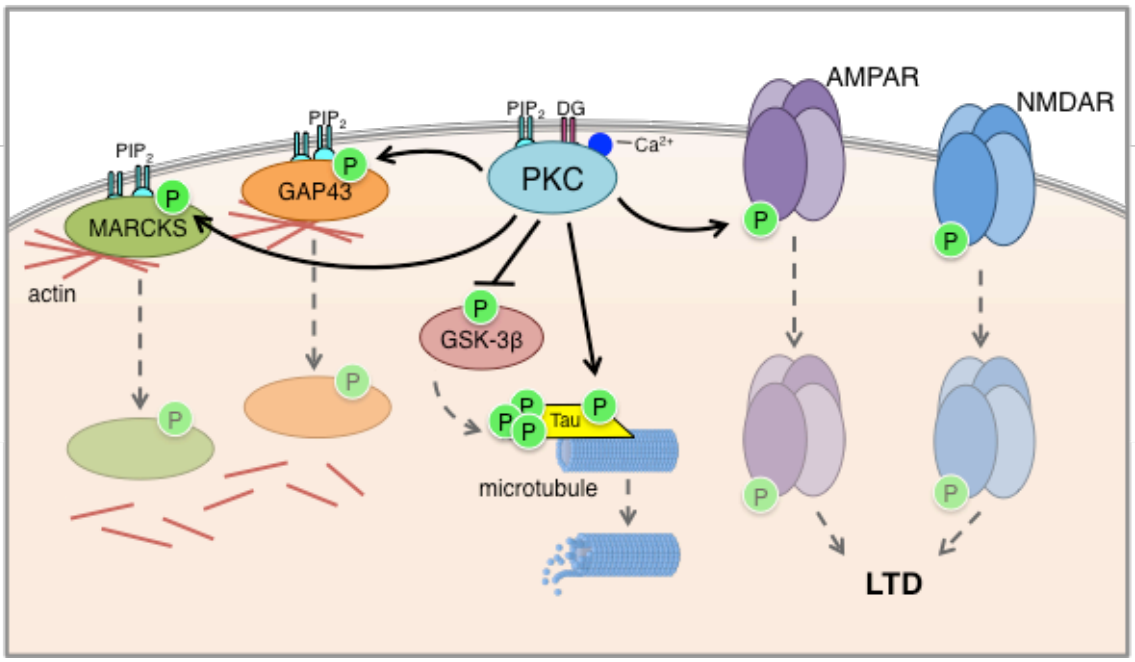

Figure 1.3: PKC substrates in the brain. PKC phosphorylates many presynaptic and postsynaptic substrates; illustrative examples are depicted here on a generic membrane for ease of viewing. PKC (cyan) regulates the actin cytoskeleton (red lines) via its phosphorylation of MARCKS (green) and GAP43 (orange). Phosphorylation by PKC causes these proteins to translocate from the plasma membrane, where they facilitate actin polymerization, to the cytosol, thus promoting actin depolarization. PKC plays a role in microtubule (small blue circles) dynamics through its effects on the microtubule-associated protein tau (yellow). PKC both directly phosphorylates tau and indirectly causes the dephosphorylation of tau by phosphorylating and inactivating GSK-3β (pink). PKC regulates synaptic plasticity by regulating postsynaptic levels of AMPA receptor (purple) and NMDA receptor (blue). Phosphorylation by PKC causes internalization of these receptors, thus promoting long-term depression (LTD).

CHAPTER 2

PROTEIN KINASE Cα REQUIRED FOR SYNAPTIC DEFECTS AND HAS GAIN OF FUNCTION MUTATIONS IN ALZHEIMER'S DISEASE

ABSTRACT

Alzheimer's disease (AD) is characterized by early synaptic degeneration. Here we examine the role of protein kinase Cα (PKCα), which in many tissues is required to keep cancer in check. We find that in mouse brain tissue, PKCα is required for synaptic degenerative effects of elevated amyloid-beta (Aβ), a likely early event in AD. Whole genome sequencing of 1345 individuals from 410 late-onset AD (LOAD) families identified three highly penetrant variants in the PKCα gene (*PRKCA*) in five families. Importantly, all variants displayed increased cellular signaling relative to wild-type PKCα. Thus, whereas loss-of-function mutations in PKCα contribute to cancer, enhanced PKCα activity may participate in AD, reinforcing the importance of maintaining a careful balance in the activity of this enzyme.

INTRODUCTION

Synaptic loss correlates well with the earliest AD symptoms in humans (133, 134) and is an early event in rodent models of AD (135-137). The loss of synapses may result from elevated levels of Aβ (123, 138, 139), a peptide central to AD development (140). Indeed, familial forms of AD are caused by mutations in genes that increase production of the most toxic form of Aβ (140). Furthermore, a minor allele of APOE (APOE-ε4), which is strongly linked with both the appearance and earlier onset of LOAD (141), may act by reducing the clearance of Aβ from the brain (140). Additional factors may also play a role, such as defects in neuronal trafficking (142-144).

We sought to identify other genes that contribute to LOAD, as their gene products may serve as therapeutic targets. We reasoned that variants of proteins participating in the detrimental effects of Aβ may contribute to the disease. We thus examined the signaling underlying Aβ-induced synaptic depression. Several clues point towards a role for Protein Kinase C (PKC): the protein scaffold PICK1—a well-known interaction partner for PKC—is required for the synaptic effects of Aβ (124). Additionally, PKC is required for a plasticity form of synaptic depression (125). Furthermore, since reduced PKC activity contributes to increased cell survival (11), we speculated that increased PKC activity could participate in AD, a disease of neuronal degeneration (140). Here, we report that not only is the conventional PKC isozyme PKCα required for Aβ-mediated synaptic depression, but also that AD-associated mutations in PKCα increase signaling output in cells.

RESULTS

PKCα is necessary for synaptic effects of beta amyloid

To test if the activity of PKC is required in Aβ-induced synaptic depression, we initially used PKC antagonists in combination with a previously established method that raises Aβ levels in neurons (123, 138, 145). Organotypic hippocampal slices were infected sparsely with a virus expressing CT100, the beta-secretase product of amyloid precursor protein (APP) and precursor to Aβ (146). 16-24 hours later, synaptic transmission was evoked by stimulating presynaptic axons (orange, **Figure 2.1A**, top left) and neighboring infected and uninfected postsynaptic CA1 neurons were simultaneously

recorded. Neurons expressing CT100 displayed depressed excitatory transmission relative to uninfected neurons (**Figure 2.1A**, top right). Previous studies have shown that the effects of CT100 expression are due to the production of Aβ leading to endocytosis of glutamate receptors and loss of synapses (123, 138, 145). To examine the role of PKC in Aβ-dependent synaptic transmission, we incubated slices (for ~12 hours before recordings) with the PKC inhibitors Gö6983, an ATP-competitive inhibitor, or Bisindolylmaleimide IV (Bis IV), a non-competitive inhibitor. Synaptic depression was effectively blocked by Bis IV but not by Gö 6983. Because PKC bound to a scaffold protein near its substrates is refractory to active site inhibitors (122), these data support a role for PKC bound to a scaffold protein mediating the synaptic effects of Aβ. Of the PKC isozymes that are modulated by these inhibitors, only PKCα has a PDZ ligand, a 3 amino-acid segment at its carboxyl terminus that binds the PDZ domains of scaffolding proteins (notably PSD95 and SAP97 (34), and PICK1 (33)). Indeed, expression of CKAR, a genetically-encoded fluorescence-based reporter of PKC activity (147), in COS7 cells revealed that endogenous PKC activity at the PSD95 scaffold was effectively inhibited by Bis IV but not Gö6983, whereas both inhibitors were equally effective at inhibiting bulk PKC activity measured at plasma membrane (**Figure 2.2**).

To test if PKCα is required for the synaptic effects of Aβ, organotypic hippocampal slices were prepared from wild-type (wt) mice as well as mice lacking PKCα (PKCα-/-) (148). 16-24 hours after infection, neurons expressing CT100 displayed depressed synaptic transmission compared to nearby neurons in slices from wt mice but showed no difference in PKCα-/- slices (**Figure 2.3 A, B**; Western blot

analysis revealed comparable levels of Aβ peptide in lysates from slices from PKCα KO or wt animals infected with virus expressing CT-100 (data not shown)). We sought to determine if absence of PKCα, rather than some developmental alteration in PKCα-/- mice, was responsible for the lack of effect by CT100 in neurons from PKCα-/- mice. For this, we used a dual promoter virus to co-express CT100 and PKCα in PKCα-/- organotypic slices. Following expression, transmission onto infected neurons was depressed compared to non-infected neurons, indicating rescue of the effect of CT100 on synapses (**Figure 2.3**). To test if the rescue of CT100-induced depression by PKCα co-expression is not due to potentiation of transmission by PKCα expression (which when added to the CT100-induced synaptic depression could normalize transmission), we co-expressed PKCα with CT84, the α-secretase product of APP that does not generate Aβ (146), nor cause synaptic depression (149). In this case no significant potentiation was observed, indicating PKCα co-expression rescued the effects of CT100 by enabling CT-100 driven signaling. To test if the effects of Aβ on synapses require that PKCα act at a scaffold, as suggested by the pharmacological results above, we co-expressed CT100 and PKCα lacking the last three amino acids (PKCα (ΔPDZ)), which prevents its binding to PDZ-domain proteins. In contrast to the co-expression of PKCα, co-expression of PKCα (ΔPDZ) did not rescue the effects of CT100 expression. These results indicate that PKCα, acting at a scaffold, is required for the depressive effects of Aβ on rodent synapses.

PKCα variants in Alzheimer's disease

To test if PKCα plays a role in human AD, we searched for rare variants in whole genome sequencing data for the PKCα gene (*PRKCA*) that were present in any of 410 pedigrees from the NIMH AD Genetics Initiative (**Figure 2.4**). In total we identified three rare variants found in LOAD patients in our families. M489V (rs34406842; Atg/Gtg; minor allele frequency = 0.0005 in 1000 genomes of the general population, http://www.1000genomes.org) was present in seven of nine affected individuals, and was absent in the single unaffected subject in these four families. V636I (rs141376042; Gtc/Atc; minor allele frequency = 0.002 in 1000 genomes) was present in two of three affected subjects in one family [no unaffected subjects available]. R324W (minor allele frequency = 0.00 in 1000 genomes), was present in one out of two affected individuals in one LOAD pedigree of three; the unaffected individual did not carry a PKCα variant. Thus, all individuals carrying a *PRKCA* variant were affected by AD, and all the individuals in these families not affected by AD did not carry a *PRKCA* variant. Thus, the *PRKCA* variants identified in the NIMH dataset appear to co-segregate with LOAD patients. A simple bootstrap test (see methods), suggests that the probability of finding such linkage in this population is less than 0.03. Given that PKCα activity is necessary for effects of Aβ on synapses (above), and reduced PKC function enhances cell survival (11), we hypothesized that the rare PKCα variants found in LOAD families would have increased activity.

AD-Linked PKCα variants display increased cellular activity

Two of the rare variants observed in LOAD patients occur in key regulatory segments of PKC: M489V is in the activation loop near the entrance to the active site,

and V636I is on the C-terminal segment that clamps over the kinase domain (**Figure 2.5**). The third variant, R324W is in a segment that controls autoinhibition: it is present in a flexible hinge, connecting the kinase domain with the regulatory moiety, that becomes exposed upon rupture of the C2-kinase domain contacts accompanying activation ((150). When visualizing the M489V variant in more detail, molecular modeling reveals that replacement of the bulky Met at position 489 on the activation loop with the smaller Val loosens the packing of this key regulatory segment (**Figure 2.5A**). This led to our prediction that the M489V substitution would either de-constrain the dynamics of the catalytic domain, lessen autoinhibition via reduced clamping of the C2 domain in that area of the catalytic domain, or both. Either scenario would be predicted to increase PKCα signaling output.

To examine the functional impact of amino acid changes, we assessed the effect of introducing these LOAD-associated rare variants on the function of PKCα. When expressed in COS7 cells, none of the three rare variants affected the processing phosphorylation of PKCα, as assessed by Western blot analysis using phospho-specific antibodies to each of the three priming phosphorylations, an indication of proper folding (151) (**Figure 2.5B**). Further analysis of the M489V mutant revealed an enhanced rate of dephosphorylation following stimulation of cells with phorbol esters, potent activators that force PKC into an open, phosphatase-sensitive conformation (152) (**Figure 2.5C**). The enhanced rate of dephosphorylation supports the looser packing of the kinase domain resulting from replacement of Met with Val, favoring a more de-constrained (i.e. active) conformation of the kinase when locked into an

"open" confirmation with phorbol esters (31). The V636I mutant did not display the same enhanced rate of dephosphorylation, indicating that there may be other structural mechanisms through which this mutation destabilizes PKC autoinhibition (data not shown).

To assess the effect of the amino acid changes on the signaling output of PKCα, we co-expressed PKCα variants or wild-type PKCα with cytosolic CKAR (147) in COS7 cells. All three rare variants showed enhanced agonist-evoked activity relative to wild-type PKCα (**Figure 2.6**; note that this assay measures the phosphorylation of CKAR and reflects the allosteric activation of PKC induced by second messenger binding. This acute stimulation by natural agonists does not cause the dephosphorylation or down-regulation of PKC that is caused by chronic activation by phorbol esters). These results indicate that all three rare PKCα variants found to co-segregate with LOAD display increased agonist-driven PKCα function.

Exposing U87 cells and primary astrocytes to $A\beta_{25-35}$ causes Ca^{2+} response and PKC activation

In order to investigate the pathway through which PKC is necessary for Aβ-mediated synaptic depression, we turned to live-cell imaging of U87 cells and primary murine astrocytes. Various forms of the Aβ peptide have been shown to cause a Ca^{2+} response in cells (153, 154). This includes (but is not limited to) a shorter toxic fragment, $A\beta_{25-35}$, which has been shown to activate the Ca^{2+}-IP3 pathway in astrocytes (155). We first sought to repeat this finding in either U87 cells (**Figure 2.7A**) or primary astrocytes isolated from wild-type mice (**Figure 2.7B**). Cells were

loaded with FURA-2 AM dye to monitor Ca^{2+} levels in the cytosol as a result of adding $A\beta_{25-35}$ peptide directly to the cell imaging media. A peptide with the reverse sequence (Aβ reverse peptide) was used as a negative control. In both U87 cells and astrocytes, $A\beta_{25-35}$ stimulation caused a robust Ca^{2+} response, which was not observed when stimulating with the reverse peptide.

Given that Ca^{2+} binding to PKC's C2 domain is the first step in PKC activation, we next asked if this Ca^{2+} response takes place concurrently with a PKC response. We transiently transfected primary astrocytes with plasma membrane-targeted CKAR (pmCKAR) in order to see if endogenous PKC is activated as a result of stimulation with $A\beta_{25-35}$ (**Figure 2.8**). Representative traces from one day of imaging are depicted in **Figure 2.8A**. Stimulation with Aβ peptide activated PKC to a comparable magnitude as subsequent UTP stimulation. PDBu treatment maximally activated all PKC in the cell, indicating that the amount of PKC activity caused by Aβ stimulation is significant (**Figure 2.8A**, top left). This PKC activation was not observed when stimulating with the reverse peptide negative control (top right), when overexpressing a non-phosphorylatable CKAR mutant (bottom left), or when pretreating with the PKC inhibitor Bis IV (bottom right). Quantification of three biologically independent experiments confirms that $A\beta_{25-35}$ stimulation is activating PKC significantly more than all the negative controls tested (**Figure 2.8B**). The lack of significance between the $A\beta_{25-35}$ treatment of cells overexpressing pmCKAR vs pmCKAR-T/A is likely due to the jump observed upon initial stimulation with $A\beta_{25-35}$ in the pmCKAR-T/A

experiment. Overall, these results support a hypothesis in which PKC is activated downstream of $A\beta_{25-35}$'s effect on cytosolic Ca^{2+} levels.

DISCUSSION

Alzheimer's Disease is a lethal neurodegenerative disorder with increasing prevalence and no effective treatment (140). Elucidating the cellular signaling events that underlie the initiation and progression of LOAD can provide potential targets amenable to therapeutic intervention. Human genetic studies (156), particularly family-based studies (141) of rare variants (157), can identify potentially important molecules in LOAD. However, delineation of LOAD pathophysiology primarily from genetic information from smaller family studies remains challenging (see comments and responses to ref. (157)). We therefore sought to combine a large genetic family study with neurophysiological and biochemical analyses to elucidate signaling employed in LOAD pathophysiology.

PKCα and Alzheimer's disease pathophysiology

While the cellular events that initiate LOAD remain unknown (140) elevated levels of pathogenic forms of Aβ, and the associated synaptic loss, is strongly implicated in its early pathophysiology (133, 134, 158, 159). PKC has been implicated in AD in a number of studies (160-162), however its exact role has not been well understood, with phorbol esters reported to both enhance and suppress Aβ production (112). Indeed, understanding the biological functions of PKC in disease, in general, has presented a

challenge given the presence of multiple isozymes and the opposing effects of phorbol esters in mediating short-term activation and long term down-regulation. By employing pharmacology, mouse genetics and acute rescue experiments, we are able to make conclusions regarding the role of a specific PKC isozyme. Our neurophysiological studies indicate PKCα, and its PDZ-ligand, are required for Aβ to produce synaptic depression (consistent with a prior study demonstrating a requirement of PICK1 (124), a PDZ-domain protein that binds PKCα). Given the evidence supporting Aβ and synaptic loss in AD, our results suggest an important role for PKCα in AD.

As conclusions regarding human disease based on physiology from immature rodent brain slices are tenuous, we turned to human genetics, which can provide unbiased insight into the function of aberrant PKC signaling in disease. By scanning the genomes of individuals from a large LOAD family study, we identified three rare variants of PKCα that co-segregated with LOAD in six families. When examined in cell-based assays, all three variants displayed increased signaling output relative to wild-type PKCα. Notably, of the 46 PKC variants observed in cancers and tested for changed activity using the same assays, none displayed increased activity (11). Furthermore, the more strongly linked M489V mutation, found in seven of nine patients and not in an unaffected subject in four LOAD families, also elicited an enhanced rate of dephosphorylation following stimulation of cells with phorbol esters, consistent with a more open and signaling competent conformation. Thus, PKCα is required for deleterious synaptic effects of Aβ, observed early in LOAD, and increased PKCα activity can contribute to human LOAD.

PKCα may be acting downstream of Aβ via a Ca^{2+}-mediated pathway

Although the pathway through which Aβ contributes to synaptic depression and neuronal death remains to be established, many studies have shown that Aβ causes a deregulation of Ca^{2+} homeostasis. This has been observed upon addition of multiple forms of the insoluble Aβ peptide to multiple types of cells, including immortalized cell lines, astrocytes, and neurons (163, 164). Here, we corroborate that addition of $A\beta_{25-35}$ to U87 cells and to primary murine astrocytes causes a Ca^{2+} response, and that this occurs concurrently with PKC activation in primary astrocytes. This provides a hint as to the mechanism through which PKCα is required for Aβ-mediated synaptic depression; PKC may be activated downstream of Aβ as a result of this Ca^{2+} dysregulation.

PKCα activity: increased in neurodegenerative diseases and decreased in cancer

It is notable that we found activating PKC mutations in LOAD patients whereas human cancer-associated PKC mutations are inactivating (11). Indeed, the neurodegenerative disease, spinocerebellar ataxia, is caused by mutations in PKCγ that promote the open, active conformation (126). Thus, our results are consistent with PKC gain-of-function mutations driving neurodegenerative diseases and loss-of-function mutations driving cell survival diseases. Supporting opposing roles of PKC in cancer vs AD, a recent meta analysis of nine independent studies reveals that AD patients exhibit an overall 45% decreased risk of cancer compared with the general population (132), consistent with earlier reports that AD and cancer display an inverse association (131, 165). It is relevant that inhibitors of PKC have failed in cancer clinical trials (9), likely because PKC activity should be restored, rather than inhibited, in cancer therapy (11). In contrast, repurposing PKC inhibitors for LOAD may prevent the effects of Aβ on

synapses and thereby mitigate loss of cognitive function. Together, our findings support inhibition of PKCα as a therapy early in LOAD and suggest that mutations in PKCα can serve as a diagnostic for disease susceptibility.

MATERIALS AND METHODS

Tissue preparation

Experiments were conducted in accordance with and received approval from the Institutional Animal Care and Use Committees at UCSD. The experiments were carried out in accordance with guidelines laid down by the NIH regarding the care and use of animals for experimental procedures.

Hippocampal slice cultures and Sindbis virus infection

Organotypic hippocampal slice cultures were made from postnatal day 6 or 7 rat pups as described (166). Slice cultures were maintained in culture for 6–8 days then infected using a Sindbis virus (pSinRep5 dp APP-CT100 tdTomato). Cells were recorded 16-30 hr after infection. For **Figure 2.3** experiments, slices were made as described above, but from either wild type (wt) or PKC -/- mouse pups and infected with the indicated Sindbis viruses.

Electrophysiology and pharmacological treatments

Slices were maintained in a solution of ACSF containing in mM: 119 NaCl, 26 $NaHCO_3$, 1 NaH_2PO_4, 11 D-glucose, 2.5 KCl, 4 $CaCl_2$, 4 $MgCl_2$, and 1.25 $NaHPO_4$ and gassed with 95% O_2 5% CO_2. In addition, the following drugs were included: 4 μm 2-

chloroadenosine (to prevent stimulus induced bursting), and 100 μm picrotoxin (to block inhibitory transmission). Simultaneous whole-cell recordings were obtained from pairs of neighboring (<50 μm) control and infected CA1 pyramidal neurons using 3–5 MΩ glass pipettes with an internal solution containing the following in mM: 115 cesium methanesulfonate, 20 CsCl, 10 HEPES, 2.5 $MgCl_2$, 4 Na_2ATP, 0.4 Na_3GTP, 10 sodium phosphocreatine, 0.6 EGTA, and 0.1 spermine, at pH 7.25. All recordings were done by stimulating two independent synaptic inputs; EPSCs were recorded while holding the cells at −60 mV, alternating pathways every 8.4 s. Results from each pathway were averaged and counted as n = 1. For pharmacological experiments, slices were incubated overnight prior to recordings with either 0.3 μM Gö 6983 or 3 μM Bisindolylmaleimide IV (Bis IV); the drug was also added to the recording chamber at the same concentration. In addition, 10 μM gabazine (to block inhibitory transmission) was added to the perfusion chamber. All data are reported as mean ± SEM. Statistical analysis employed bootstrap (resampling) methods (167). For instance, in **Figures 2.1-2.2**, we calculated the probability by bootstrap resampling (100,000 times) the data from groups a, b and c, and measuring the frequency with which (A>C or B>C) is true (where caps indicates mean); for **Figure 2.3**, we bootstrap resampled (100,000 times) data groups, measuring the frequency with which (A>B or C>B or A>D) is true. For **Figure 2.5**, we bootstrap resampled (100,000 times) data groups, measuring the frequency with which [(MV at t=3hrs > wt at t=3hrs) or (MV at t=6hrs > wt at t=6hrs)] is true.

Plasmid Constructs

The C Kinase Activity Reporter (CKAR) and plasma membrane-localized PKC reporter (PM-CKAR) were described previously (147). The PSD95 specific PKC reporter (PSD95-CKAR) contains CKAR with PSD95 fused to its N-terminus via a four amino acid linker (EPGQ) in a pcDNA3 vector (Life Technologies). PKC constructs were prepared as described previously (11). For HA-PKCα, human PKCα was N-terminally HA-tagged via Gateway cloning into pDEST-HA generated from ligating the Reading Frame Cassette C into the EcoRV site of pcDNA3-HA. All mutants were generated using QuikChange site-directed mutagenesis (Agilent Technologies).

Antibodies and Reagents

The pan anti-phospho-PKC activation loop antibody (pT497) was previously described (168). The anti-phospho-PKCα/βII (pT638/641; 9375S) and pan anti-phospho-PKC hydrophobic motif (βII pS660; 9371S) antibodies were purchased from Cell Signaling. The α-HA antibody (anti-HA, 11867423001, clone 3F10) purchased from Roche. Phorbol 12,13-dibutyrate (PDBu), Uridine-5'-triphosphate (UTP) trisodium salt, Gö 6983, and Bis IV were obtained from Calbiochem. FURA-2 AM dye (F1221) was obtained from Thermo Fisher Scientific. $A\beta_{25-35}$ peptide and the reverse peptide negative control were both obtained from Sigma-Aldrich (A4559 and A2201, respectively).

Cell Culture, Transfection, and Immunoblotting

All cells were maintained in DMEM (Corning) containing 10% fetal bovine serum (Atlanta Biologicals) and 1% penicillin/streptomycin (Corning) at 37˚C, in 5% CO_2. Transient transfection of COS7 was carried out using FuGENE 6 transfection

reagent (Roche) for ~24h. Transient transfection of U87 cells and primary astrocytes was carried out using Lipofectamine 3000 reagent (Thermo Fisher Scientific) for ~48h. Cells were lysed in 50 mM Tris, pH 7.4, 1% Triton X-100, 50 mM NaF, 10 mM $Na_4P_2O_7$, 100 mM NaCl, 5 mM EDTA, 1 mM Na_3VO_4, 1 mM PMSF, 50 µg/mL Leupeptin, 1 µM Microcystin, 1 mM DTT, and 2 mM Benzamidine. Whole cell lysates were analyzed by SDS-PAGE and immunoblotting via chemiluminescence on a FluorChemQ imaging system (ProteinSimple). For cellular dephosphorylation experiments, cells were treated with 200 nM PDBu for the indicated times at 37˚C before lysis.

Isolation of primary astrocytes for culturing and imaging

Astrocytes were isolated from P1-P3 postnatal wild-type C57BL/6 mice as previously described (169). Pups were briefly submerged in 70% ethanol and immediately decapitated. The cerebral hemispheres were dissected from the cranium and the meninges were removed by rolling the cerebral hemispheres on sterile filter paper or paper towels. The hemispheres were then transferred to cold Hanks' balanced salt solution (HBSS). The tissue was dissociated and homogenized with small scissors, collected in a total volume of 7ml HBSS per brain and transferred to a 50 ml falcon tube. 700 µl/brain of 2.5% trypsin and 200 µl/brain of 2.5 g/L pancreatin were added and the mixture was incubated at 37˚C for 30 minutes, shaking to mix after 15 minutes. 8 ml of cell growth medium was added and cells were centrifuged for 3 minutes at 1200 rpm. The supernatant was removed and 10 ml of growth medium was added. The cell pellet was then triturated with a 5ml pipette until the cell suspension was homogeneous (avoiding frothing). Cells were then plated at a density of ~1 brain per T75 flask and placed in a

37˚C / 5% CO_2 incubator for 4 days. Media was changed after 4 days and every 3 days thereafter. On the 11th day, fresh culture media was added to the flasks and oligodendrocytes were shaken off at 240rpm for 16-22 hours. Supernatant was discarded, with the remaining cells being astrocytes. Cells were washed with PBS twice, trypsinized to detach from the flask, and each T75 flask was split 1:3 into three 10 cm plates. The cells were left to grow for 3-4 days before being frozen down in 10% DMSO/90% FBS. Astrocytes were thawed before experiments, the media was changed on day 2 after thawing, and the astrocytes were split into imaging dishes on day 3 or day 4.

FRET imaging, FURA-2 imaging, and analysis

Cells were imaged as described previously (170). COS7 cells were co-transfected with the indicated mCherry-tagged PKC and either CKAR, plasma membrane-targeted CKAR (PM-CKAR), or CKAR fused to PSD95 (PSD95-CKAR), as specified. Cells were rinsed once with and imaged in Hanks' balanced salt solution containing 1mM $CaCl_2$. Images were acquired on a Zeiss Axiovert microscope (Carl Zeiss Microimaging, Inc.) using a MicroMax digital camera (Roper-Princeton Instruments) controlled by MetaFluor software (Universal Imaging, Corp.). Using a 10% neutral density filter, CFP, YFP, FRET, and mCherry images were obtained every 15 seconds. YFP emission was monitored as a control for photobleaching and mCherry was measured to ensure that overexpressed PKC levels were equal in all experiments. Base-line images were acquired for ≥ 2 min before ligand addition and data were normalized to the baseline FRET ratios. The normalized average FRET ratio is the average of these normalized values ± S.E. Area under curve from 3-6 min was quantified and plotted in the bar graph in Figure 2.6,

and statistical significance was determined as indicated above, except for the astrocyte imaging, where significance was calculated using an ANOVA test.

FURA-2 AM dye (5 μM) was loaded into U87 cells or primary astrocytes in serum-free cell growth medium for 30 minutes at room temperature and in the dark. After loading, the cells were rinsed three times in Hanks' balanced salt solution. Fura-2 images were obtained every 7 s through a 380/10-nm or 340/10-nm excitation filter, a 450-nm dichroic mirror, and a 535/45-nm emission filter. $A\beta_{25-35}$ peptide was resuspended in DMSO to form a 10mM 1000X stock. During imaging, Aβ peptide was added directly to the imaging buffer as described previously (155).

3D PKC Structure Modeling

The PKCα structure was visualized using the PyMOL Molecular Graphics System (Version 1.7.4.1, Schrödinger, LLC).

Genetics

Family cohort

The National Institute of Mental Health (NIMH) Alzheimer's Disease Genetics Initiative Study (171) originally ascertained for the study of genetic risk factors in AD with family-based methods, was used in the WGS analyses in this study. The basis for ascertainment in the NIMH collection was the existence of at least two affected individuals within a family, typically siblings. The complete NIMH study cohort contains a total of 1,536 subjects from 457 families. For the purpose of this analysis, only subjects of self-reported European ancestry were included, consisting of 1,376 participants (941

definitely affected and 404 definitely unaffected and the remainder could not be determined as definitely unaffected or definitely affected) from 410 families.

To test the likelihood of finding the observed linkage in the mutant carrier families by chance, we conducted the following bootstrap analysis. We generated a 'parent' set containing 941 ones (indicating affected) and 404 zeros (indicating unaffected), which is the nature of the definitely assessed population in this cohort. We wished to test the likelihood that choosing a set of 16 individuals, (i.e. based on being in a family with a PKCα variant), would show the observe linkage; that is the likelihood that choosing 10 individuals (variant carriers) would all show AD, and choosing 6 individuals (variant non-carriers), at least two would be AD negative. We conducted the following sampling (allowing resampling) procedure: we chose 10 and 6 elements from the 'parent' set to generate 2 subsets, y(1) and y(2). We then tested if all values in y(1) were 1 [test 1] and at least 2 values in y(2) were zero [test2]. If both tests were true, the result of the procedure was 1 (i.e. chance could account for observed linkage); if any of the tests was false, the result of the procedure was 0. This procedure was conducted 100,000 times (run five times). The number of times the result of the procedure was 1, in the five runs was 1598, 1626, 1675, 1628, and 1631. Thus (dividing these values by 100,000) the likelihood of finding the observed linkage distribution by chance in this population is < 2000/100,000 = 0.02.

Standard Protocol Approvals, Registrations, and Patient Consents

Diagnosis of AD dementia was established according to NINCDA-ADRDA criteria. Informed consent was provided by all participants, and research approval was established by the relevant institutional review boards in the study cohort.

WGS Data Generation

3 μg of total genomic DNA (150 ng/μL) obtained from Rutgers repository was sequenced at Illumina, Inc (San Diego, CA 92122 USA) using their latest HiSeq 2500, paired-end sequencing platform. An average of 48X coverage of 98% of the genome was observed in the resulting 120 GB data from each sample. Genomic variants were called in-house using FreeBayes (v0.9.9.2-18) and GATK best practices method (172), resulting in close to 400 Tera-Bytes of high-quality sequencing data in a fully annotated GEMINI database (173).

Chapter 2 is in large part published online as "Gain-of-function mutations in protein kinase Cα (PKCα) may promote synaptic defects in Alzheimer's disease." Alfonso SI*, Callender JA*, Hooli B*, Antal CE, Mullin K, Sherman MA, Lesné SE, Leitges M, Newton AC, Tanzi RE, Malinow R. in *Science Signaling*, 2016 May 10;9(427). The dissertation author was one of the primary investigators and authors of this work (*, co-first authors).

FIGURES AND TABLES

Figure 2.1: Aβ-mediated synaptic depression is blocked by a non-competitive PKC antagonist. [A] Top left, experimental design; organotypic hippocampal slices were infected with a virus expressing CT100, the precursor to Aβ. 16-24 hours later, synaptic transmission was evoked by stimulating presynaptic axons (orange) and neighboring infected and uninfected postsynaptic CA1 neurons were simultaneously recorded. Neurons expressing CT100 exhibit synaptic depression, with the red triangle depicting the drop in average synaptic transmission onto infected neurons. Line, X=Y. Scale bars, 50 ms, 50 pA. [B] Bar graph (left; ni, non-infected) for indicated conditions (right). Error bars, SEM throughout; **, $p < 0.03$, bootstrap (see methods).

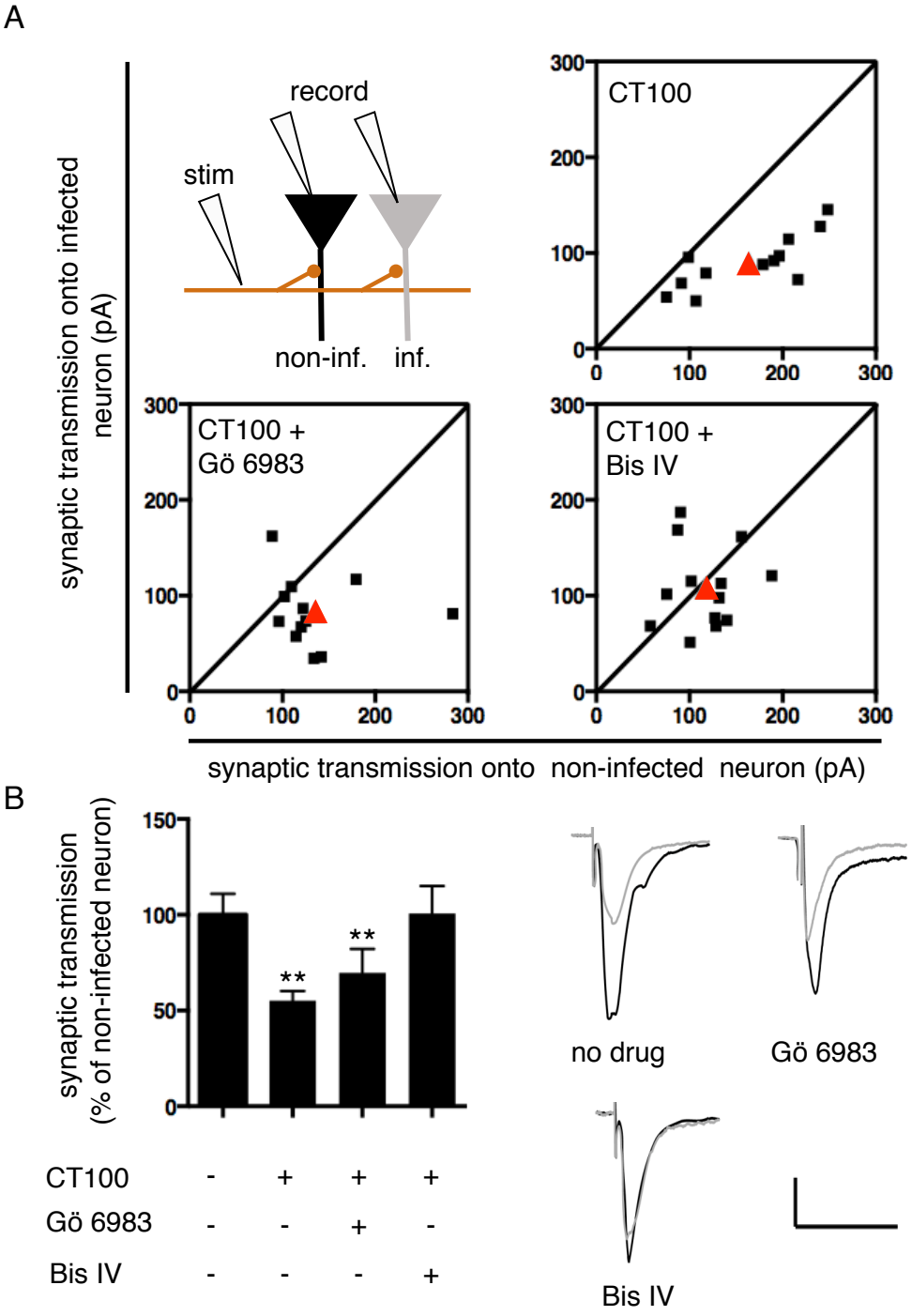
A
record
stim
non-inf.
inf.
CT100
CT100 +
Gö 6983
CT100 +
Bis IV
synaptic transmission onto infected neuron (pA)
synaptic transmission onto non-infected neuron (pA)
0
100
200
300
B
synaptic transmission
(% of non-infected neuron)
150
100
50
0
**
**
CT100 - + + +
Gö 6983 - - + -
Bis IV - - - +
no drug
Gö 6983
Bis IV

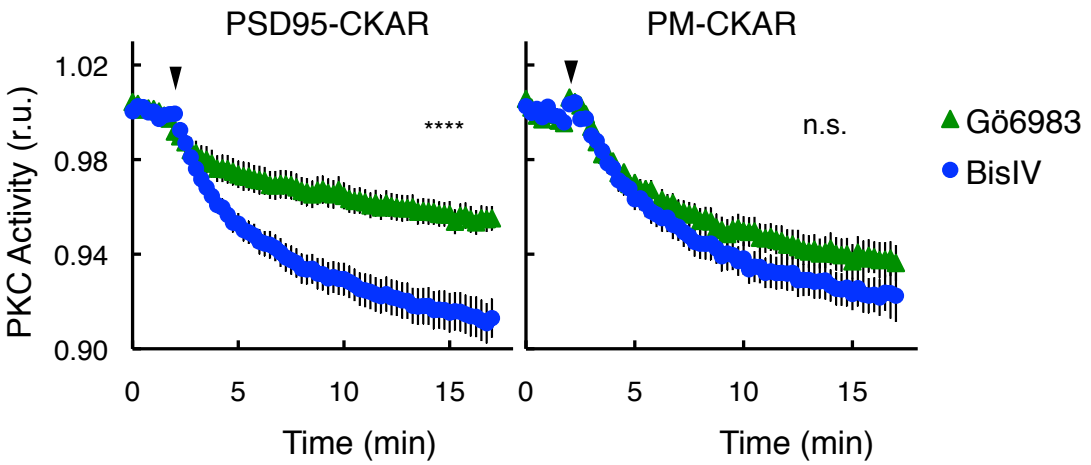

Figure 2.2: PKC at protein scaffolds exhibits differential response to ATP-competitive inhibitors. Normalized average PKC activity in COS7 cells expressing PKC activity reporter (147) fused to PSD95 (left) or targeted to plasma membrane (right); inhibitor added where indicated (arrow head); N > 16 cells; ****, $p < 0.0001$, bootstrap (see methods).

Figure 2.3: Requirement of PKCα for effects of Aβ on synaptic transmission. [A-B] Plot (and example traces, bottom right) of evoked synaptic response amplitudes recorded in infected versus non-infected neurons; infection and number of cell pairs recorded indicated in table (B, right). Bar graph (B, left) of same data; ** indicates $p<0.03$, bootstrap (see methods).

A

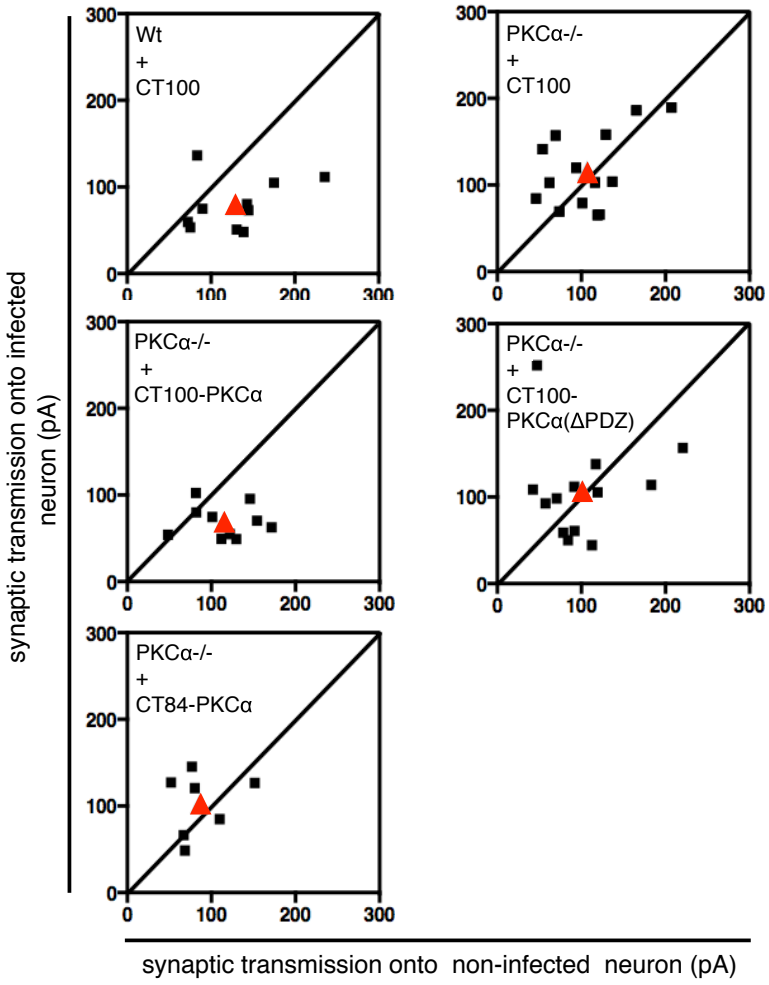
Wt
+
CT100
PKCα-/-
+
CT100
PKCα-/-
+
CT100-PKCα
PKCα-/-
+
CT100-
PKCα(ΔPDZ)
PKCα-/-
+
CT84-PKCα
synaptic transmission onto infected neuron (pA)
synaptic transmission onto non-infected neuron (pA)
0
100
200
300

B

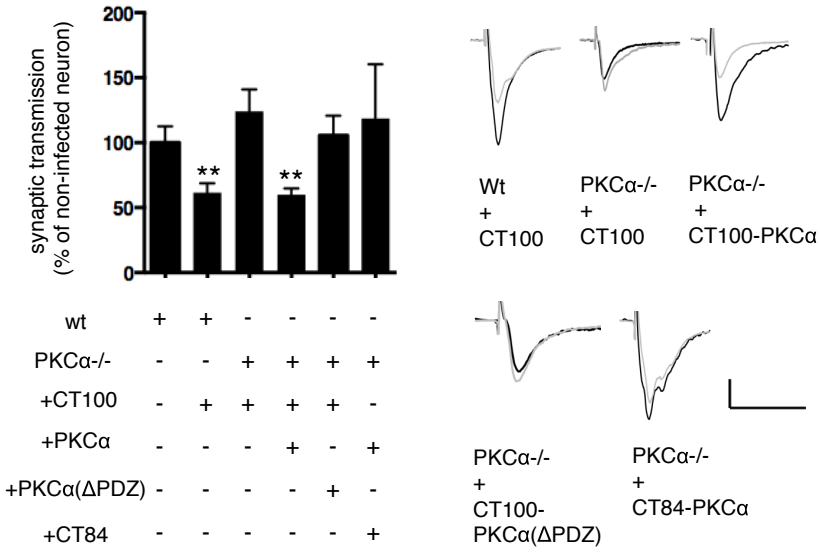
synaptic transmission (% of non-infected neuron)
0
50
100
150
200
**
**
wt + + - - - -
PKCα-/- - - + + + +
+CT100 - + + + + -
+PKCα - - - + - +
+PKCα(ΔPDZ) - - - - + -
+CT84 - - - - - +
Wt + CT100
PKCα-/- + CT100
PKCα-/- + CT100-PKCα
PKCα-/- + CT100-PKCα(ΔPDZ)
PKCα-/- + CT84-PKCα

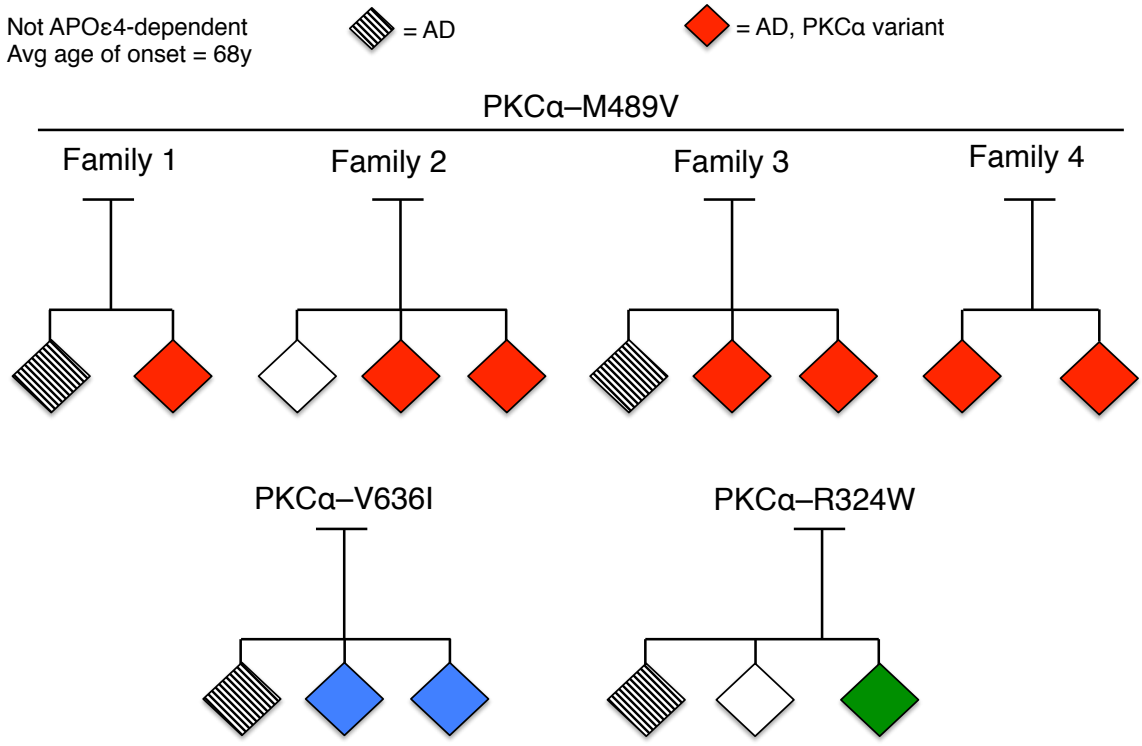

Figure 2.4: Human genetics of rare PKCα variants. Diagrams indicating number of families, along with phenotype and genotype of individuals, carrying M489V, V636I or R324W PKCα variants. Note that all PKCα variant carriers displayed AD and both individuals without AD (white) lacked a PKCα variant.

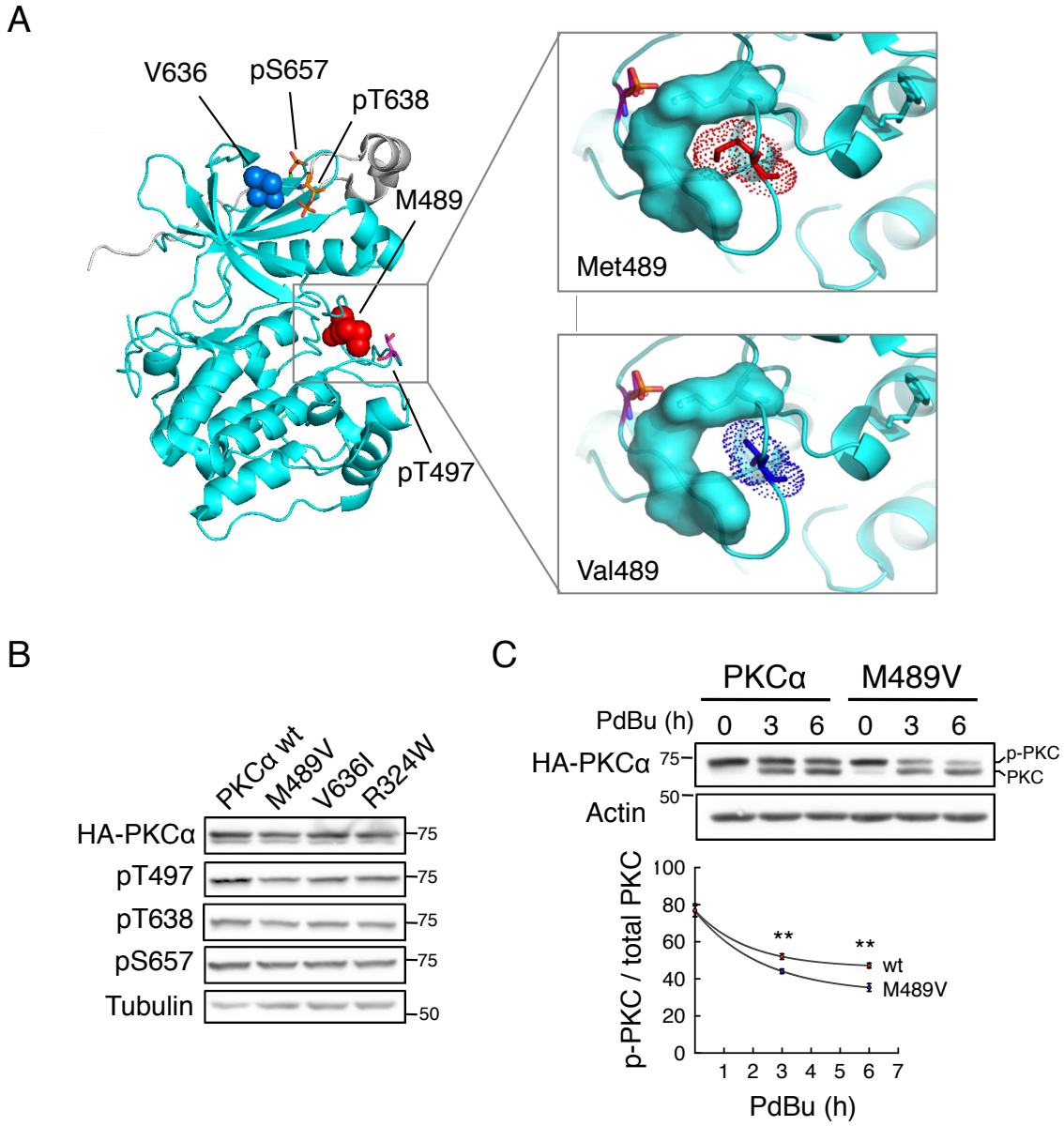

Figure 2.5: AD associated rare variants in PKCα. [A] PKCα kinase domain structure (54) showing the two residues altered in AD: Met489 and Val636. Both are near key regulatory phosphorylation sites (stick representation). Enlargement of activation loop segment (right panels) showing that substitution of Met489 with Val loosens the structural packing of this segment. [B] Western blot showing phosphorylation of the indicated HA-tagged PKCα proteins. [C] Western blot of COS7 cells expressing wt or M489V PKCα and treated with phorbol dibutyrate (PDBu) for the indicated times, and probed for HA. Quantification depicted below of phosphorylated/total PKC from 5 independent experiments. **, $p < 0.01$, by bootstrap (see methods).

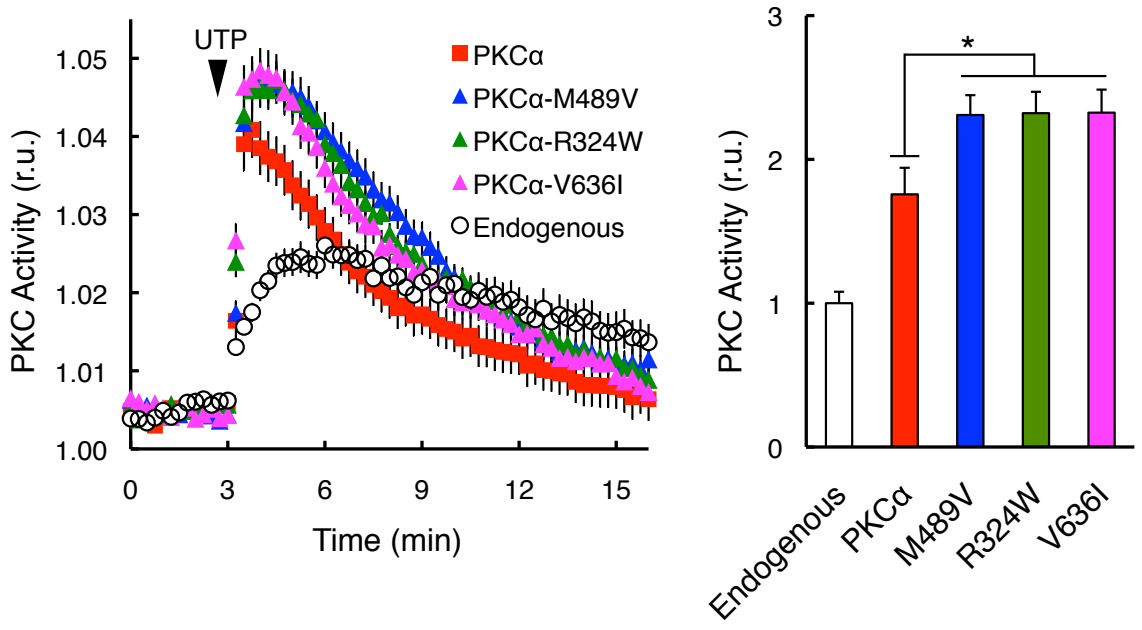

Figure 2.6: Live cell imaging reveals higher signaling output of both AD-associated rare variants. [A] Normalized FRET ratios (mean ± SEM) representing PKC activity in COS7 cells co-expressing a PKC activity reporter (147) and indicated PKCα. Addition of UTP (100 μM) where indicated (black arrow). N > 25 cells for each construct. Data represent the average ± SEM from at least 3 biologically independent experiments measuring > 16 cells. Right, area under the curve from 3-6 minutes; *, $p < 0.05$, bootstrap (see methods).

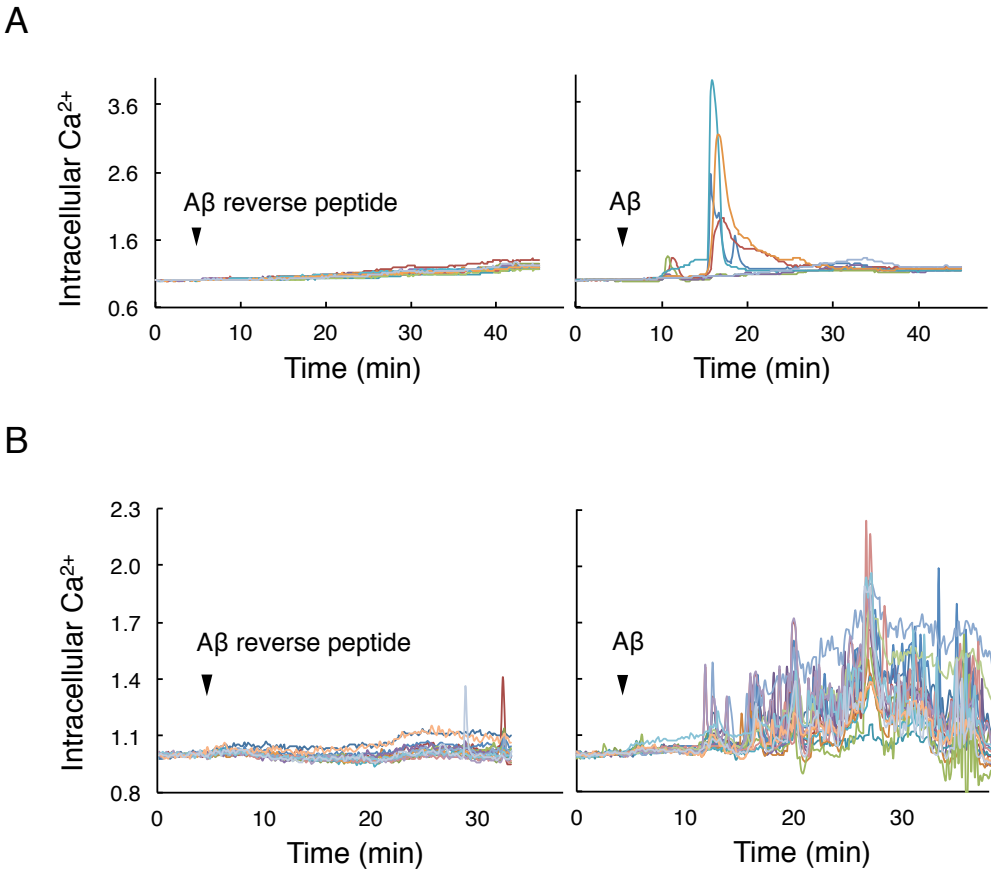

Figure 2.7: Live cell imaging reveals that $A\beta_{25-35}$ peptide causes Ca^{2+} response in both U87 cells and in primary murine astrocytes. [A] Normalized 350/380 ratios depicting changes in cytosolic Ca^{2+} in U87 cells, as assessed using the Ca^{2+} indicator FURA-2, upon addition (black arrow) of Aβ peptide comprised of residues 25-35 (10 μM; right) or Aβ reverse peptide, residues 35-25 (10 μM; left). Each trace corresponds to one cell. [B] Normalized 350/380 ratios depicting changes in cytosolic Ca2+ in primary murine astrocytes, as assessed using the Ca2+ indicator FURA-2, upon addition (black arrow) of $A\beta_{25-35}$ (10 μM; right) or reverse peptide negative control (10 μM; left).

Figure 2.8: Live cell imaging reveals that $A\beta_{25-35}$ peptide causes PKC activation in primary murine astrocytes. [A] Normalized FRET ratios representing endogenous PKC activity in astrocytes expressing plasma membrane-targeted CKAR (pmCKAR). Cells expressing either normal pmCKAR or a non-phosphorylatable CKAR as a negative control (pmCKAR-T/A, bottom left panel) were treated with $A\beta_{25-35}$ or Aβ reverse peptide negative control (10 μM each), UTP (100 μM), or PDBu (200 nM) where indicated (black arrows). Each trace represents one cell, N ≥ three cells for each experiment. [B] Quantification of experiments depicted in [A]. Quantification was calculated as the area under the curve of the traces from minutes 5-40. *, $p < 0.05$; **, $p < 0.01$ using one-way ANOVA.

A

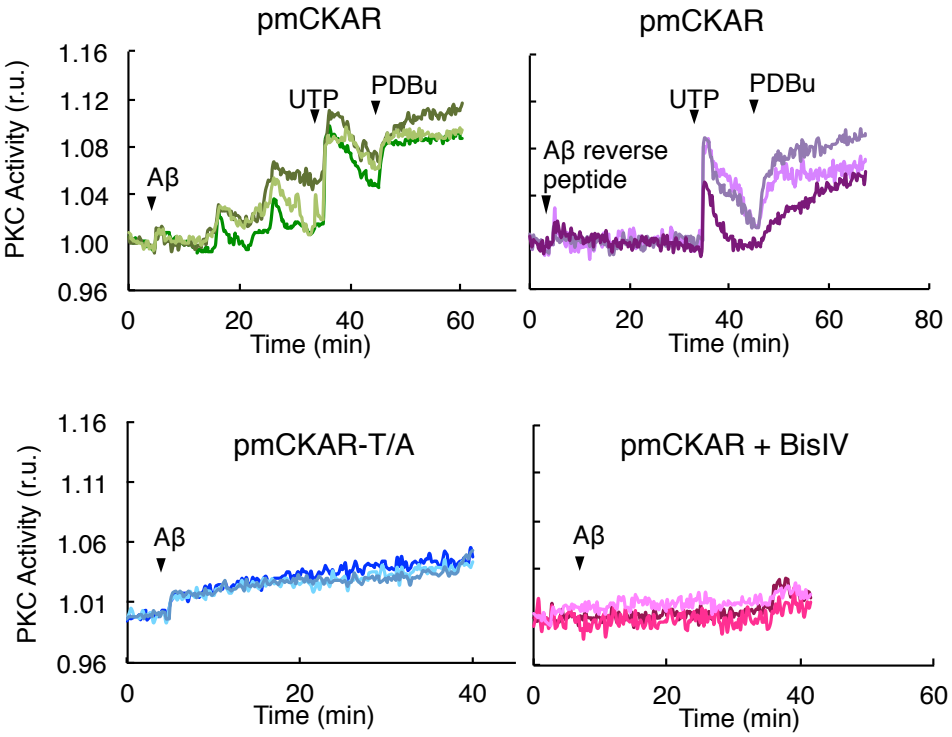
pmCKAR
pmCKAR
PKC Activity (r.u.)
1.16
1.12
1.08
1.04
1.00
0.96
Aβ
UTP
PDBu
Aβ reverse peptide
0
20
40
60
80
Time (min)
pmCKAR-T/A
pmCKAR + BisIV
1.11
1.06
1.01

B

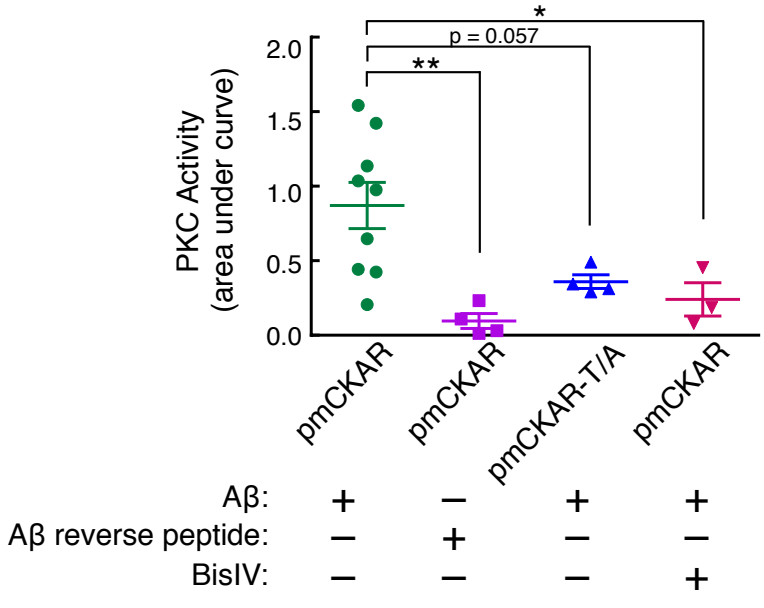
PKC Activity (area under curve)
2.0
1.5
1.0
0.5
0.0
*
p = 0.057
**
pmCKAR
pmCKAR
pmCKAR-T/A
pmCKAR
Aβ: + − + +
Aβ reverse peptide: − + − −
BisIV: − − − +

CHAPTER 3

PROTEIN KINASE Cα GAIN-OF-FUNCTION VARIANT IN ALZHEIMER'S DISEASE DISPLAYS ENHANCED CATALYSIS BY MECHANISM THAT EVADES DOWN-REGULATION

ABSTRACT

Conventional protein kinase C (PKC) family members are reversibly activated by binding to the second messengers Ca^{2+} and diacylglycerol, events that break autoinhibitory constraints to allow the enzyme to adopt an active, but degradation-sensitive, conformation. Perturbing these autoinhibitory constraints, resulting in protein destabilization, is one of many mechanisms by which PKC function is lost in cancer. Here, we address how a gain-of-function germline mutation in PKCα in Alzheimer's Disease (AD) enhances signaling without increasing vulnerability to down-regulation. Biochemical analyses of purified protein demonstrate that this mutation results in an approximately 30% increase in the catalytic rate of the activated enzyme, with no changes in the concentrations of Ca^{2+} or lipid required for half-maximal activation. Molecular dynamics simulations reveal that this mutation has both localized and allosteric effects, most notably decreasing the dynamics of the C-helix, a key determinant in the catalytic turnover of kinases. Consistent with this mutation not altering autoinhibitory constraints, live cell imaging studies reveal that the basal signaling output of PKCα-M489V is unchanged. However, the mutant enzyme in cells displays increased sensitivity to an inhibitor that is ineffective towards scaffolded PKC, suggesting the altered dynamics of the kinase domain may influence protein interactions. Lastly, we show that phosphorylation of a key PKC substrate, Myristoylated Alanine-rich C-kinase Substrate (MARCKS), is increased in brains of CRISPR-Cas9 genome-edited mice containing the PKCα-M489V mutation. Our results unveil how an AD-associated

mutation in PKCα permits enhanced agonist-dependent signaling via a mechanism that evades the cell's homeostatic down-regulation of constitutively active PKCα.

INTRODUCTION

Protein kinase C α (PKCα) is a ubiquitously-expressed member of the protein kinase C (PKC) family of Serine/Threonine kinases that transduces signals mediated by the second messengers Ca^{2+} and diacylglycerol (DG) (21, 174). It plays a major role in suppressing cell proliferation (175-179) and survival (13, 180). Studies both in mice, where its deletion causes the spontaneous development of colon tumors (181), and in patients, where loss of protein expression is associated with colon cancer (182), have long supported a role as a tumor suppressor. It is the first PKC in which a cancer-associated mutation was reported: over 20 years ago, Joubert and colleagues reported that a mutation in PKCα in human pituitary tumors resulted in mislocalization, thus allowing growth in soft agar in ectoptic expression studies (183-185). Loss-of-function somatic mutations in PKCα have now been identified in many diverse cancers (11). Mounting evidence suggests that PKCα opposes oncogenic survival signaling by its phosphorylation and inactivation of oncogenes such as K-Ras (12, 13), growth factor receptors (14-16) and phosphatidylinositol-3 kinase (17-19), among others. The key role of PKCα in suppressing proliferative and survival pathways poise it to play a role not only in cancer via its loss-of-function, but also in degenerative diseases via gain-of-function.

We recently identified gain-of-function mutations in PKCα in Alzheimer's Disease (AD) (121), a degenerative pathology characterized by the accumulation of amyloid-β (Aβ) protein aggregates in the brain and synaptic degeneration (139). Whole genome sequencing of individuals from 410 families with late-onset AD identified germline PKCα mutations in affected, but not in disease-free, individuals in six of the families. These mutations all enhanced the agonist-evoked signaling output of PKCα assessed using a genetically encoded PKC activity sensor in overexpression studies (121). While the mechanisms by which Aβ aggregation leads to synaptic degeneration are not fully understood, electrophysiological studies established that the synaptic effects of Aβ depend on PKCα via a mechanism requiring PKCα's PDZ ligand (which scaffolds to PDZ domain-containing proteins such as PSD95, SAP97, and PICK1 (33, 34)) and its interaction with the scaffold PICK1 (121, 124). Thus, enhanced activity of PKCα may augment the degenerative pathways activated by Aβ. Supporting a general role of enhanced PKC activity in AD, a recent unbiased phosphoproteomics study identified increased phosphorylation of PKC substrates, including MARCKS, as a primary early event in AD (109). These activity-enhancing mutations are in stark contrast to loss-of-function cancer-associated mutations. Indeed, with the possible exception of a mutation in PKCβ in Adult T Cell Leukemia (186), it is noteworthy that no gain-of-function mutations in any of the nine PKC isozymes have been identified (11).

PKCα is an exquisitely tuned enzyme, whose signaling output depends not only on binding to second messengers, but also on the abundance of inputs that control its steady-state levels in the cell. Following its biosynthesis, PKCα becomes constitutively

phosphorylated at three priming sites, allowing it to adopt an autoinhibited conformation in the cytosol that protects the enzyme from dephosphorylation and degradation (21). Due to this autoinhibited species being resistant to degradation, PKCα is a particularly long-lived enzyme. It is transiently and reversibly activated by signals that promote phospholipid hydrolysis to generate its two second messengers, Ca^{2+} and diacylglycerol: Ca^{2+} binds the C2 domain, promoting association to the plasma membrane via a Ca^{2+}-dependent bridge with anionic phospholipids, and diacylglycerol binds one of two tandem C1 domains (187). Engagement of both membrane-targeting modules with the plasma membrane results in release of an autoinhibitory pseudosubstrate segment from the substrate-binding cavity, positioning PKC in an "open" and signaling-competent conformation. Metabolism of diacylglycerol results in PKC disengaging from the membrane and regaining the stable, autoinhibited conformation (187). Phorbol esters, potent competitive ligands for diacylglycerol binding, are not readily metabolized and therefore result in irreversible binding of PKC to the membrane, leading to acute activation but chronic down-regulation of PKC protein levels (188, 189). The paradoxical effect of these potent tumor promoters—initial activation followed by eventual degradation—confounded understanding the role of PKC in cancer (180). Given that the active conformation of PKC is sensitive to degradation, how do AD-associated mutations result in enhanced cellular kinase activity while also evading down-regulation?

Here, we examine the mechanism by which one AD-associated variant PKCα-M489V enhances PKCα signaling. This variant was identified in seven individuals in four families: it is heterozygous, with one allele encoding a protein with a Met to Val

substitution at position 489 in the activation loop, a segment near the entrance to the active site that critically controls catalysis (190). Our findings support a model in which altered dynamics of the kinase domain enhance the activity of the PKCα-M489V variant by increasing the intrinsic catalytic rate of the enzyme without affecting autoinhibitory constraints. Thus, the enzyme's on/off dynamics are unaffected, but when on, it catalyzes phosphorylation at a faster rate. This provides a previously undescribed mechanism by which a disease-associated mutation enhances PKC activity without compromising its stability.

RESULTS

PKCα-M489V mutation confers an enhanced catalytic rate.

We previously established that PKCα-M489V displays enhanced agonist-evoked signaling output relative to wild-type PKCα in cells (121). Specifically, the M489V variant overexpressed in COS7 cells has approximately 25% greater activity compared to wild-type enzyme following agonist stimulation of cells to generate Ca^{2+} and DG, as assessed using the genetically-encoded FRET-based C Kinase Activity Reporter (CKAR) (147, 191). This variant has a replacement of Met to Val at position 489 in the activation loop, nine residues before the constitutive phosphorylation site (Thr497) for the upstream kinase PDK-1 (**Figure 3.1A**). It is also two residues removed from an interaction network that connects the activation loop to the C helix, in turn connecting to the C-terminal phosphorylation site Ser657 (**Figure 3.1C**). Furthermore, this face of the kinase domain for the related PKCβII has been shown to interface with the C2 domain to maintain the

enzyme in an autoinhibited conformation (32), as schematized in **Figure 3.1B**. Thus, this residue is positioned to potentially perturb autoinhibitory constraints, catalysis, or both.

To elucidate the molecular mechanism through which the M489V mutation confers enhanced PKC activity in cells, we analyzed the kinetics of activation of the purified wild-type and M489V mutant protein. GST-tagged PKCα was purified to homogeneity from insect cells using a baculovirus expression system. Western blot analysis confirmed that both the wild-type and PKCα-M489V proteins were processed by priming phosphorylations at the activation loop (Thr497) and the two C-terminal sites (Thr638 and Ser657) (**Figure 3.2A**).

To assess whether autoinhibitory constraints were altered in the PKCα-M489V protein, we examined the dependence for activation on [1] Ca^{2+} or [2] mol fraction phosphatidylserine (PS) in DG-containing micelles. Triton X-100 lipid mixed micelles afford a highly sensitive system to dissect the lipid dependence of PKC activation, which displays high cooperativity with respect to phosphatidylserine (192-194). Kinase assays revealed no differences in the two proteins with respect to the concentration of Ca^{2+} or phosphatidylserine resulting in half-maximal activity (**Figure 3.2B** and **Table 1**). Nor was the basal activity different between the two proteins, which both displayed approximately 10% of co-factor induced activity when activators were absent from the assay. We did note, however, that the V_{max} was consistently higher for the PKCα-M489V protein compared to wild-type enzyme. These data reveal that while the autoinhibitory constraints were unaffected in the PKCα-M489V variant, the maximal velocity was higher.

We next assessed whether peptide substrate or ATP dependencies were altered in the AD variant. When assayed in the presence of saturating Ca^{2+} and lipid, the K_m for peptide substrate and the K_m for ATP were indistinguishable from wild-type enzyme (**Figure 3.2B, Table 1**). However, the V_{max} was higher for PKCα-M489V (V_{max} = (2.7 ± 0.2) x 10^3 nmol phosphate per minute per mg PKC) compared to wild-type (V_{max} = (2.0 ± 0.2) x 10^3 nmol phosphate per minute per mg PKC), an increase observed in each of five separate protein preparations. Analysis of protein obtained from three separate preparations, under conditions of saturating Ca^{2+} and lipid, 100 μM peptide, and 300 μM ATP, revealed a 29 ± 9% increase in the specific activity of purified PKCα-M489V compared to wild-type. These data reveal that neither the degree of autoinhibition nor the cofactor-dependent release of autoinhibition is altered by the M489V mutation. Rather, Met to Val substitution increases the intrinsic catalytic rate of the enzyme.

Molecular dynamics simulations reveal altered dynamics of the catalytic domain in PKCα-M489V.

To gain insight into how the M489V mutation increases the catalytic rate without altering sensitivity to cofactors, binding of peptide substrate, or the K_m for ATP, we compared the dynamics of the kinase domain of wild-type or PKCα-M489V using molecular dynamics (MD) simulations (**Figure 3.3**). These simulations reveal both localized and long-range changes in the dynamics of the kinase core. Notably, altered dynamics were observed in two key segments of the ATP binding pocket: [1] motion was increased in the Gly-rich loop, a key determinant between the βI and βII strands (β1/βII)

that anchors the β-phosphate of ATP (190), and [2] motion was decreased in the C-helix (αB/αC), a segment that stabilizes the active conformation of kinases. For PKCα, Arg389 in the C-helix forms an electrostatic interaction with Glu487 in the activation loop (AL), two residues removed from Met489, whereas the flanking Lys388 forms an H-bond with the main chain carbonyl of Gly655, part of a conserved FXXF motif (190) and two residues removed from phosho-Ser657, a key determinant of stability of PKCα's kinase domain (see **Figure 3.1C**). Additionally, the simulations indicated that motions in the distal αG and αI helices were increased in the M489V mutant compared to wild-type PKCα. These studies support a model in which replacing Met with Val at position 489 impacts the dynamics not only around the active site, but also at distal surfaces on the kinase domain.

PKCα-M489V is not more basally active than wild-type PKCα in a cellular environment.

Given that the M489V mutation does not affect autoinhibitory constraints in the pure protein, we hypothesized that basal (unstimulated) signaling by PKCα-M489V would be similar to that of wild-type PKCα in cells. We overexpressed a FRET-based reporter for PKC activity (CKAR, (147)) alone or with either wild-type or mutant mCherry-PKCα in COS7 cells and monitored the decrease in phosphorylation of CKAR, assessed by the decrease in FRET ratio, following addition of the general PKC inhibitor bisindolylmaleimide IV (Bis IV) (**Figure 3.4A**). Bis IV caused a drop in the FRET ratio of cells transfected with CKAR alone, representing inhibition of the basal activity of

endogenous PKC isozymes (empty triangles). This drop was larger in cells overexpressing PKCα (blue), with the difference reflecting the basal activity of the overexpressed PKCα. Importantly, Bis IV caused the same drop in cells overexpressing comparable levels of PKCα-M489V (red). Thus, the M489V mutation does not enhance the basal signaling output of PKCα; enhanced signaling is only observed following agonist stimulation and removal of autoinhibitory constraints (121).

In order to assess if the M489V mutation confers increased basal signaling in the absence of autoinhibitory constraints, we introduced this mutation into a PKCα construct that lacked its N-terminal regulatory moiety (thus lacking the pseudosubstrate, C1 domains, and C2 domain). We then measured the effect of inhibiting PKC activity in cells co-expressing the isolated catalytic domains (αCat) and CKAR (**Figure 3.4B**). Addition of Bis IV produced a significantly higher drop in FRET for cells expressing the isolated PKCα catalytic domain containing the M489V mutation (red) compared with the wild-type PKCα catalytic domain (blue). For these experiments, cells expressing comparable amounts of each kinase domain were selected for imaging: **Figure 3.4C** depicts the average mCherry-PKCα intensity for the experiments in **Figures 3.4A** and **3.4B**. Thus, the findings in **Figures 3.4A** and **3.4B** do not result from differences in the amount of overexpressed protein. Note, the expression levels for the isolated catalytic domains were lower than that of the full-length enzyme because of the enhanced sensitivity of the exposed kinase domain to degradation.

PKCα-M489V confers enhanced sensitivity to ATP-competitive inhibitors in cells.

We next took advantage of pharmacological tools to address whether the M489V mutation alters signaling on protein scaffolds. We have previously shown that scaffold-bound PKC is refractory to ATP-competitive inhibitors such as Gö6976 and Gö6983, but is fully sensitive to the uncompetitive inhibitor Bis IV (121, 122, 195). We overexpressed both CKAR and mCherry-PKCα wild-type or M489V in COS7 cells, stimulated with the PKC activator phorbol 12,13-dibutyrate (PDBu) to maximally activate all PKC in the cell, and followed by treatment with sub-threshold amounts of the ATP-competitive inhibitor Gö6976 (**Figure 3.5A**). Cells expressing PKCα-M489V displayed a greater drop in activity compared to wild-type PKCα at all three inhibitor concentrations tested. In contrast, sub-saturating amounts of the ATP-uncompetitive inhibitor Bis IV caused an identical drop in the cellular activity of both wild-type and PKCα-M489V (**Figure 3.5B**). These results reveal that PKCα-M489V has enhanced sensitivity to the ATP competitive inhibitor (Gö6976) that discriminates between scaffolded and non-scaffolded PKC, but not to the non-discriminatory inhibitor (Bis IV).

To determine whether the altered inhibitor sensitivity reflected an intrinsic property of the kinase or altered cellular interactions, we measured the K_I of purified GST-PKCα for Gö6976: the K_I of M489V (109 ± 20 nM) and wild-type enzyme (113 ± 10 nM) were the same within the error of the assay (**Figure 3.5C**). These data suggest that the enhanced sensitivity of the M489V variant to Gö6976 results from altered interactions with the cellular environment, rather than from an innate property of the enzyme itself.

Phosphorylation of MARCKS is increased in the brains of PKCα-M489V mice.

The M489V mutation was identified in affected, but not unaffected, siblings in four unrelated families suggesting that it is causal in the disease (121). Because increased phosphorylation of MARCKS has been identified as one of the earliest and most robust phosphorylation change in post-mortem brains from AD patients compared to controls (109), we assessed whether the AD-associated single amino acid change altered phosphorylation of MARCKS in an animal model. To this end, we used CRISPR-Cas9 mediated genome editing to develop a genetically engineered mouse containing a homozygous M489V mutation in its *Prkca* gene (Taconic Biosciences GmbH developed for Cure Alzheimer's Fund). We obtained whole-brain lysates from either wild-type or homozygous M489V mice and analyzed them via SDS-PAGE and Western blotting for a known PKC phosphorylation site on MARCKS protein (**Figure 3.6**). The mice containing the M489V mutation displayed a 41 ± 20% increase in phosphorylation of MARCKS at Ser 159/163 compared to wild-type mice. We also blotted for total PKCα levels in order to assess whether the M489V mutation affected the PKCα stability and protein levels in an endogenous, whole-brain environment. Importantly, the total PKCα protein levels were not significantly different between the wild-type and M489V samples. This establishes that the M489V mutation both changes PKCα signaling in the brain to enhance the phosphorylation of one of its major down-stream targets and also does so in a manner that does not alter the steady-state levels of total PKCα protein.

DISCUSSION

Here we unveil a previously undescribed mechanism by which a disease-associated mutation in a conventional PKC has enhanced activity without threatening the stability of the protein (**Figure 3.7**). Biochemical, molecular dynamics, cellular studies, and analysis of brains from genome-edited mice reveal that the Alzheimer's disease-associated PKCα-M489V variant has the same on/off dynamics as wild-type enzyme, but catalyzes reactions at a faster rate when on, resulting in a significant increase in phosphorylation of endogenous PKC substrates without causing a reduction in the levels of PKCα. We show that autoinhibitory constraints are unperturbed by mutation of this residue, with basal signaling both *in vitro* and in cells unchanged from wild-type PKCα. Rather, this mutation alters the dynamics of the kinase core in a manner that enhances the rate of catalysis by approximately 30% while it is open and active, accounting for the previously described increase in agonist-evoked signaling in cells (121). Furthermore, these altered dynamics affect the cellular pharmacology of the PKCα-M489V variant, rendering it more sensitive to an ATP competitive inhibitor but not to an uncompetitive inhibitor. Lastly, we demonstrate that brains from mice with this PKCα mutation contain higher phosphorylation levels of the canonical PKC substrate MARCKS. Given this finding, it is of note that a recent unbiased phosphoproteomics study of brains from human Alzheimer's Disease patients revealed that an increase in MARCKS phosphorylation is the major upregulated pathway in early stages of this disease (109).

The altered catalytic rate resulting from mutation of a bulky Met to the smaller Val in a key regulatory segment involved in structuring the catalytic domain's active site exemplifies how structural dynamics and protein plasticity play a critical role in catalysis.

Notably, elegant NMR relaxation studies with wild-type and mutant forms of cis-trans isomerase cyclophilin A provide strong experimental evidence that protein motions limit the turnover rate of the enzyme (196). Consistent with protein dynamics determining the rate of catalysis, our *in silico* molecular dynamics simulations support a model in which substituting Met for Val at position 489 alters both localized and distal structural flexibility of the catalytic domain. Such allosteric effects are not surprising given the interlinked functional communities that populate the kinase core (190, 197). The activation loop, in particular, acts as a hub for these communities. For example, numerous studies with the archetypical kinase, protein kinase A (PKA), and with the Tec family kinases have established that altering residues in the activation loop region alters the dynamics of the catalytic domain (198, 199). Mechanistic studies with PKA have revealed that the rate-limiting step in catalysis is the release of ADP (200). If this is the case for PKCα, then the altered motions in the active site may reduce the constraints that limit ADP release, thereby increasing the catalytic rate. It is noteworthy that, like many enzymes (201), PKA and PKC are relatively inefficient, with PKA catalyzing on the order of 20 reactions per second (200) and PKCα on the order of 3 reactions per second (this study). Thus, minor changes are likely to have significant effects on catalysis. Interestingly, the residue at position 489 varies amongst different PKC isozymes (Figure 3.7A). Whether the residue at this position generally serves to tune catalytic efficiency unique to each PKC enzyme remains to be established. Indeed, there exists a precedent for residues in this position playing a key role in tuning the catalysis of kinases; namely, the large hydrophobic residue at the DFG+5 position in c-Src has been shown to act as a

"hydrophobic latch" in its control of c-Src activity (202). In contrast, the flanking residues in PKC contain the highly conserved DFG and APE motifs that are frequently mutated in cancer to result in loss of function.

We have previously established that PKC bound to protein scaffolds is refractory to inhibition by ATP-competitive inhibitors (122). This is relevant to the cellular pharmacology of PKCα in the context of AD because the species of PKCα that mediates Aβ's effects on synaptic transmission depends on PKCα's PDZ ligand, which scaffolds to the PDZ domain-containing proteins PICK1 and PSD95 (33, 34). In this study, we found that PKCα-M489V gained sensitivity to the ATP competitive inhibitor Gö6976 in cells, with sensitivity to the uncompetitive inhibitor Bis IV remaining similar to that of wild-type PKCα. In contrast, the M489V mutation did not change the IC_{50} for inhibition by Gö6976 *in vitro* relative to wild-type protein, revealing that this altered sensitivity is specific to the cellular environment. One possible explanation is that the altered dynamics conferred by the M489V mutation now allow inhibition by ATP competitive inhibitors, regardless of whether the kinase is bound to protein scaffolds. Alternatively, the altered dynamics may alter residency time on scaffolds. It is of note that that the enhanced sensitivity of PKCα-M489V to the ATP competitive inhibitor highlights a weakness that might be pharmacologically exploited in the treatment of this disease.

The amount of PKC activity in the cell exquisitely controls cellular homeostasis. This is exemplified by the finding that PKCβII is haploinsufficient in a colon cancer cell line: two alleles of this isozyme effectively suppress growth in 3D whereas one allele does not (11). Thus, small changes in the activity of PKC have large effects on cellular

function. Given the multiple regulatory inputs necessary for PKC activity, PKC can be readily inactivated by mutations that prevent processing phosphorylations, impede second messenger binding, or impair catalysis. Indeed, such loss-of-function mutations are prevalent in cancer (11, 203, 204). However, mechanisms to enhance the activity of PKC are more difficult to envision. Conventional PKC isozymes engage in intramolecular autoinhibition in order to prevent downstream signaling in the absence of activating ligands, and disruption of this autoinhibition by prolonged treatment with potent PKC activators such as phorbol esters and bryostatins causes the degradation of PKC (38, 188, 189) (**Figure 3.7B**, right). Indeed, patients receiving prolonged bryostatin infusions in a clinical trial for advanced metastatic cancer were reported to have decreased levels of PKC in peripheral blood monocytes (205). Thus, any mutations that decrease autoinhibition of PKCα to promote less constrained or constitutive activation would effectively lead to its degradation, thus paradoxically serving as loss-of-function mutations. Here, we show that one mechanism to evade this is by increasing the reaction rate of PKC, in the absence of any perturbations of autoinhibitory constraints **(Figure 3.7B**, left). The approximately 30% increase in the reaction rate of PKCα harboring the M489V germline mutation, accumulating over a patient's lifetime, could contribute to AD pathogenesis.

The results reported here not only reveal how a subtle Met to Val mutation in a key region of the catalytic domain of PKCα can significantly alter molecular dynamics to increase activity—thus promoting degenerative pathology—but also highlight the

importance of maintaining exactly the right level of PKC signaling, an endeavor that requires precise biochemical and molecular regulation.

MATERIALS AND METHODS

Plasmid Constructs, Antibodies, and Reagents

The C-Kinase Activity Reporter (CKAR) was previously described (147, 191). Human PKCα was N-terminally tagged with mCherry via Gateway cloning as described (11, 121). All mutants were generated using QuikChange site-directed mutagenesis (Agilent Genomics). The anti-PKCα antibody (610108) was from BD Transduction Laboratories. The anti-phospho PKCα/βII (pT638/641; 9375S) and pan anti-phosphorylated PKC hydrophobic motif (βII pS660, 9371S) antibodies were from Cell Signaling Technology. The pan anti-phospho-PKC activation loop antibody was previously described (168). The phospho-MARCKS (sc-12971-R) and the total MARCKS (sc-6454) antibodies were purchased from Santa Cruz Biotechnology. β-actin antibody was purchased from Sigma-Aldrich (A2228). Phorbol 12,13-dibutyrate (PDBu), Gö6976, and bisindolylmaleimide IV (Bis IV) were from Calbiochem. Lipids used in kinase assays (diacylglycerol (DG), 800811C, and phosphatidylserine (PS), 840034C) were from Avanti Polar Lipids.

Mammalian Cell Culture and Transfection

COS7 cells were maintained in DMEM (Cellgro) containing 10% fetal bovine serum (Atlanta Biologicals) and 1% penicillin/streptomycin (Gibco) at 37 °C in 5% CO_2.

Transient transfection was carried out using jetPRIME (PolyPlus Transfection) or FuGENE 6 transfection reagents (Roche Applied Science) for ~24h.

PKCα-M489V mouse generation

C57BL/6NTac-*Prkca* mice containing the M489V mutation in *Prkca* were generated by Taconic Biosciences GmbH for Cure Alzheimer's Fund. The point mutation was inserted using a standard CRISPR/Cas9-mediated gene editing approach. In short, a ribonucleoprotein complex comprising the Cas9 protein complexed with a guide and a transactivator crRNA molecules were injected in fertilized C57BL/6NTac oocytes along with a single-stranded oligonucleotide containing the desired point mutation. Insertion of the oligonucleotide sequence resulted in the mutation of the Methionine 489 to Valine and introduction of an AflIII restriction site for genotyping purposes. Founder mice were genotyped by sequencing and bred to C57BL/6NTac WT mice for germline transmission. G1 heterozygous mice were identified by restriction analysis and confirmed by sequencing. HET G1 animals were then crossed to C57BL/6NTac WT mice for another generation before establishing HET x HET mating to generate cohorts for analysis. 12-15 week old mice were used for sample preparation. All animal handling and procedures were approved by the Institutional Animal Care and Usage Committee.

Murine Brain Sample Preparation and Immunoblotting

3-month old wild-type and homozygous M489V mice were euthanized and hemibrains were obtained and immediately snap-frozen. Frozen tissue was then homogenized in a dounce tissue grinder with RIPA buffer (50 mM Tris, pH 7.4, 150 mM NaCl, 2 mM EDTA, 1% Triton X-100, 1% NaDOC, 0.1% SDS, 10 mM NaF, 1 mM

Na_3VO_4, 1 mM PMSF, 50 μg/ml leupeptin, 1 μM microcystin, 1 mM DTT, and 2 mM benzamidine). Homogenates were sonicated and protein was quantified using a BCA protein assay kit (Thermo Fisher Scientific). 30 μg of protein were separated by standard SDS-polyacrylamide gel electrophoresis (SDS-PAGE) and transferred to PVDF membranes (BioRad). Membranes were blocked with 5% bovine serum albumin or 5% milk for one hour at room temperature and analyzed by immunoblotting with specific antibodies. Detection and quantification of immunoreactive bands was conducted by chemiluminescence on a FluorChem Q imaging system (ProteinSimple). Statistical significance was determined using a Student's t test.

FRET Imaging and Analysis

Cells were imaged as described previously (121, 147, 170) with the following modifications: COS7 cells were co-transfected with the indicated mCherry-tagged PKC construct and CKAR (147) at a 0.8:1 ratio of DNA, respectively. Baseline images were acquired every 15 seconds for ≥ 2 minutes before ligand addition, and data were normalized to the baseline FRET ratios. The data are graphed as average normalized FRET ratio ± SEM from at least 3 independent experiments.

Insect Cell Culture and Protein Purification

Human GST-PKCα protein was expressed and purified from insect cells using the Bac-to-Bac expression system (Invitrogen). GST-PKCα protein was batch purified using glutathione sepharose beads as previously described (206) with the following protocol changes: Sf-21 insect cells expressing GST-tagged protein were rinsed with PBS and lysed in 50 mM HEPES pH 7.5, 1 mM EDTA, 100 mM NaCl, 0.1 % Triton X-100, 100

μM PMSF, 1 mM DTT, 2 mM benzamidine, 50 μg/ml leupeptin, and 1 μM microcystin. Purified protein was exchanged into 20 mM HEPES, pH 7.5, 1 mM EDTA, 1 mM EGTA, and 1 mM DTT using 10 kDa Amicon centrifugal filter unit (EMD Millipore). An equal volume of glycerol was then added to a final concentration of 50% glycerol for storage at -20˚C. Protein concentration was determined using [1] BSA standards on an SDS-PAGE gel stained with Coomassie Brilliant Blue stain, and [2] A_{595} of BGG standards or PKC protein after mixing 5 μl of protein solution with 45 μl of buffer (0.05 M NaOH, 20 mM Tris) and 500 μl of Coomassie (Bradford) Protein Assay Reagent (1856209, Thermo Fisher Scientific).

Kinase Assays

The activity of purified GST-PKCα (typically 2.4 nM) towards a peptide substrate (Ac-FKKSFKL-NH_2) was assayed as described previously (207). Standard assay conditions contained (unless otherwise specified in figure legends): Ca^{2+} (200 μM free Ca^{2+} in the presence of 500 μM EGTA), 100 μM ATP, 100 μM substrate, 5 mM $MgCl_2$, 200 μM $CaCl_2$, 0.06 mg/ml BSA, and Triton X-100 (0.1 % w/v) mixed micelles containing 15 mol % PS and 5 mol % DG in 50 mM HEPES pH 7.5, 1 mM DTT. The quantities of GST-PKCα wild-type or M489V used in the assay were additionally verified post-assay by Western blot using a PKCα antibody. The dependence of PKC activity on Ca^{2+} or mol % PS was analyzed by a nonlinear least squares fit to a modified Hill equation as described (208) using GraphPad Prism version 6 (GraphPad Software). The Km for peptide substrate or ATP was fit to the Michaelis Menten equation using GraphPad Prism version 6 (GraphPad Software). The concentration of free Ca^{2+} was

calculated using a program that takes into account pH, Ca^{2+}, Mg^{2+}, EGTA, and ATP concentrations (maxchelator.stanford.edu CaMgATPEGTA program, (209)).

Structure Modeling and Molecular Dynamics Simulations

Homology models of PKCα wild-type and M489V were created using Modeller 9.16 from PDB ID: 3IW4 (residues 339 to 597). Molecular dynamics simulations were performed using GROMACS version 5.0 with the GROMOS96 53a6 force field parameter set. All titratable amino acids were assigned their canonical state at physiological pH, short-range interactions were cut off at 1.4 nm and long-range electrostatics were calculated using the particle mesh Ewald summation (210). Dispersion correction was applied to energy and pressure terms accounting for truncation of van der Waals forces and periodic boundary conditions were applied in all directions. Protein constructs were placed in a cubic box of 100 nM NaCl in simple point charge water with at least 1 nm distance between the protein construct and box edge in all directions. Neutralizing counter ions were added and steepest decent energy minimization was performed, followed by a two-step NVT/NPT equilibration. Both equilibration steps maintained a constant number of particles and temperature, and NVT equilibration was performed for 100 ps maintaining a constant volume, followed by 10 ns of NPT equilibration maintaining a constant pressure. Temperature was maintained at 37 ^{o}C by coupling protein and non-protein atoms to separate temperature coupling baths (211), and pressure was maintained at 1.0 bar (weak coupling). All position restraints were then removed and simulations were performed for 400 ns using the Nose-Hoover thermostat (212) and the Parrinello-Rahman barostat (213). Root-mean-squared fluctuation (RMSF)

analysis compared the standard deviation of the atomic position of each α-carbon in the trajectory, fitting to the starting structure as a reference frame. Images were created using PyMol version 1.7.2.3.

Chapter 3 in its entirety is published online as "Protein Kinase Cα gain-of-function variant in Alzheimer's disease displays enhanced catalysis by a mechanism that evades down-regulation." Callender JA, Yang Y, Lordén G, Stephenson NL, Jones AC, Brognard J, Newton AC in *Proc Natl Acad Sci U S A*. 2018 Jun 12;115(24). The dissertation author was the primary investigator and author of this work.

FIGURES AND TABLES

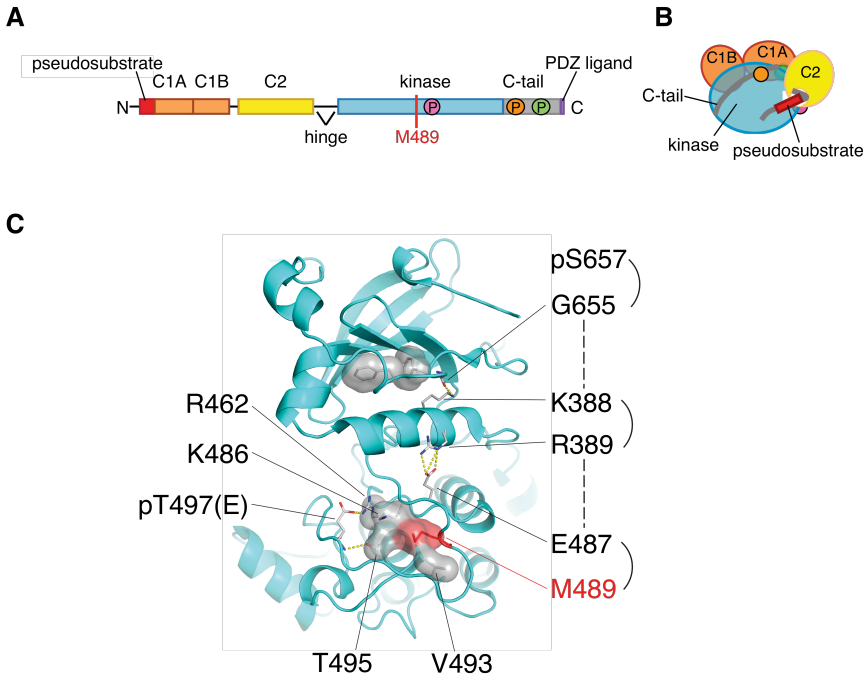

Figure 3.1: Alzheimer's Disease-associated PKCα mutation in key region of catalytic domain. [A] Primary structure of PKCα showing pseudosubstrate (red), C1A and C1B domains (orange), C2 domain (yellow), kinase domain (cyan), C-terminal tail (grey) and PDZ ligand (purple). Indicated are the three processing phosphorylation sites, Thr497 (magenta circle) in the activation loop and Thr638 (orange circle) and Ser657 (green circle) in the C-terminal tail. [B] Cartoon representation showing autoinhibitory constraints in the full-length inactive form of PKCα wherein the pseudosubstrate occupies the substrate binding cavity, an interaction locked in place by the C2 domain. [C] Structure of PKCα kinase domain (PDB 3IW4) showing position of Met489 (red space filling) in the activation loop; note this structure has a Glu at the position of the activation loop phosphorylation site (pT497(E)). Indicated in stick representation is the network of interactions from the activation loop to the C-terminal tail that involves a salt bridge from Glu487 in the activation loop to Arg389 in the C-helix and H-bonding between the Lys388 in the C-helix to the main chain of Gly655 in the C-terminal tail; H-bonds and salt bridges are indicated by yellow dots. Gly655 is in a conserved FXXF motif that directly precedes the hydrophobic phosphorylation site (phospho-Ser657); the two Phe are indicated in grey space filling model. Residues that pack into the activation loop (Arg462, Lys486, Val493, and Thr495) are also presented in grey space filling model.

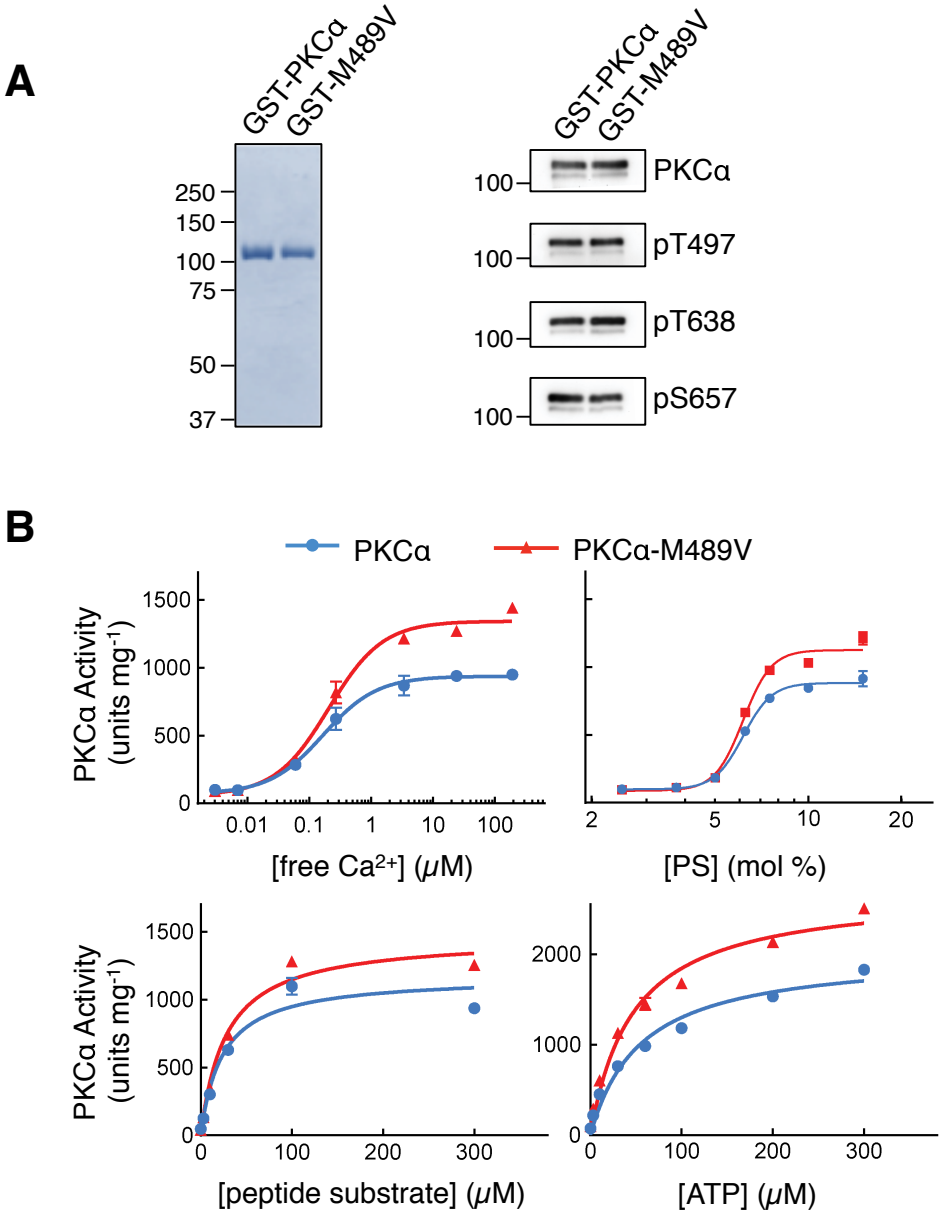

Figure 3.2: Purified PKCα-M489V displays higher V_{max} than wild-type PKCα under activating conditions. [A] Coomassie blue-stained SDS-PAGE gel of purified GST-PKCα wild-type and GST-PKCα M489V (left). Western blot of pure proteins probed with antibodies for total PKCα, or with phospho-specific antibodies to the priming phosphorylation sites, pT497, pT638, and pS657 (right). [B] The activity of PKCα wild-type (blue) or M489V (red) (typically 2.4 nM) measured as a function of Ca^{2+}, phosphatidylserine (PS), peptide substrate, or ATP concentration. Data are graphed in units (nmol phosphate per minute) per mg GST-PKC. Data represent the average ± S.E.M. of triplicate samples.

Table 2.1: Kinetic values for *in vitro* kinase assays using purified PKCα or PKCα-M489V.

Kinetic values from the data shown in Figure 2B are listed. Data represent the average ± S.E.M. of triplicate samples. Unless otherwise indicated in the figure legends, the standard reaction component concentrations were as follows: 200 μM free Ca^{2+}, Triton X-100 mixed micelles containing 5 mol% diacylglycerol and 15 mol% phosphatidylserine, 100 μM peptide substrate, and 100 μM ATP. V_{max} is obtained from the experiment varying ATP concentration (all other components are as noted for the standard reaction). V_{max} is reported as units per mg GST-PKC where one unit is defined as one nmol phosphate hydrolyzed per minute.

	Ca^{2+}_{50} (μM)	PS_{50} (mol%)	$Km_{substrate}$ (μM)	Km_{ATP} (μM)	V_{max} (units mg^{-1})
PKCα	0.17 ± 0.05	6.16 ± 0.05	24 ± 5	55 ± 8	(2.0 ± 0.2) x 10^3
PKCα-M489V	0.21 ± 0.07	6.16 ± 0.06	28 ± 4	47 ± 6	(2.7 ± 0.2) x 10^3

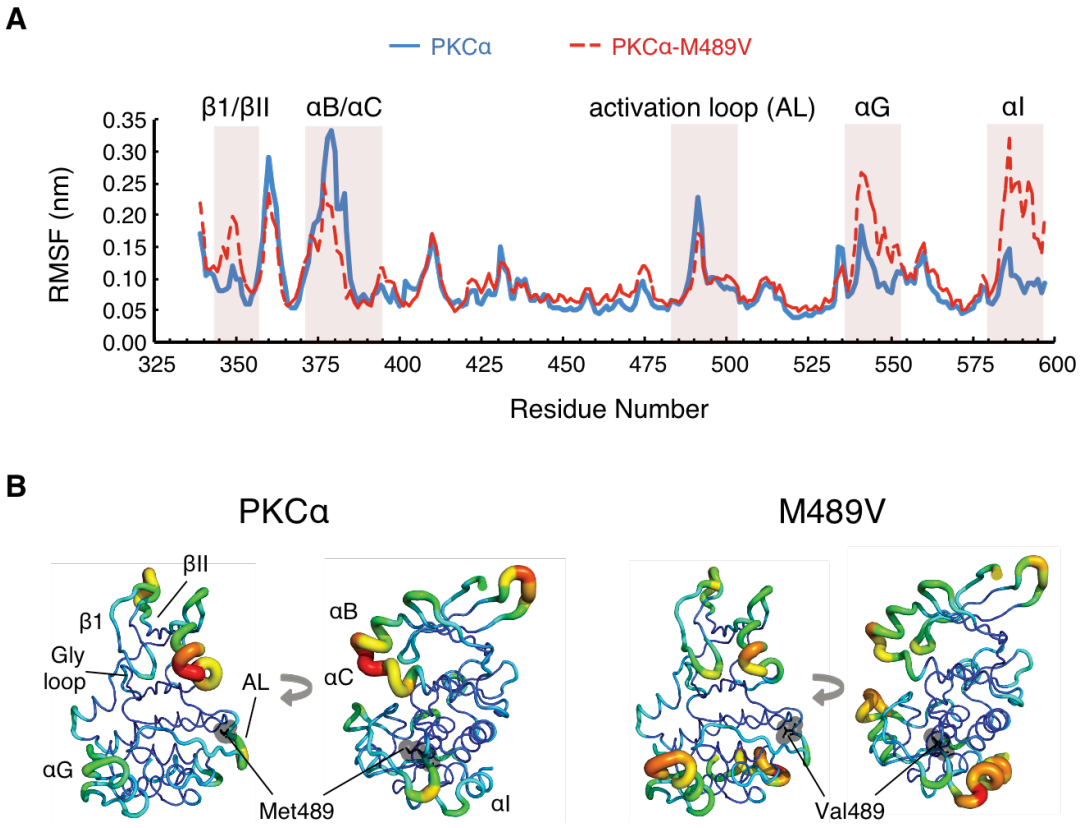

Figure 3.3: M489V mutation causes key alterations in the dynamics of the kinase domain structure. [A] Molecular dynamics simulations showing altered flexibility around the ATP binding site, αG helix and αI helix of the M489V variant. Root-mean-squared fluctuations (RMSF) of each residue are shown [A] graphically and [B] structurally, with width and color of the ribbon corresponding to the level of fluctuations observed. Key regions are highlighted as is the residue at position 489.

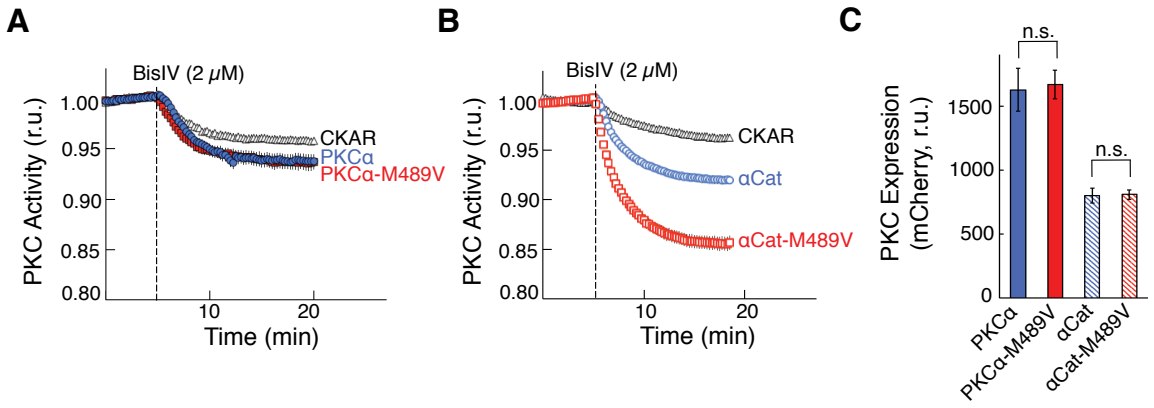

Figure 3.4: Basal activity of wild-type and PKCα-M489V is the same, but removal of regulatory moiety unmasks enhanced activity of the M489V kinase domain.
[A] COS7 cells overexpressing CKAR alone (empty triangles) or co-expressing CKAR and full-length mCherry-PKCα wild-type (blue circles) or M489V (red squares) were exposed to 2 μM Bis IV and the change in FRET monitored. ($n \geq 20$ from at least three separate biological replicates). [B] COS7 cells overexpressing CKAR alone (empty triangles) or co-expressing CKAR and the catalytic domain of PKCα (αCat) wild-type (empty blue circles) or M489V (empty red squares). 2 μM Bis IV was added and the change in FRET was monitored. ($n \geq 54$ from at least three separate biological replicates). For both [A] and [B], data were normalized to the first five minutes prior to Bis IV addition and are graphed as average ± S.E.M. Note that in some cases, the error bars are obscured by the symbols. [C] Quantification of average mCherry-PKC expression for each overexpressed PKC depicted in panels [A] and [B]. Data are graphed as average mCherry intensity ± S.E.M. (n.s., not significantly different using a Student's t test).

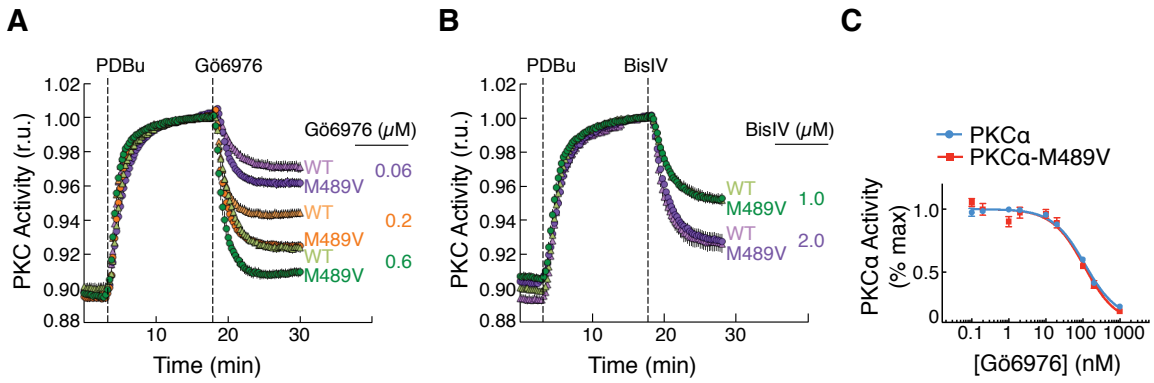

Figure 3.5: PKCα-M489V in cells is more sensitive to Gö6976 inhibition.
[A-B] COS7 cells overexpressing mCherry-PKCα wild-type or M489V and CKAR were exposed to PDBu (200 nM) followed by sub-saturating amounts of [A] Gö6976: 0.06 μM (purple), 0.2 μM (orange), or 0.6 μM (green) or [B] Bis IV: 1 μM (green) or 2 μM (purple). Data were normalized to the maximal FRET after PDBu addition. ($n \geq 14$ from three separate biological replicates). Data are depicted as average ± S.E.M.; note that in some cases, the error bars are obscured by the data points. [C] Purified GST-PKCα wild-type (blue) or M489V (red) activity in the presence of Gö6976. Data represent the average ± S.D. of triplicate samples.

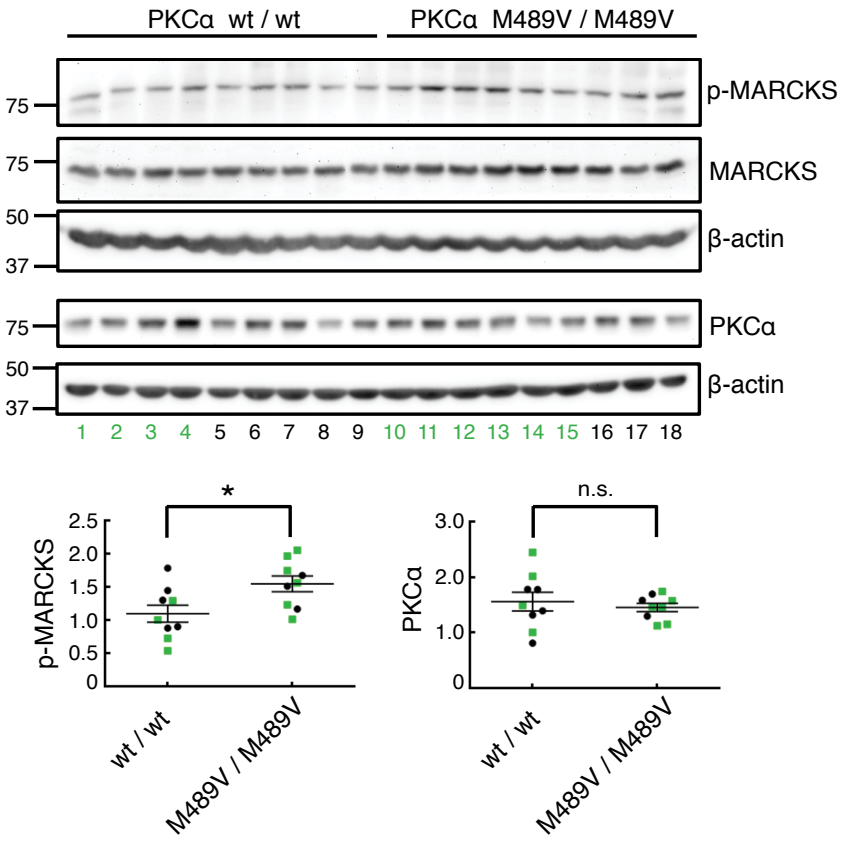

Figure 3.6: Phosphorylation of MARCKS is increased in the brains of PKCα-M489V mice. Western blot of lysates of whole brain obtained from nine male and female three-month-old wild-type (lanes 1-4, males; lanes 5-9, females) or nine male and female genome-edited mice containing a homozygous PKCα-M489V mutation (lanes 10-15, males; lanes 16-18, females). Western blots were probed with antibodies specific to a known PKC phosphorylation site on MARCKS (Ser 159/163) or to total PKCα (top). Bands were quantified using densitometry and the phospho-MARCKS signal was normalized to total MARCKS signal and PKCα signal was normalized to its β-actin loading control. Normalized data from the depicted Western blot were plotted (bottom) as average normalized intensity ± S.E.M. (*, $p<0.05$; n.s., not significantly different using a Student's t test). Males indicated in green squares and females in black circles.

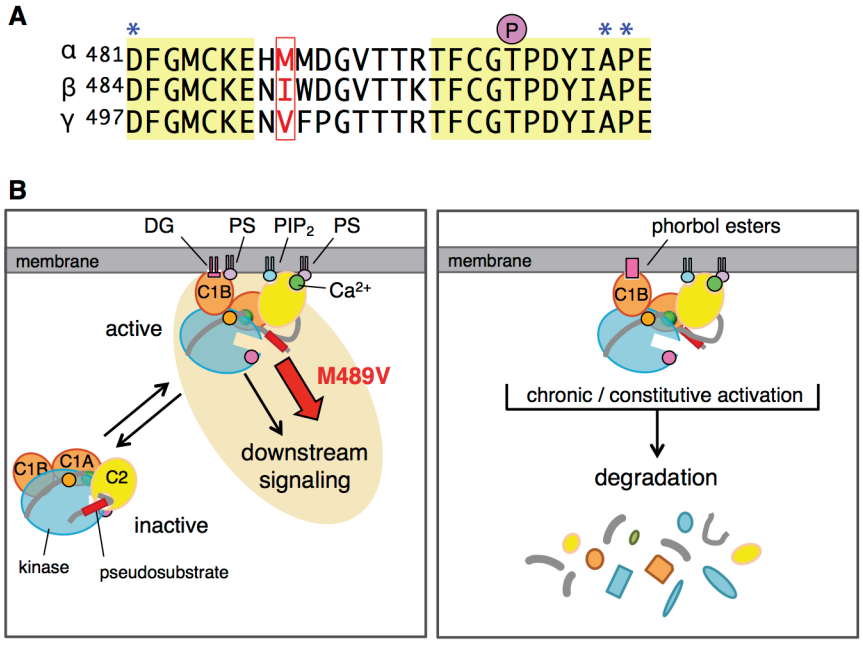

Figure 3.7: PKCα-M489V mutation increases PKCα signaling output without causing PKCα degradation. [A] Alignment of the activation loop of conventional PKC isozymes showing conserved regions, including the flanking DFG and APE motifs, (yellow); residues that frequently harbor loss-of-function mutations in cancer (blue asterisk); and the variable residue at the position corresponding to Met489 in PKCα (red). [B] Left: model depicting normal PKCα signaling, in which the enzyme is in an autoinhibited and stable conformation that is transiently and reversibly activated. Right: model showing the homeostatic downregulation of PKCα after either chronic activation by phorbol esters (which trap PKC in an open and labile conformation) or as a result of mutations that disrupt autoinhibitory constraints to constitutively activate PKCα signaling. Rather than promoting the constitutively active form of PKCα that would be subsequently degraded, the PKCα-M489V mutation instead enhances the normal signaling output of the enzyme without leading to its degradation (left). Domains and phosphorylation sites (small circles) are color coded as in Figure 1.

CHAPTER 4

STRUCTURAL REGULATION OF PROTEIN KINASE Cα: AUTOINHIBITORY INTRAMOLECULAR CONTACTS AND TYROSINE PHOSPHORYLATION

ABSTRACT

Conventional protein kinase C (PKC) family members are reversibly activated by binding to the second messengers Ca^{2+} and diacylglycerol, events that break autoinhibitory constraints to allow the enzyme to adopt an active, but degradation-sensitive, conformation at the plasma membrane. The Ca^{2+}-regulated plasma membrane sensing C2 domain of conventional PKC isozymes plays a key role in controlling both autoinhibition and the movement of PKC on and off the plasma membrane, with impaired C2 function accounting for one of the many mechanisms of PKC loss-of-function in cancer. In this study, we establish two mechanisms through which the C2 domain of the conventional isozyme PKCα regulates its signaling: [1] intramolecular contacts between the C2 domain and the C-terminal tail of are crucial for autoinhibition, and [2] phosphorylation of a conserved tyrosine residue in the C2 domain of conventional PKCα (Tyr195) sustains the signaling output of PKC by promoting plasma membrane association. We use a combination of live-cell FRET-based PKC translocation experiments to show that mutation of residues that engage in intramolecular contact between the C2 domain and C-tail "open" up PKCα and promote unmasking of membrane-sensing domains. We use FRET-based translocation and activity experiments to show that tyrosine phosphorylation of PKCα promotes plasma membrane localization, and that introducing a Y195F mutation ablates this effect. A phospho-antibody specific for this site reveals the transient nature of this phosphorylation, which can only be observed in active PKCα at the plasma membrane. Taken together, our results suggest that activation of PKC breaks intramolecular interactions to unmask the C2 domain, thus

allowing for phosphorylation on Tyr195, a modification that promotes the membrane association and thus activity of PKCα. This residue is conserved among all conventional PKCs, suggesting a key regulatory mechanism for this class of PKC isozymes. Consistent with this, we show that a cancer-associated mutation at this site in the related conventional isozyme PKCβII (Y195H) prevents agonist-dependent activation, providing another mechanism for loss-of-function of PKC in cancer.

INTRODUCTION

The PKC family consists of nine isoforms organized into three subfamilies: conventional (PKCs α, β, and γ); novel (PKCs δ, ε, θ, and η); and atypical (PKCs ζ and ι) (214). Each PKC consists of a kinase domain that is relatively conserved across subfamilies, a carboxy-terminal tail that is conserved across subfamilies, and a regulatory domain that differs between subfamilies (20, 215). PKC regulatory domains include the C1 domains, which bind diacylglycerol, and the C2 domain, which bind anionic lipids in a Ca^{2+} dependent manner (216-220). The pseudosubstrate domain maintains PKC in an inactive conformation by occupying the active site of the kinase domain. All PKC isoforms are immature when first translated and must undergo a series of stabilizing phosphorylations to produce a fully mature and catalytically competent PKC (20, 215). The three sites of constitutive phosphorylation are the activation loop, the turn motif, and the hydrophobic motif (151, 221, 222). A fully processed and phosphorylated PKC remains in the cytosol in its inactive, auto-inhibited form. In this conformation, only one of the C1 domains is available to bind diacylglycerol (31) and the pseudosubstrate binds

the active site. Signals that cause membrane lipid hydrolysis recruit PKC to the membrane, where the C1B domain binds diacylglycerol and phosphatidylserine, and the C2 domain binds phosphatidylinositol-4,5-bisphosphate (PIP_2). Once at the membrane, the pseudosubstrate vacates the active site, yielding an open and active enzyme that can propagate downstream signaling.

Many crystallographic studies have contributed to the clarification of the structure of PKC. The kinase domain alone has been crystallized for PKC α, βII, θ, and ι (50-54). The C2 domain has been crystallized for PKC α, βII, δ, η, and ε (55-60). The C1 domains of PKC α, γ, and δ have been crystallized as well (61-63). The structure of full-length PKC was not solved until 2011, when Hurley and colleagues successfully crystallized full-length rat PKC βII and resolved the C1B, C2, and kinase domain (64). Using the crystal packing data from this study, we observed a pose in the crystal lattice in which the C2 domain clamps against the catalytic domain, leading us to hypothesize that this allows the C2 domain to autoinhibit signaling output in the inactive state. We tested the validity of the pose observed in the crystal structure by mutating residues predicted to lie along this interface and using rate of plasma membrane translocation in live cells to show that these mutations broke the intramolecular contacts and "opened" PKCβII (38). Given the high degree of homology between the conventional PKC isozymes, it is likely that they share this mechanism of structural autoinhibition. Indeed, a study recently published by Igumenova and colleagues used molecular modeling and NMR spectroscopy to propose that the C2 domain of PKCα interacts with the C-terminal tail in the autoinhibited form of the enzyme (65). Based on our studies establishing the interface through which PKCβII

engages in autoinhibition, we produced a model of how we predict the C2 domain of PKCα would interact with the catalytic domain by docking the C2 domain against the kinase domain (**Figure 4.1C**). Shown in red are the residues mutated by Igumenova and colleagues. In this study, we seek to test the Igumenova model of PKCα autoinhibition by introducing their interface mutations (**Figure 4.1A, C** red) into PKCα overexpressed in live cells and observing plasma membrane translocation, as was done to support our autoinhibition model for PKCβII.

In addition to the intramolecular interactions between unmodified amino acid sidechains, we also investigated a different aspect of PKCα regulation: tyrosine phosphorylation. Although many studies have addressed the role of phosphorylation at the activation loop, the turn motif, and the hydrophobic motif sites, relatively little is known about tyrosine phosphorylation in PKC. Previous studies have supported that tyrosine phosphorylation enhances the activity of PKCδ (223, 224) and PKCα (225, 226). We used PhosphoSite Plus to compare the amount of studies referencing different phosphorylation sites in PKCα (**Figure 4.1B**) (227). The most frequently annotated PKCα phosphorylation in PhosphoSite is pY195 in the C2 domain, with a close second being the oft-referenced phosphorylation at the activation loop (pT497). However, every reference containing PKCα-pY195 is an unbiased phosphoproteomics screen, and no targeted studies have investigated the role of phosphorylation at this site to date. Therefore, we sought to investigate the role of tyrosine phosphorylation in general and phosphorylation of Tyr195 specifically in PKCα signaling. Overall, we address two questions relating to the structural regulation of PKCα signaling: [1] do residues in the

C2 domain and C-terminal tail interact to autoinhibit PKCα, and [2] what is the function of phosphorylation of Tyr195 in PKCα.

RESULTS

PKCα autoinhibition is regulated by intramolecular contacts

Previous studies conducted on PKCα, PKCβII, and PKCγ established that membrane-binding surfaces of the C1 domains are masked by intramolecular interactions in inactive forms of the enzymes (228-230). Therefore, the sensitivity of C1 domains to their activators can be used to probe the conformational state of PKCα in live cells. Igumenova and colleagues recently modeled a predicted interface between the C2 domain and the C-terminal tail of PKCα, and these intramolecular contacts are predicted to contribute to autoinhibition in the inactive form of the enzyme (65). In order to test this model, we generated YFP-PKCα variants with mutations along this interface and observed their translocation to the plasma membrane (**Table 4.1**).

We used FRET to monitor the translocation of YFP-PKCα to the CFP-tagged plasma membranes in COS7 cells (**Fig. 4.2**). We initiated membrane translocation by treating the cells with a potent C1 domain agonist, phorbol ester PDBu. In the simplest model (see Methods), the translocation rate is mono-exponential and depends on the sum of the on and off-rate constants, ($k_{on}+k_{off}$), while the total translocation level is proportional to the $(1+k_{off}/k_{on})^{-1}$ term.

Our first finding was that, unlike the translocation kinetics of the related PKCβII, the translocation kinetics of wild-type PKCα are biphasic and can be fit with a sum of exponential and linear terms (**Figure 4.2B**). The first component is "fast," with an apparent rate constant 1.10 ± 0.06 min^{-1}; the second component is "slow," with an apparent rate constant of $(4.1 \pm 0.3) \times 10^{-3}$ min^{-1}. One plausible interpretation is that inactive PKCα in the cell exists as two conformational states with a distinct kinetic response to C1 agonists. Our data suggest that mutations at the C2-C-terminal tail interface alter this conformational equilibrium.

Alanine mutations of Ser657, Phe656, and the aromatic residues at the predicted C2-C terminal tail interface eliminated the *slow* translocation phase (**Figure 4.2B**). All three variants: S657A, F656A, and FYYW showed mono-exponential saturatable translocation kinetics with the rate constants of 1.20 ± 0.04, 1.22 ± 0.05, and 1.28 ± 0.03 min^{-1}, respectively. Western blot analysis of cell lysates (**Figure 4.2C**) showed that these variants have very low phosphorylation levels of the turn motif, Thr638, whose phosphate group anchors the C-terminal tail domain to the N-terminal lobe of the kinase (50, 54, 64). Because S657A and F656A mutants purified from insect cells were phosphorylated at Thr638 (data not shown), we concluded that these variants are sensitive to phosphatases and undergo rapid dephosphorylation in mammalian cell lysates, as recently published for PKCβ mutants(48). The FYWW variant was not phosphorylated at Thr638 in either cell lysates or purified form. The observed membrane translocation behavior is therefore indicative of the "open" state of the kinase, in which the C1 membrane binding sites are partially unmasked. Stensman and colleagues (229)

reported similar observations, with respect to the turn motif phosphorylation and DAG-stimulated membrane translocation, on the S657A variant of PKCα. The apparent translocation rate constant of the "fast" conformation of wild-type PKCα was ~90% of that observed for the aromatic/pSer657 variants, indicating that the "fast" conformer has highly accessible C1 membrane binding sites.

In contrast to the aromatic/pS657 mutations, disruption of the salt bridge between Asp652 and lysines of the lysine-rich cluster eliminated the *fast* translocation phase (**Figure 4.2D**). Our interpretation is that the mutation of charged residues preferentially stabilizes the "slow" conformation of PKCα. In this conformation, the C2 domain would clamp over the active site similarly to the structure for PKCβII, such that mutations of this residue breaks ionic interactions between the C2 and kinase domain (231). Based on the translocation levels alone, we rank the (k_{off}/k_{on}) ratios as D652K << KK ≈ DKK. With respect to the effective membrane translocation rate constants ($k_{off}+k_{on}$), the order is D652K (0.23 ± 0.07 min^{-1}) ≈ DKK (0.22 ± 0.01 min^{-1}) < KK (0.70 ± 0.01 min^{-1}). Previous studies demonstrated that mutations of lysine residues of the lysine-rich cluster increase the kinetic off-rate constant due to disrupted binding to PtdIns(4,5)P_2 (232). If the membrane dissociation behavior of the KK and DKK variants is not significantly different, the only condition under which we can obtain comparable effective rate constants for D652K and DKK is when k_{on}(D652K) > k_{on}(DKK). This means that the DKK mutation restores the stabilizing effect of electrostatic interactions in the "slow" conformer of PKCα.

We noted that the apparent translocation rate constant of the PKCα-D652K variant, 0.23 ± 0.07 min^{-1}, is similar to that observed for the wild-type PKCβII, 0.19 ± 0.01 min^{-1} (230, 231). In the βII isoform, the salt bridge between Glu655 (the equivalent of D652 in α) and Lys205 of the lysine-rich cluster contributes significantly to the stabilization of the inactive state (38). We introduced K205E and charge reversal D652K/K205E mutations into PKCα and characterized the membrane translocation behavior of the variants. The results were very similar to those obtained for the D652K, KK and DKK trio (compare **Figures 4.2D** left and middle), producing comparable ($k_{on}+k_{off}$) values for the D652K (0.23 ± 0.07 min^{-1}) and D652K/K205E (0.28 ± 0.01 min^{-1}) variants, and a larger value for the K205E variant (1.05 ± 0.04 min^{-1}). Taken together, these data indicate that electrostatic interactions between the lysine residues of the lysine-rich cluster and the C-terminal tail contribute to the stabilization of the "slow" inactive conformation of PKCα. An interesting observation is that charge reversal of Asp652 to Lys resulted in a significant increase of the steady-state translocation levels compared to other variants. This was not observed when Asp652 was mutated to Ala (**Figure 4.2D**, right), suggesting that the introduction of a positive charge at this position enhanced interactions of PKC with anionic phospholipids.

PKCα and PKCβII exhibit different translocation behavior

The closely-related conventional PKC isozymes PKCα and PKCβII both visibly translocate to the plasma membrane in cells as a result of binding the same second messengers: Ca^{2+}, PIP_2, diacylglycerol, and phosphatidylserine. However, the

translocation behavior exhibited by PKCα was highly divergent from that of PKCβII. As discussed above, PKCα exhibited a biphasic translocation behavior characterized by a "fast" component (rate constant = 1.10 ± 0.06 min^{-1}) and a "slow" component (rate constant = (4.1 ± 0.3) x 10^{-3} min^{-1}). In contrast, PKCβII translocation exhibited a monophasic translocation behavior, with a rate constant of 0.19 ± 0.01 min^{-1} (31, 38). Indeed, the translocation behaviors also differ in the extent of visible translocation after 15 minutes of PDBu stimulation (**Figure 4.3**). We overexpressed either wild-type YFP-PKCα or wild-type YFP-PKCβII in COS7 cells and compared the extent of translocation after 15 minutes of PDBu treatment. The cell images showed that PKCβII exhibits more robust translocation to the plasma membrane when compared to PKCα, indicating that there may be differing mechanisms or cellular processes contributing to the k_{on} and/or k_{off} of these two enzymes.

PKCα translocation to the plasma membrane is controlled by Tyrosine phosphorylation

While p-Tyr195 is the most frequently identified PKCα phosphorylation in unbiased phosphoproteomics studies, the role this phosphorylation plays in the regulation of PKCα signaling is unknown (**Figure 4.1B**). To investigate this further, we observed YFP-PKCα translocation to the plasma membrane in COS7 cells.

First, we overexpressed either YFP-PKCα wild-type or a non-phosphorylatable Y195F variant in COS7 cells along with CFP tagged to the plasma membrane. We initiated translocation with PDBu and measured the change in FRET between these two

fluorophores (31). Representative cell images are depicted in **Figure 4.4A**, with quantification of translocation depicted in **Figure 4.4B**. Both wild-type (black) and PKCα-Y195F (blue) translocated to the plasma membrane to a similar extent upon PDBu stimulation. Since the upstream kinase that phosphorylates this residue is unknown, we increased the amount of pY195 by pre-treating the cells with the tyrosine phosphatase inhibitor peroxyvanadate ($NaVO_4$). Pre-treatment with peroxyvanadate caused a robust increase in the amount of wild-type PKCα translocation to the plasma membrane (red), which can be seen in both the cell images in **Figure 4.4A** and the quantifications in **Figure 4.4B**. In contrast, the PKCα-Y195F variant did not exhibit the same increase in translocation after peroxyvanadate pretreatment (orange), although there was a relative increase in translocation to the plasma membrane compared to PKCα-Y195F without peroxyvanadate. It should be noted that peroxyvanadate treatment will nonspecifically increase phosphorylation of any exposed tyrosines present in PKCα. Therefore, comparing the wild-type and PKCα-Y195F data is crucial to distinguish the contribution of phosphorylation at Tyr195. These data indicate that, while tyrosine phosphorylation in general promotes PKCα retention on the plasma membrane, phosphorylation at Tyr195 significantly contributes to this retention.

p-Tyr195 affects C2 domain sensing of plasma membrane

Tyr195 is situated along the predicted autoinhibitory interface between the C2 domain and the C-terminal tail, according to modeling by Igumenova and colleagues (see **Figure 4.1C**). Therefore, we asked if the Y195F variant was preventing PKCα

translocation to the plasma membrane via [1] promoting autoinhibitory intramolecular contacts, or [2] affecting the C2 domain's innate ability to act as a plasma membrane sensor. We overexpressed an isolated YFP-PKCα C2 domain, wild-type or containing a Y195F mutation, and stimulated movement towards the plasma membrane by raising cytosolic Ca^{2+} levels with thapsigargin (**Figure 4.4C**). Wild-type PKCα C2 domain translocated to the plasma membrane in response to Ca^{2+} binding (black), and introduction of the Y195F mutation dramatically reduced this translocation (blue). Similarly to the full-length protein, pretreatment with peroxyvanadate to promote p-Tyr195 in the isolated C2 domain caused a significant increase in translocation to the plasma membrane upon Thapsigargin stimulation (red). Peroxyvanadate pretreatment increased the amount of translocation exhibited by the Y195F C2 domain (orange), although not to the extent exhibited by the wild-type C2 domain. Therefore, our findings with the isolated C2 domain recapitulate what was seen with the full-length protein: while phosphorylation of other tyrosine residues in the C2 domain (of which there are three) appear to contribute to plasma membrane sensing, Tyr195 specifically plays a significant role in this process.

PKCα-Tyr195 phosphorylation requires tyrosine phosphatase inhibition and unmasking of the C2 domain.

According to our model of how the C2 domain interfaces with the C-terminal tail in the inactive form of the enzyme, Tyr195 would be masked when PKCα is autoinhibited (see **Figure 4.1C**). In order to test this, we used an antibody specific for

phospho-Tyr195 (pY195) to investigate what conditions would allow for phosphorylation of this site in COS7 cells (**Figure 4.5**). We overexpressed HA-tagged wild-type or PKCα-Y195F in COS7 cells, treated with PDBu to lock PKC in an "open" conformation, then lysed the cells and probed whole cell lysates with the phospho-antibody (**Figure 4.5A**, left). Under normal conditions, no phosphorylation signal was detected, even with PDBu treatment. However, when pre-treating with peroxyvanadate to inhibit tyrosine phosphatase activity ($NaVO_4$), we detected phosphorylation of Y195, but only in the presence of PDBu. This phosphorylation signal was more clear when we immunoprecipitated the HA-PKCα and probed for pY195 (**Figure 4.5A**, right). There is a clear pY195 signal that only appears when [1] PKCα is locked in an "open" state, and [2] tyrosine phosphatases are inhibited.

In order to test if the phosphorylation of Y195 in the presence of PDBu is due to activation of PKCα or to the unmasking of the C2 domain, we overexpressed isolated YFP-αC2 domain in COS7 cells and treated with peroxyvanadate to stimulate accumulation of pY195 (**Figure 4.5B**). We observed pY195 in the isolated C2 domain in the presence of peroxyvanadate, and this signal was partially ablated by pretreatment with the promiscuous kinase inhibitor staurosporine. These data support that PDBu allows for the accumulation of pY195 in the full-length protein due to the unmasking of the C2 domain that takes place as a result of PDBu binding the C1B domain.

PKCα-Tyr195 is not phosphorylated by Src-family kinases that are targeted by PP2 inhibition.

Based on the motif surrounding Y195, we sought to determine if any Src family kinases were responsible for phosphorylation of this site (**Figure 4.6**). We overexpressed HA-tagged PKCα wild-type or Y195F in COS7 cells and treated the cells for one hour with the general Src family kinase inhibitor PP2, PP3 (a negative control for PP2), or staurosporine. We then treated with peroxyvanadate ($NaVO_4$) for 30 minutes prior to lysing, and PDBu for 15 minutes prior to lysing. HA-PKCα was immunoprecipitated and probed for p-Y195. As seen previously, pY195 was only detectable in the presence of both peroxyvanadate and PDBu. Staurosporine blocked this signal, indicating that a kinase targeted by this highly promiscuous inhibitor is responsible for phosphorylating this site. However, neither PP2 nor PP3 reduced the pY195 signal, indicating that the kinase of interest is not one that is targeted by PP2 inhibition.

Cancer-associated mutation PKCβII-Y195H is loss-of-function

Tyr195 is highly conserved among conventional PKC isozymes (**Figure 4.7A**), indicating that it is crucial for proper regulation of conventional PKC signaling. Indeed, consulting the cBioPortal database reveals a cancer-associated mutation (Y195H) at this site in PKCβII (233, 234). In order to test if this disease-associated amino acid substitution has a functional effect, we overexpressed mCherry-tagged PKCβII, either wild-type or Y195H, in COS7 cells along with CKAR and stimulated with UTP and with PDBu (**Figure 4.7B**). The Y195H mutation ablates PKCβII's response to the physiological agonist UTP, and is therefore loss-of-function. This is consistent with the

fact that, to date, every cancer-associated mutation in PKC has either been loss-of-function or has had no effect (11).

Neither cancer-associated PKCβII-Y195H nor PKCα-Y195F exhibit neomorphic signaling at the Golgi apparatus.

When observing the cell images for the translocation experiments with PKCα-Y195F (**Figure 4.4**) and the CKAR experiments with PKCβII-Y195H (**Figure 4.7**), we noted that these variants translocate to the Golgi to a greater degree than wild-type upon PDBu stimulation. This indicates that mutating Y195 lessens the C2 domain's ability to guide translocation to PIP2 in the plasma membrane, thus resulting in PKC movement being determined by the C1B domain's affinity for the highly concentrated pool of diacylglycerol in Golgi membranes (235). This is further supported by our finding that the isolated C2 domain is less able to sense the plasma membrane when it contains the Y195F mutation (see **Figure 4.4C**).

In order to determine if these variants exhibit neomorphic signaling at the Golgi, we took advantage of a Golgi-targeted CKAR construct (170) (**Figure 4.8**). We stimulated with UTP and then inhibited with Bis IV. We first observed that PKCβII-Y195H is less active at the Golgi compared to wild-type, which recapitulates our findings with cytosolic CKAR. Next, we observed that PKCα-Y195F exhibited the same amount of activity at the Golgi as wild-type. Thus, neither the cancer-associated PKCβII-Y195H nor the non-phosphorylatable PKCα-Y195F mutant exhibit neomorphic signaling at the Golgi when compared to wild-type. The increased translocation to the Golgi seen in cell

images is likely an artifact of PDBu stimulation, and not reflective of how these variants behave under physiologically relevant scenarios.

DISCUSSION

We have investigated two distinct mechanisms through which PKCα signaling is regulated: [1] autoinhibition of signaling output using intramolecular contacts between the C2 domain and the C-terminal tail of the catalytic domain, and [2] phosphorylation of a conserved tyrosine in the C2 domain that promotes plasma membrane localization and activation (**Figure 4.9**). These two mechanisms preferentially affect the k_{on} and k_{off} of PKC membrane binding that is required for activation, respectively. Both de-autoinhibition and retention on the plasma membrane affect the equilibrium between cytosolic, inactive PKCα and membrane-bound, active PKCα, thus regulating the global signaling output of this enzyme.

We used mutagenesis followed by observation of the rate and extent of translocation to the plasma membrane to show that several residues in the C2 domain and the C-terminal tail participate in hydrophobic and electrostatic interactions in the inactive form of PKCα (**Figure 4.9A**). A large number of studies support that domains other than the pseudosubstrate contribute to PKC autoinhibition (64, 231, 236-238), including most recently a study published by Igumenova and colleagues supporting a model of PKCα autoinhibition in which the C2 domain interacts with the C-terminal tail (65). Based on this model, we selected mutated residues that were predicted to lie upon this intramolecular interface. Our translocation experiments support the autoinhibition model

put forth by Yang et al. (**Figure 4.9A**, mode ii). However, the biphasic nature of phorbol ester-induced PKCα translocation (which is not observed during PKCβII translocation) indicates that PKCα is present in the cell in two distinct conformational states, rather than the single state previously hypothesized by Igumenova and colleagues. Since the Ca^{2+}-binding regions of the C2 domain are highly accessible to solvent in the model presented in Yang et al., it is likely that this represents the dominant conformation of PKCα that is responsible for the "fast" membrane translocation behavior that we observe (**figure 4.9A**, mode ii). The "slow" conformation of PKCα may be similar to that of PKCβII, whose C2 domain interacts not only with the C-terminal domain through the Glu255-Lys205 salt bridge (231), but also clamps onto the C-lobe of the kinase domain using the Ca^{2+}-binding loop region (**Figure 4.9A**, mode i). It may also be likely that the biphasic translocation is due to two pools of PKCα that contain different post-translational modifications that affect plasma membrane affinity. Indeed, we have shown that tyrosine phosphorylation enhances PKCα's translocation to the plasma membrane (see **Figure 4.4**), so it is possible that these different states of PKCα differ in their level of tyrosine phosphorylation. The observed differences between the membrane translocation behavior of PKCβII (mono-exponential, "slow") and PKCα (biphasic, "fast" and "slow") illustrate both the isoform-specific differences and conformational plasticity of this class of enzymes. We note that the concentration of Ca^{2+} required for half-maximal activation of PKCα is 25-fold lower than that required for half-maximal activation of PKCβII, likely reflecting the enhanced accessibility of the C2 domain in the "fast" conformation adopted by PKCα but not PKCβII (239). Further supporting that divergent mechanisms regulate

PKCα and PKCβII signaling, we note that in addition to the rates of translocation differing, the degree of translocation to the plasma membrane upon PDBu stimulation is visibly different when comparing these two closely-related enzymes (**Figure 4.3**).

We also establish that a previously uncharacterized phosphorylation site in the C2 domain of PKCα plays a crucial role in the regulation of PKCα translocation and localization (**Figure 4.9B**). We show that general tyrosine phosphorylation promotes PKCα retention on the plasma membrane, as supported by the robust increase in plasma membrane translocation in the presence of peroxyvanadate. Tyr195 specifically plays an important role in this process, as this effect is ablated by introducing a non-phosphorylatable Y195F variant (**Figure 4.9B**, mode iii). Phosphorylation of this site takes place when the C2 domain is exposed in the "open" form of PKCα, as supported by the finding that PDBu is required to observe this phosphorylation on a western blot (**Figure 4.9B**, mode ii). Based on our hypothesis that the C2 domain interfaces with the kinase domain in the inactive form of PKCα, Tyr195 would be masked when PKCα is in the cytosol (**Figure 4.9B**, mode i). pY195 is also transient and easily removed by tyrosine phosphatases, as shown by the finding that—even when PDBu is present—peroxyvanadate is always necessary in order to observe phosphorylation at this site. These results may be explained if we hypothesize that the kinase phosphorylating this site does so at the plasma membrane. Any kinases that are inhibited by PP2 can be ruled out, as PP2 treatment did not decrease the pY195 signal seen on a western blot. It should be noted that, as the upstream kinase that phosphorylates this site remains unknown, these experiments were conducted in the absence of stimulation of this kinase. Therefore,

identifying the upstream kinase is a crucial future direction, as stimulation of this kinase may change the conditions required to observe phosphorylation at this site.

Lastly, we show that a cancer-associated mutation at Tyr195 in PKCβII is loss-of-function in that it completely ablates any response to UTP stimulation. This establishes that Tyr195 is a crucial residue that regulates the signaling of both PKCα and PKCβII. These studies also support PKC's general role as a tumor suppressor by identifying yet another cancer-associated mutation that is loss-of-function (11, 180).

In summary, these studies widen our view of how PKCα signaling output is regulated. Our data suggest that—like the related PKCβII—the C2 domain serves to autoinhibit the inactive form of the enzyme by interacting electrostatically with the C-terminal tail of the catalytic domain. This autoinhibition serves to mask the positively-charged lysine-rich cluster until Ca^{2+} binds and facilitates bridging to anionic phospholipids in the plasma membrane. However, our data also highlight the differences between PKCα and PKCβII translocation to the plasma membrane, which requires further study to elucidate the mechanisms contributing to these variable behaviors. Finally, we show for the first time that a previously unstudied phosphorylation in the C2 domain of PKCα promotes retention on the plasma membrane, and that this residue is crucial for proper PKCα and PKCβII signaling. These studies all serve an ultimate goal of understanding the interplay between the autoinhibited, cytosolic form of PKCα and the active, plasma membrane-bound form. Understanding the mechanisms that stabilize one or the other state of PKCα may potentially open up new approaches for pharmacologically modulating PKC activity in an isozyme-specific manner.

MATERIALS AND METHODS

Plasmid Constructs, Antibodies, and Reagents

The C-Kinase Activity Reporter (CKAR) was previously described (147, 191). Human YFP-PKCα for translocation experiments was generated by sub-cloning PKCα into pcDNA3 with YFP at the N-terminus. Human mCherry-PKCβII for CKAR activity experiments was N-terminally tagged with mCherry via Gateway cloning. Human PKCα isolated C2 domain was N-terminally tagged with YFP via Gateway cloning. Gateway cloning procedure was as previously described (11, 121). Membrane-targeted CFP for translocation experiments (240) has been previously described. All mutants were generated using QuikChange site-directed mutagenesis (Agilent Genomics). The anti-PKCα antibody (610108) was from BD Transduction Laboratories. The anti-phospho PKCα/βII (pT638/641; 9375S) and pan anti-phosphorylated PKC hydrophobic motif (βII pS660, 9371S) antibodies were from Cell Signaling Technology. The pan anti-phospho-PKC activation loop antibody was previously described (168). The anti-α-Tubulin (T6074) antibody was from Sigma-Aldrich. The GAPDH (2118) and GFP (2555S) antibodies were purchased from Cell Signaling Technology. The mouse anti-HA (901533) antibody was purchased from BioLegend, and the rat anti-HA (3F10) antibody was purchased from Roche. The phospho-Y195 antibody for PKCα (AB-PK764) was purchased from Kinexus. Phorbol 12,13-dibutyrate (PDBu), uridine-5'-triphosphate (UTP), thapsigargin, PP2, PP3, staurosporine, and bisindolylmaleimide IV (Bis IV) were purchased from Calbiochem. Na_3VO_4 for making peroxyvanadate was purchased from New England Biolabs. Hydrodgen peroxide (H_2O_2) 30% was purchased from Thermo

Fisher Scientific. Peroxyvanadate was prepared immediately before use by combining 10 mM Na_3VO_4 (30 µl) with 30% H_2O_2 (0.8 µl). Protein A/G PLUS-Agarose beads for immunoprecipitation were purchased from Santa Cruz Biotechnology (sc-2003).

Mammalian Cell Culture, Transfection and Drug Treatments

COS7 cells were maintained in DMEM (Cellgro) containing 10% fetal bovine serum (Atlanta Biologicals) and 1% penicillin/streptomycin (Gibco) at 37 °C in 5% CO_2. Transient transfection was carried out using jetPRIME (PolyPlus Transfection) for ~24h. For drug treatments, cells were treated first with inhibitor where indicated for 45 minutes, followed by peroxyvanadate (3.5 µl per 2 ml of cell media) where indicated for 15 minutes, followed by PDBu (200 nM) where indicated for 15 minutes. For non-immunoprecipitation experiments, cells were lysed in 50 mM Tris, pH 7.4, 1% Triton X-100, 50 mM NaF, 10 mM $Na_4P_2O_7$, 100 mM NaCl, 5 mM EDTA, 1 mM Na_3VO_4, 1 mM PMSF, 50 µg/mL Leupeptin, 1 µM Microcystin, 1 mM DTT, and 2 mM Benzamidine. Whole cell lysates were analyzed by SDS-PAGE and immunoblotting via chemiluminescence on a FluorChemQ imaging system (ProteinSimple).

Immunoprecipitation

To immunoprecipitate overexpressed PKCα, cells were lysed in RIPA buffer: 50 mM Tris, pH 8, 150 mM NaCl, 1% NP-40, 0.5% sodium deoxycholate, 0.1% SDS, 1 mM PMSF, 1 mM Na_3VO_4, 50 µg/mL Leupeptin, 1 µM Microcystin, 1 mM DTT, and 2 mM Benzamidine. Mouse anti-HA antibody was added to the whole cell lysates at a 1:100 dilution (2 µl per 200 µl of whole cell lysate), and samples were rocked overnight at 4˚C. 30 µl of Protein A/G PLUS-Agarose bead slurry were added to the 200 µl of lysate, and

the mixture was rocked at 4˚C for 2-4 hours. Beads were washed three times with RIPA buffer, the final wash was removed, and the HA-tagged PKCα was eluted from the beads by adding 4X sample buffer and boiling for 5 min at 100˚C. Immunoprecipitated product was then analyzed by SDS-PAGE and immunoblotting via chemiluminescence on a FluorChemQ imaging system (ProteinSimple).

FRET Imaging and Analysis

Cells were imaged as described previously: translocation experiments in **Figure 4.2** were carried out as described by Gallegos et al. (241), and all other imaging experiments were carried out as described by Callender et al. (242). For translocation experiments, COS7 cells were co-transfected with the indicated YFP-tagged PKC and plasma membrane-targeted CFP at a 1:1 ratio of DNA. For CKAR activity experiments, COS7 cells were co-transfected with the indicated mCherry-tagged PKC and CKAR at a 1:1 ratio of DNA. Cells were rinsed once with and imaged in Hanks' balanced salt solution containing 1 mM Ca^{2+}. Images were acquired on a Zeiss Axiovert microscope (Carl Zeiss Microimaging, Inc.) using a MicroMax digital camera (Roper-Princeton Instruments) controlled by MetaFluor software (Universal Imaging, Corp.). Using a 10% neutral density filter (translocation experiments in **Figure 4.2**) or a 5% neutral density filter (all other imaging experiments), CFP, YFP, mCherry, and FRET images were obtained every 7 or 15 seconds. For translocation experiments, YFP emission was monitored as a control for photo bleaching and to ensure that overexpressed PKC levels were equal in all experiments. For CKAR activity experiments, mCherry emission was used to ensure that overexpressed PKC levels were equal between conditions. Base-line

images were acquired for ≥ 2 min before first ligand addition and for ≥ 2 min after maximum response to the final ligand had been achieved. Data were normalized to the baseline FRET ratios prior to ligand addition (**Figures 4.2, 4.4, and 4.7**) or the baseline FRET ratios after maximum response to inhibitor (**Figure 4.8**). Data are plotted as the average ± S.E.M. of normalized FRET ratio for n > 20 cells from at least 3 biologically independent experiments.

The FRET-detected translocation curves, with baseline FRET ratios normalized to 1, were fit using the following equation:

$$y = 1.0 + A\left[1 - e^{-kt}\right],$$

where y is the FRET ratio; k is the sum of the on- and off- rate constants, ($k_{on}+k_{off}$); A is the steady-state FRET ratio that reflects the amount of translocated protein and is ~$(1+k_{off}/k_{on})^{-1}$. For variants that showed non-saturatable behavior (e.g. wild-type PKCa), a linear term, D×t, was added to describe the time dependence.

ACKNOWLEDGEMENTS: Chapter in part is unpublished material generated in collaboration with Tatyana Igumenova, Alexandr Kornev, Susan Taylor, and Ronit Ilouz. We thank Tatyana Igumenova for fitting of translocation data and calculation of rate constants for **Figure 4.2**. We also thank Alexandr Kornev for modeling and docking the C2 domain of PKCα onto the catalytic domain, which is depicted in **Figure 4.1C**.

FIGURES AND TABLES

Figure 4.1: Amino acids predicted to regulate PKCα signaling. [A] Primary structure of PKCα. Depicted in red are the residues in the C2 domain and the C-tail that are predicted by Igumenova and colleagues to lie upon the C2:C-tail interface in the autoinhibited enzyme (65). Shown in blue is the location of Tyr195. [B] PhosphoSitePlus graph depicting frequency of references to phosphorylation sites in PKCα (227). [C] Residues from [A] shown on a model in which the PKCα C2 domain (PDB 4DNL) is docked against the catalytic domain (PDB 3IW4). Shown in red are the residues studied by Igumenova and colleagues, shown in green is the site of hydrophobic motif phosphorylation, and shown in blue is Tyr195.

A

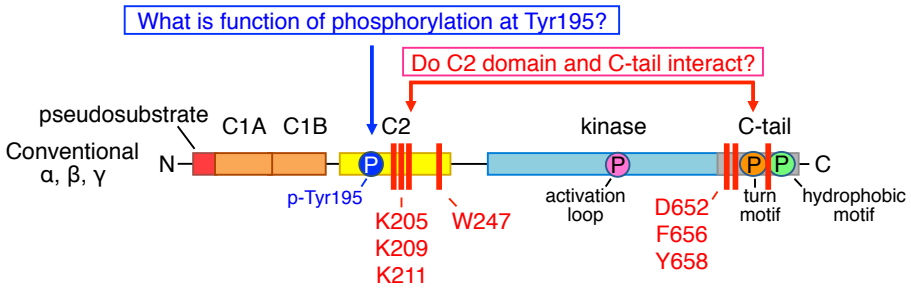
What is function of phosphorylation at Tyr195?
Do C2 domain and C-tail interact?
pseudosubstrate
C1A
C1B
C2
kinase
C-tail
Conventional
α, β, γ
N
C
P
p-Tyr195
K205
K209
K211
W247
activation
loop
D652
F656
Y658
turn
motif
hydrophobic
motif

B

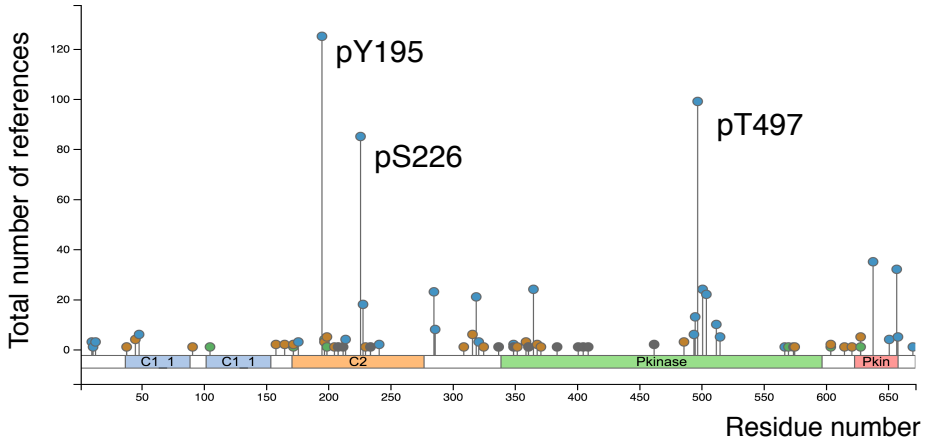
Total number of references
pY195
pS226
pT497
C1_1
C1_1
C2
Pkinase
Pkin
Residue number

C

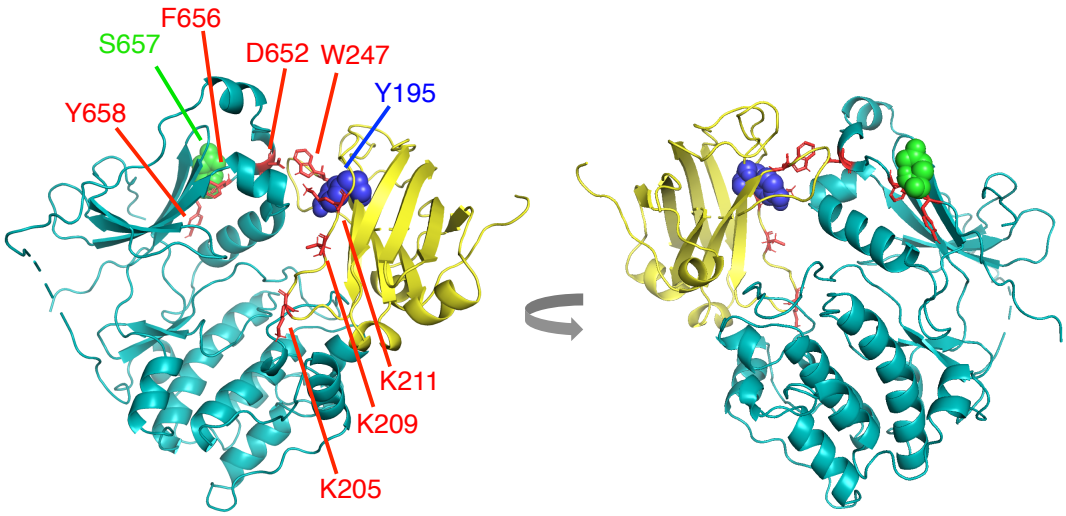
F656
S657
D652
W247
Y195
Y658
K211
K209
K205

Table 4.1: PKCα C2-catalytic domain interface mutations. Table establishing abbreviations for all the PKCα variants tested. Residues were selected based on modeling of PKCα C2 domain-kinase domain interface published by Igumenova and colleagues (65).

Variant	*C2*	*C-tail*
WT		
S657A (hydrophobic motif)		S657A
F656A		F656A
FYYW	Y195A/W247A	F656A/Y658A
D652K		D652K
KK	K209E/K211E	
DKK	K209E/K211E	D652K
K205E	K205E	
DK	K205E	D652K
D652A		D652A

Figure 4.2: PKCα autoinhibition is regulated by intramolecular contacts. [A] Schematic depicting current model for PKCα autoinhibition and activation. When inactive, PKCα remains in the cytosol in a "closed" state, in which residues in the C2 domain and the C-tail participate in intramolecular interactions. Note that Tyr195 is located in this interface. Upon stimulation by second messengers, PKCα translocates to the plasma membrane, where autoinhibitory constraints are removed and the C2 domain and catalytic domain both become "opened" and unmasked. [B] Absolute FRET ratio changes (mean ± S.E.M.) representing the kinetics of PDBu (200 nM)-induced translocation of YFP-PKCα variants with mutations targeting pSer657 (blue) and aromatic interactions (orange, grey) to CFP-tagged plasma membrane. Wild-type translocation trace (black) shows both "slow" and "fast" translocation kinetics of wild-type PKCα. [C] Western blots showing whole cell lysates of COS7 cells transfected with PKCα constructs. The PKCα phosphorylation sites are the activation loop (Thr497), turn motif (Thr638), and hydrophobic motif (Ser657). [D] PDBu-induced translocation of YFP-PKCα variants targeting residues predicted to engage in electrostatic interactions. All FRET data represent the average ± SEM from at least 3 biologically independent experiments measuring > 20 cells.

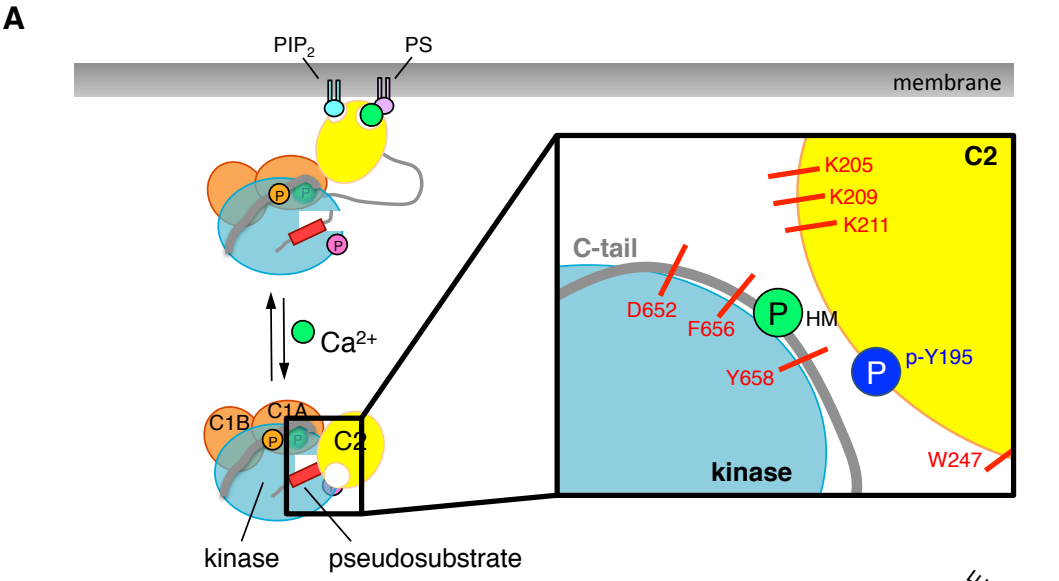
A
PIP2
PS
membrane
Ca2+
C1B
C1A
C2
kinase
pseudosubstrate
C2
K205
K209
K211
C-tail
D652
F656
HM
Y658
p-Y195
kinase
W247

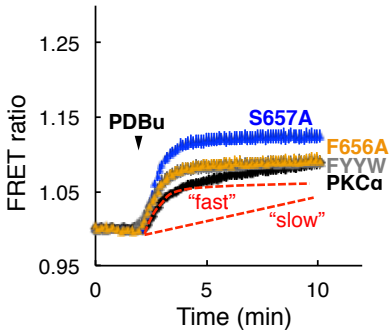
B
FRET ratio
1.25
1.15
1.05
0.95
PDBu
S657A
F656A
FYYW
PKCα
"fast"
"slow"
0
5
10
Time (min)

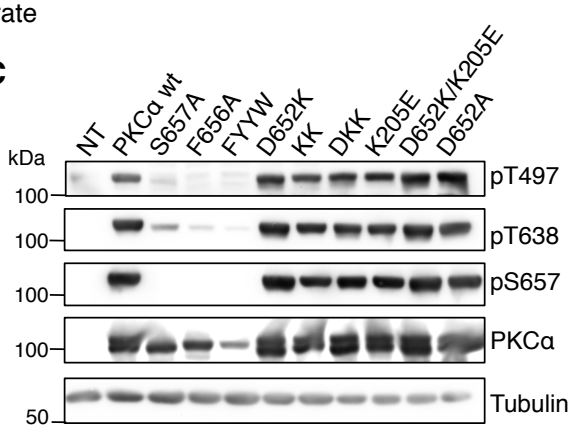
C
NT
PKCα wt
S657A
F656A
FYYW
D652K
KK
DKK
K205E
D652K/K205E
D652A
kDa
100
100
100
100
50
pT497
pT638
pS657
PKCα
Tubulin

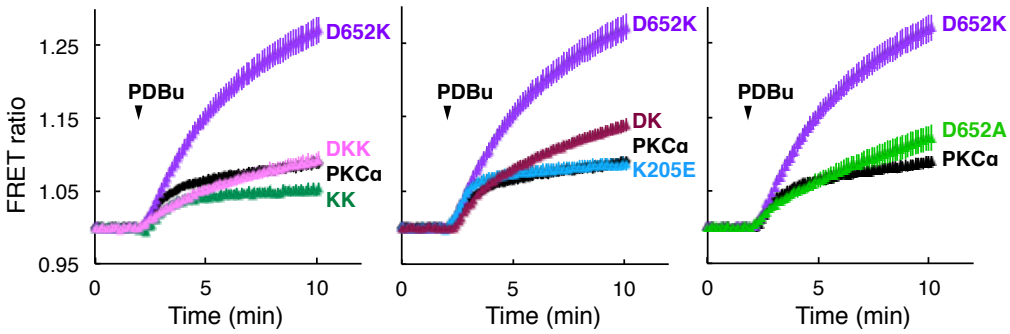
D
FRET ratio
1.25
1.15
1.05
0.95
PDBu
D652K
DKK
PKCα
KK
DK
K205E
D652A
0
5
10
Time (min)

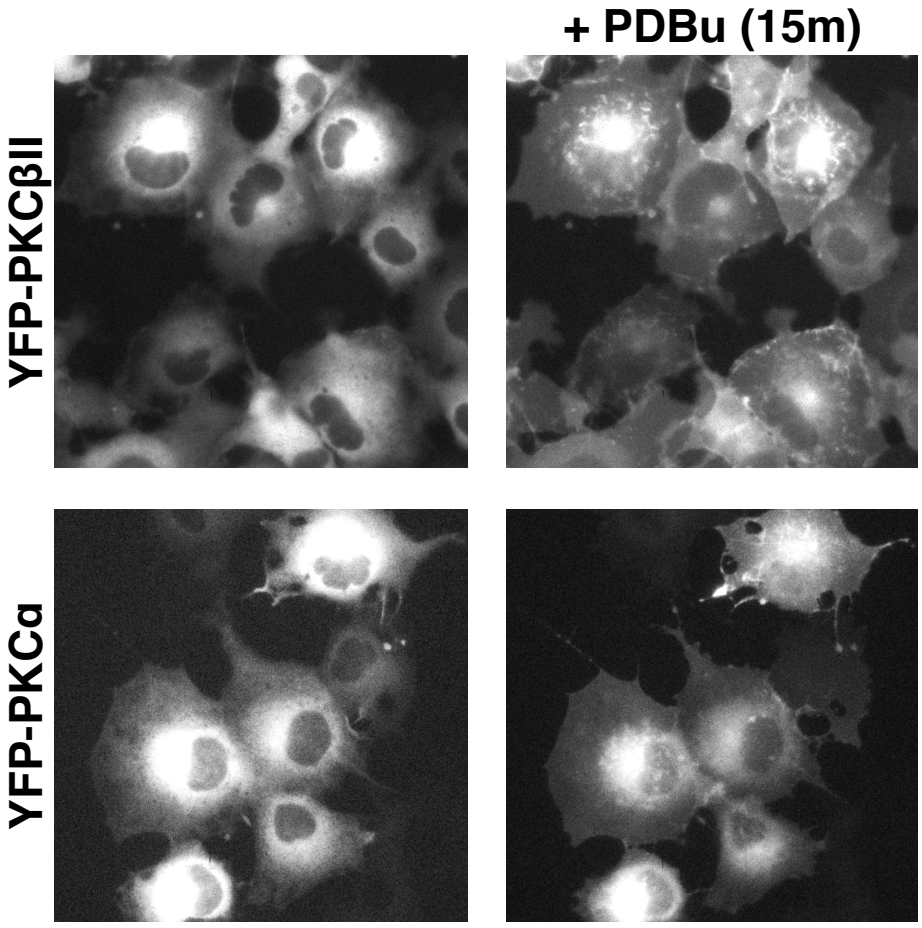

Figure 4.3: YFP images depicting translocation behaviors of PKCα and PKCβII. YFP-PKCα and YFP-PKCβII were overexpressed in COS7 cells and translocation to the plasma membrane stimulated by 200 nM PDBu. Images depict either before translocation was initiated (left) or 15 minutes after PDBu had been added (right).

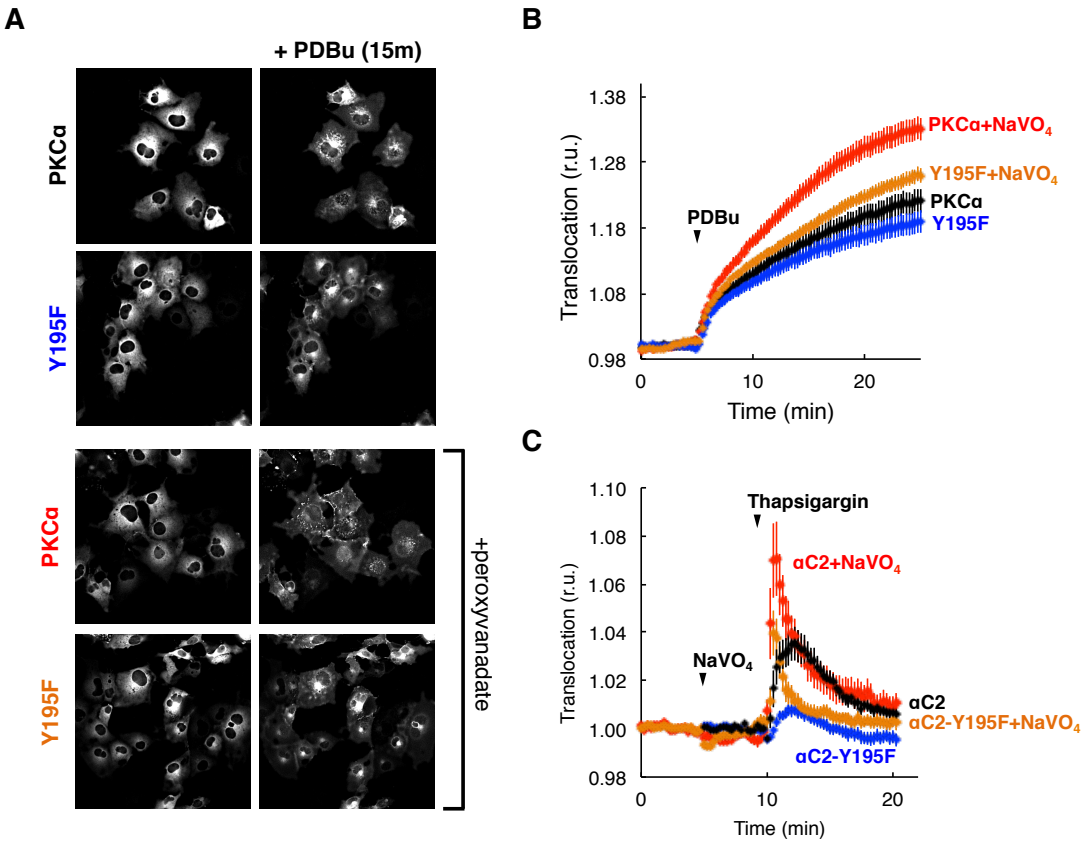

Figure 4.4: Tyrosine phosphorylation of PKCα promotes enhanced translocation to the plasma membrane. [A] COS7 cell images depicting YFP signal in YFP-PKCα translocation experiments. Images depict either before translocation was initiated (left) or 15 minutes after 200 nM PDBu had been added (right). Cell images depict translocation without (top) or with (bottom) peroxyvanadate pretreatment. [B] Absolute FRET ratio changes representing translocation of full-length YFP-PKCα wild-type (black) or Y195F (blue) after PDBu stimulation (200 nM, black arrow where indicated). Also shown are translocation traces after pre-treatment with peroxyvanadate at 0 minutes ($NaVO_4$) followed by PDBu stimulation (black arrow) for both wild-type (orange) and Y195F (red). [C] FRET ratio changes depicting translocation of isolated YFP-αC2 domain to CFP-tagged plasma membrane in response to thapsigargin (5 μM). Depicted are wild-type C2 domain (black) and C2 domain containing Y195F mutation (blue). Peroxyvanadate pre-treatment (3.5 μl per 2 mL of imaging buffer) prior to PDBu addition is shown for both wild-type C2 domain (red) and Y195F C2 domain (orange). Data represent the average ± SEM from at least 3 biologically independent experiments measuring > 20 cells.

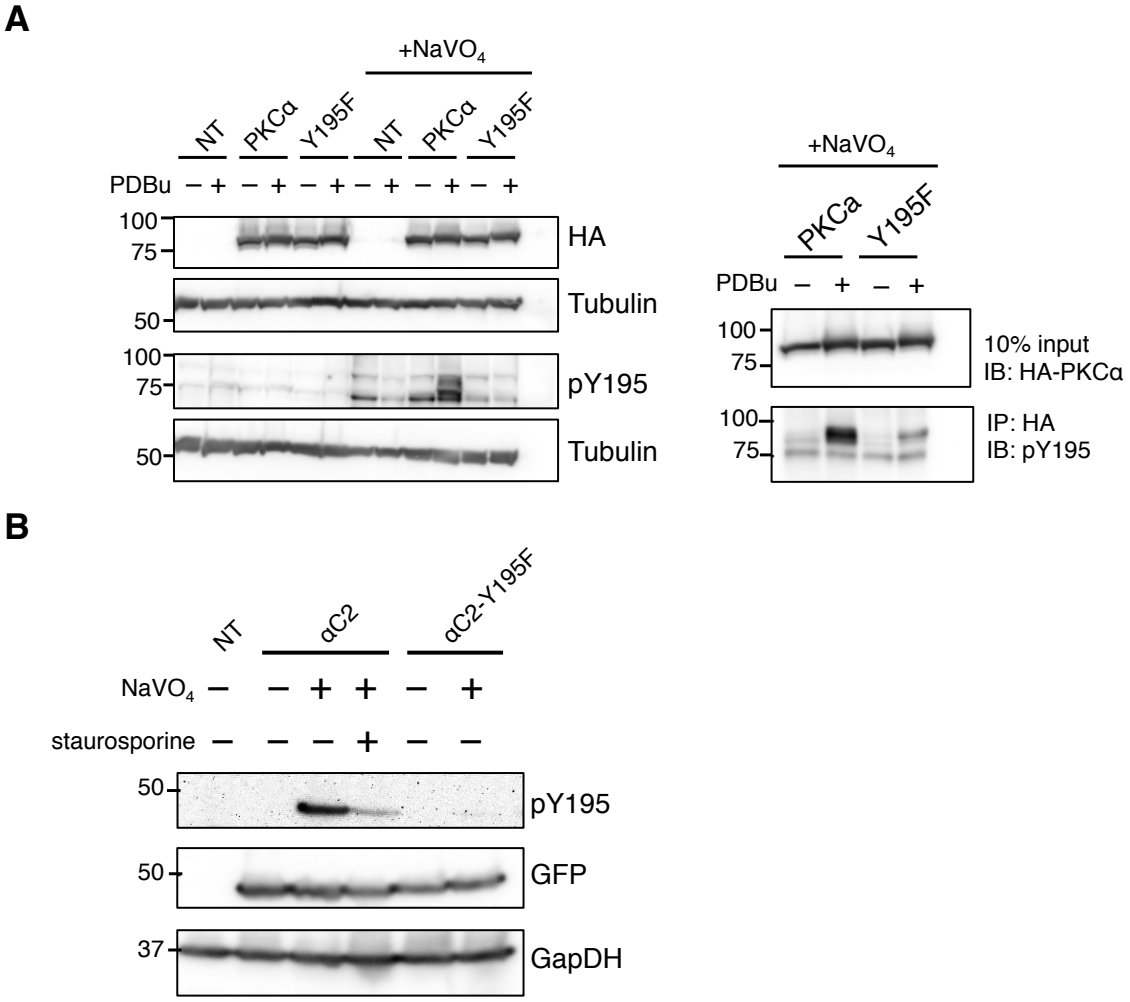

Figure 4.5: PKCα-Tyr195 phosphorylation requires both peroxyvanadate and unmasking of the C2 domain. [A] Western blot depicting conditions necessary for phosphorylation of Y195 in full-length HA-PKCα overexpressed in COS7 cells. Shown are experiments using either whole cell lysates (left) or HA-PKCα immunoprecipitated from whole cell lysates (right). NT, not transfected control. Cells were treated with either 200 nM PDBu or with DMSO control for 15 minutes. Peroxyvanadate pre-treatment ($NaVO_4$) was added where indicated for 15 minutes prior to PDBu addition (3.5 µl per 2 mL growth media). [B] Western blot depicting conditions necessary for phosphorylation of Y195 in isolated YFP-αC2 domain overexpressed in COS7 cells. Staurosporine (1 µM) was added to cells for 60 minutes where indicated, followed by peroxyvanadate for 15 minutes where indicated.

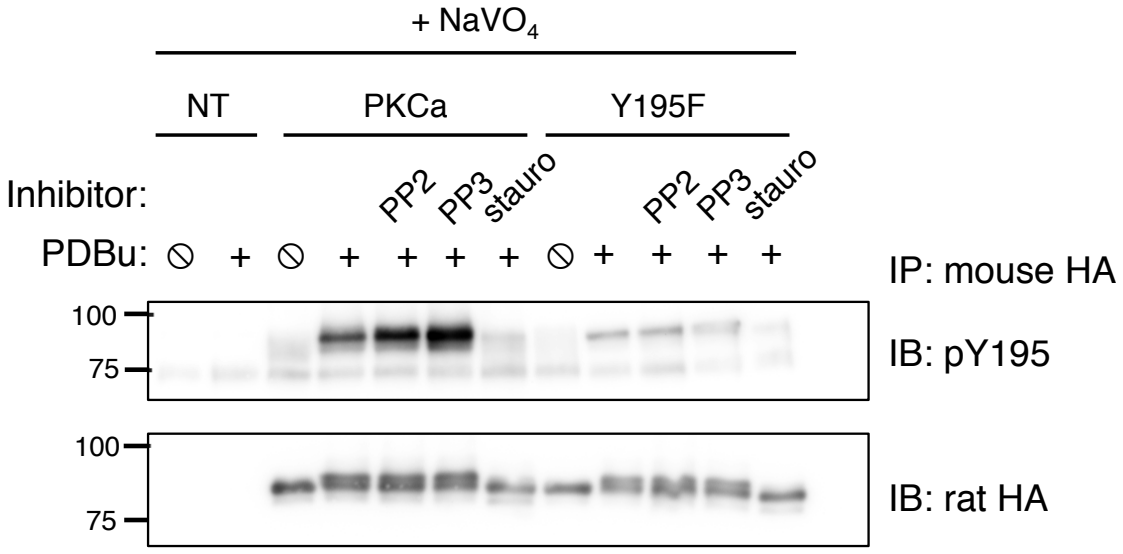

Figure 4.6: PKCα-Tyr195 is not phosphorylated by Src-family kinases that are targeted by PP2 inhibition. Western blot depicting pY195 signal when overexpressing and immunoprecipitating full-length HA-PKCα from COS7 cells. Cells were treated with inhibitors (10 μM PP2, 10 μM PP3, or 1 μM staurosporine) where indicated for 60 minutes, followed by peroxyvanadate ($NaVO_4$) where indicated for 15 minutes, followed by PDBu where indicated for 15 minutes. NT, not transfected control.

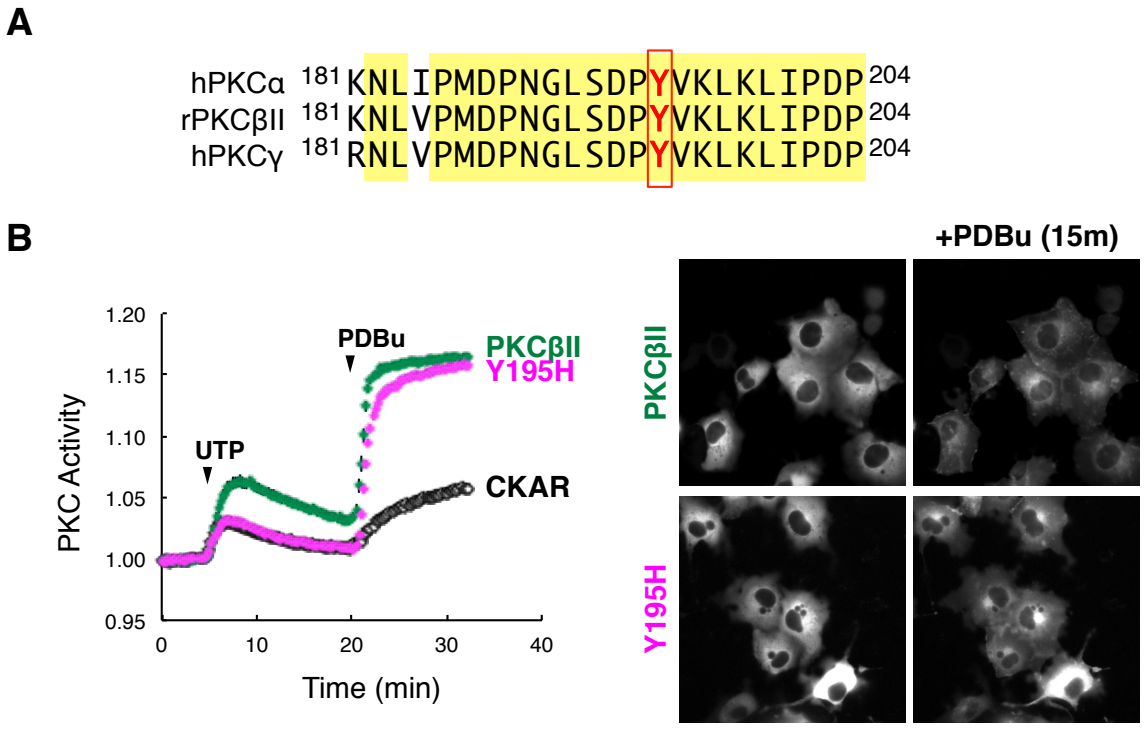

Figure 4.7: Cancer-associated PKCβII-Y195H mutant is loss-of-function. [A] Sequence alignment depicting highly conserved nature of Tyr195 (red) and surrounding residues in conventional PKC isozymes. [B] Normalized FRET ratio depicting PKC phosphorylation of CKAR activity reporter (147) in COS7 cells. UTP (100 μM) or PDBu (200 nM) were added where indicated (black arrows). Data represent average ± SEM from at least 3 biologically independent experiments measuring > 20 cells. On the right are representative cell images depicting YFP-PKCβII localization before (left) and after (right) PDBu addition.

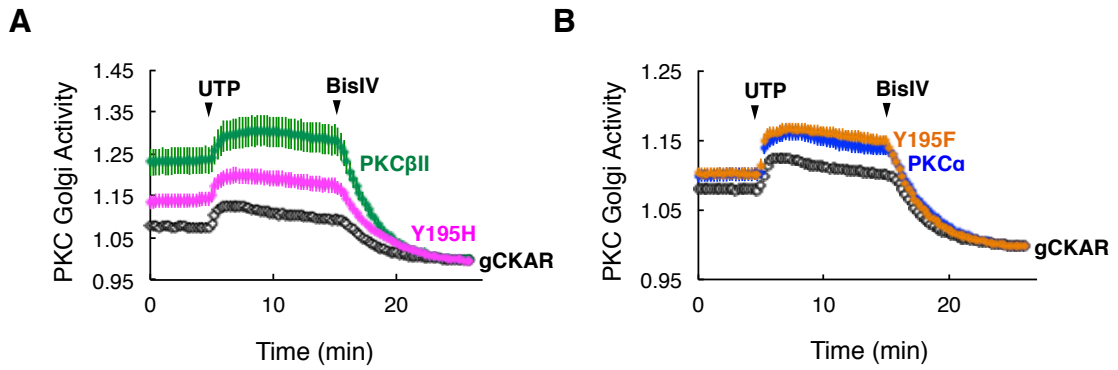

Figure 4.8: Neither cancer-associated PKCβII-Y195H nor PKCα-Y195F are gain-of-function at the Golgi apparatus. [A-B] Normalized FRET ratio depicting mCherry-PKCβII [A] or mCherry-PKCα [B] phosphorylation of CKAR activity reporter targeted to the Golgi (147, 170). UTP (100 μM) and Bis IV inhibitor (2 μM) added where indicated (black arrows). Data represent average ± SEM from at least 3 biologically independent experiments measuring > 20 cells.

Figure 4.9: PKCα autoinhibition and signaling output is regulated by both intramolecular contacts and by tyrosine phosphorylation. [A] Schematic depicting intramolecular contacts that contribute to PKCα autoinhibition. (i-ii) In the inactive state, PKCα is "closed" in the cytosol, and positively-charged residues in the C2 domain interact with negatively-charged residues in the kinase domain. We propose that there are two distinct conformational states are in equilibrium in this pool of PKCα. One of these states constitutes the "slow" translocation phase when PKCα translocates to the plasma membrane (i), and the other constitutes the "fast" translocation phase (ii). Once at the plasma membrane, PKCα's C2 domain is removed from intramolecular contact with the catalytic domain, yielding an "open" and active catalytic domain. [B] Schematic depicting tyrosine phosphorylation regulating PKCα signaling and autoinhibition. When PKCα responds to second messengers to move from the inactive, cytosolic state (i) to the membrane-bound, active state (ii), it accumulates a transient phosphorylation at Tyr195. Inhibiting tyrosine dephosphorylation promotes continued accumulation of PKCα at the plasma membrane (iii). Preventing phosphorylation at this site, or, in the case of the cancer-associated mutation Y195H, introducing a positively-charge amino acid side chain at this site, ablates PKCα's ability to respond to second messengers (iv).

A

PKCα autoinhibition is regulated by intramolecular contacts

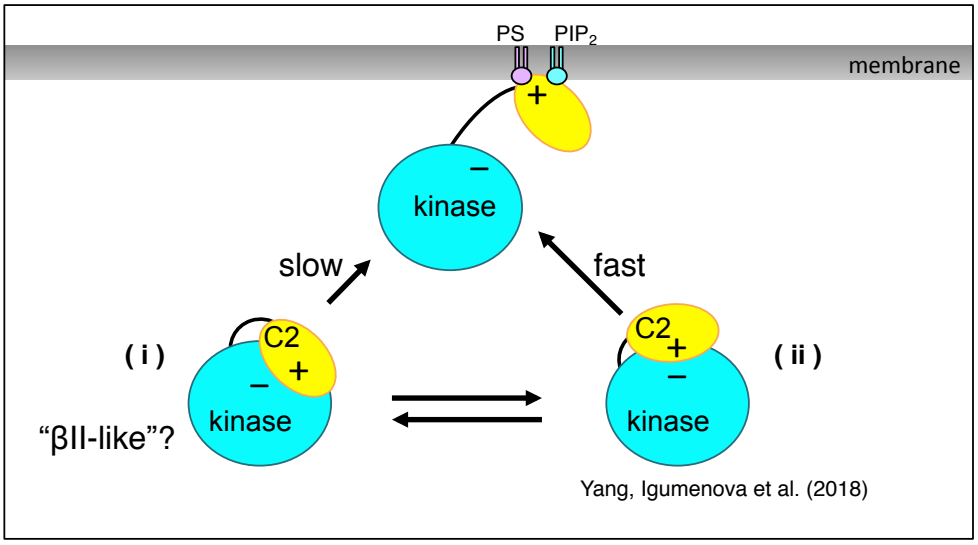

B

PKCα autoinhibition is regulated by Tyrosine phosphorylation

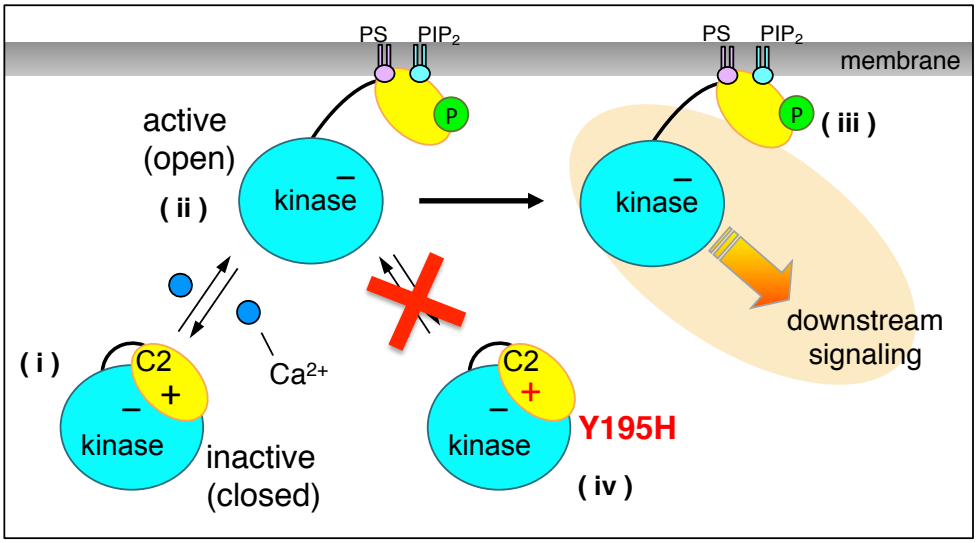

CHAPTER 5

CONCLUSIONS AND FUTURE WORK

5.1 Conclusions

The work within this thesis describes both the mechanisms that regulate PKCα signaling and also how deregulation of these mechanisms supports the development of neurodegenerative pathophysiologies. PKCα is a ubiquitously-expressed signaling enzyme that plays a role in a myriad of cellular processes, and as such, precise regulation of its signaling output is crucial to maintain cellular homeostasis. PKCα, like all PKC isozymes, differs from the majority of kinases in that its C-terminal catalytic domain is phosphorylated at its activation loop not as a result of activation, but rather as a result of a constitutive priming and processing pathway. This catalytic domain would therefore exhibit constitutive activity, were it not for the evolution of an elegant mechanism through which PKCα's own N-terminal regulatory domains autoinhibit the catalytic domain. Thus, the cell maintains a precise balance of PKCα signaling output (**Figure 5.1**). In this vein, if the catalytic domain were to be locked open and activated in a constitutive fashion, PKCα would be dephosphorylated and shunted into a degradation pathway (48), thereby restoring the necessary equilibrium. The mechanism through which this balance in PKCα signaling is properly regulated—and how pathology circumvents this balance in Alzheimer's disease—has been the main focus of these studies. The two primary stories investigated in this thesis (PKCα signaling in Alzheimer's disease and structural regulation of PKCα signaling by its C2 domain) serve to support each other in telling a complete narrative: PKCα has evolved elegant mechanisms through which its autoinhibition and signaling is regulated by its own N-

terminal domains, and perturbation of these mechanisms can lead to an aberrant increase in PKCα activity and neurodegenerative pathologies.

Chapter 2 describes a novel role for PKCα signaling in Alzheimer's disease. We used a combination of genetic, electrophysiology, and biochemistry experiments to show that [1] PKCα (and its ability to engage in protein scaffold interactions via its PDZ ligand) is necessary for Amyloid β (Aβ)-induced synaptic depression in hippocampal slices, [2] Alzheimer's disease-associated mutations in PKCα enhance signaling output in cells, and [3] exposing live cells to Aβ causes a Ca^{2+} response and activates PKC. Coupled with previous studies from our group identifying that PKC signaling is lost in cancer, a disease of proliferation, these experiments highlighted that deregulation of PKCα in the opposite direction promotes biochemical alterations that support the development of Alzheimer's disease, thus strengthening our model that PKCα signaling must be maintained in a precise balance to avoid pathological consequences. These studies also sparked our interest in the biochemistry of how these disease-associated mutations increase PKCα signaling output in cells without compromising stability of the enzyme, which would lead to protein degradation and a paradoxical loss-of-function. This led us to pursue a more rigorous biochemical characterization of one of the mutations, PKCα-M489V.

Chapter 3 describes our in-depth investigation into how the M489V amino acid substitution in PKCα could enhance signaling output in cells without sensitizing it to dephosphorylation and degradation. We performed *in vitro* kinase assays with purified protein to show that while the M489V mutation did not affect sensitivity to cofactors,

peptide substrate binding, and ATP binding, it conferred a V_{max} that was approximately 30% higher than the wild-type protein. We used *in silico* molecular dynamics simulations to model how a modest amino acid substitution (a Met to a Val) could in fact cause robust changes in the molecular dynamics of the entire kinase domain. This is unsurprising when considering that this mutation is in the activation loop region, a key area that is connected to other functional communities in the kinase domain via electrostatic and hydrophobic interactions (see **Figure 3.1C**). These findings led to our hypothesis that this mutation increases PKCα signaling output without compromising stability because it does not perturb autoinhibition, as evidenced by the unchanged sensitivity to cofactors. Rather, when autoinhibitory constraints are removed, this mutation changes the dynamics of the kinase domain to cause in increase in the catalytic output. We confirm this hypothesis by removing the N-terminal autoinhibitory domains and assessing basal signaling output in cells, which is robustly increased after introduction of the M489V mutation. Lastly, we generated a mouse model containing this M489V mutation. We showed that not only is phosphorylation of a key PKCα substrate (MARCKS) known to be involved in the early stages of Alzheimer's disease pathology increased in the brains of these mice, but also that the steady-state levels of PKCα are the same in the M489V mice and wild-type mice, thus confirming that this mutation confers enhanced PKCα activity without compromising stability. These studies therefore describe a novel mechanism through which a disease-associated mutation cleverly evades the cell's normal homeostatic response to aberrantly active PKC.

Chapter 4 describes a variety of studies undertaken to understand how PKCα signaling is regulated by intramolecular autoinhibition and by tyrosine phosphorylation. Previous work by our group has established that the closely-related conventional isozyme PKCβII experiences autoinhibition by its N-terminal regulatory domains in its inactive, cytosolic form, and that this autoinhibition can be tested by introducing mutations that perturb this interface and observing membrane translocation kinetics of the PKCβII variants. We used FRET-based cell translocation assays to show that while this autoinhibitory mechanism also regulates PKCα signaling, there are key differences in the behavior of PKCβII and PKCα in cells. Using modeling from a recent publication by Igumenova and colleauges (65), we introduced mutations in residues predicted to engage in intramolecular interactions and observed that they "opened" PKCα, as was seen previously with PKCβII. However, we observed that PKCα translocates to the plasma membrane in a biphasic manner, which is in contrast to PKCβII's monophasic translocation behavior. This suggests that PKCα exists in the cytosol in two conformational states. We then showed that PKCα signaling is regulated by phosphorylation of a conserved tyrosine residue in the C2 domain. This phosphorylation site, while frequently picked up in unbiased phosphoproteomics screens, was completely unstudied in the PKCα literature. We detected the accumulation of tyrosine phosphorylation on PKCα by inhibiting tyrosine phosphatases and observed a robust increase in PKCα translocation and retention on the plasma membrane. This effect was partially ablated by introducing a non-phosphorylatable residue at Tyr195 (Y195F), thus confirming that this tyrosine in particular plays a crucial role in promoting PKCα

association with the plasma membrane. These studies provide new insight into how PKCα autoinhibition and signaling is regulated, which is crucial for understanding how to target PKCα in an isozyme-specific manner in various diseases.

5.2 Future Work

With regards to the role played by PKCα in Alzheimer's disease, a number of exciting avenues remain unexplored. Our findings in Chapter 2 serve as a proof-of-concept for a powerful new approach for tackling diseases for which there is no cure: identification of new rare variants that co-segregate with a particular disease will yield novel protein targets and signaling pathways that play roles in disease pathogenesis. Identifying these alternative signaling pathways—which may be understudied in the context of a particular disease—will be a crucial in the development of novel therapeutic approaches.

After having established that the PKCα-M489V variant displays enhanced activity in mouse brains, the most important future direction will be a more thorough characterization of the M489V mouse model. These studies are currently under way, and will involve a variety of biochemical, behavioral, histopathological, and phosphoproteomics approaches to further elucidate how this variant affects the whole organism. This PKCα-M489V mouse will be crossed with an Alzheimer's disease model mouse (APP/swe), which will allow for experiments observing how the M489V variant affects the progression of the disease phenotype. Additionally, this mouse would allow for follow-up experiments regarding the activation of PKCα downstream of Aβ. In Chapter 2, we establish that PKC is activated as a result of exposing primary astrocytes

isolated from wild-type mice to $A\beta_{25-35}$ peptide (see **Figures 2.7-2.8**) Repeating these experiments in primary cells isolated from the PKCα-M489V mouse presents a fascinating opportunity to assess if this variant enhances this effect. In this vein, this experiment should be repeated in primary cells of different lineages (for example, primary hippocampal neurons or cortical neurons as opposed to primary astrocytes). Additionally, future studies should focus on testing how different forms of Aβ cause this PKC activation, as the mixture used to stimulate cells in Chapter 2 may have been monomers, oligomers, fibrils, or some combination of all of the above. Given the differential biological roles played by different forms of Aβ, elucidating which form of Aβ is at play is crucial. Lastly, we show that the PKCα-M489V variant exhibits differential response to certain PKC inhibitors. Future work can continue in this vein, with the ultimate goal of understanding how to decrease PKCα signaling in Alzheimer's disease in an isozyme-specific manner. Along these lines, our work in Chapter 4 provides some hints as to how this might be accomplished by providing a more in-depth look at the structural regulation of PKCα signaling.

With regard to the studies presented in Chapter 4, future directions should focus on identifying the upstream kinase that phosphorylates Tyr195 in PKCα. This can be accomplished either through a general tyrosine kinase screen or through a more targeted approach, such as pharmacologically inhibiting candidate tyrosine kinases or using RNA interference (RNAi) to knock down kinases of interest. Further studies could also focus on the discrepancies between PKCα and PKCβII translocation, as this research path help

to elucidate how to pharmacologically target one of these enzymes while not affecting the other.

Therapeutically targeting PKCα in Alzheimer's disease should be an ongoing goal of future studies. PKCα activity would need to be decreased, and luckily, many methods to inhibit PKC have already been developed for use in clinical trials to treat cancer. While these PKC modulators universally failed (and in some cases, worsened patient outcome) in the context of cancer, they can be repurposed to inhibit PKCα in neurodegenerative diseases. Indeed, the potent PKC agonist Byrostatin has recently completed a successful Phase II clinical trial for the treatment of Alzheimer's disease (243). Prolonged infusion of Bryostatin into cancer patients has been shown to cause a decrease in blood levels of PKCα, as would be expected of potent C1 agonists that lock PKC into an open and degradation-sensitive conformation (205). Therefore, it's likely that Bryostatin will see success in treating Alzheimer's disease due to its ability to chronically decrease steady-state PKC levels in the patient, rather than its acute activation of PKC.

In regards to treating Alzheimer's disease, PKCα inhibition should be pursued while keeping in mind the following concerns: [1] only PKCα activity—and not the activity of any of the related PKC isozymes—should be decreased, and [2] this inhibition of PKCα activity should ideally be limited to the brain, as global inhibition of PKC signaling may promote the development of cancer pathologies. The first goal can be accomplished via a myriad of approaches that are highlighted by the findings of this thesis work. For example, studies in Chapter 2 establish that PKCα's ability to engage with PDZ domain-containing protein scaffolds is necessary for Aβ-mediated synaptic

depression. Therefore, small molecules that disrupt this protein interaction would target this specific pool of PKCα. In Chapter 3, we show that the PKCα-M489V mutation confers enhanced sensitivity to ATP-competitive active site inhibitors. This effect must be attributed to the M489V mutation changing the way PKCα interacts with the cellular environment, as this difference in sensitivity was not observed in the purified protein. While not all patients contain the PKCα-M489V mutation, these studies indicate that the pool of PKCα contributing to Alzheimer's disease exists separately from the pool of regular PKCα, and that this pool may be more sensitive to this specific class of competitive inhibitors. Lastly, in Chapter 4, we investigate the ways in which PKCα and PKCβII translocation differ. While more work will be necessary to determine the mechanisms that contribute to these different behaviors, they may provide a clue as to how to target PKCα signaling without affecting the related conventional PKC isozymes. In regards to specifically targeting PKCα signaling in the brain rather than in the whole organism, this remains a primary focus of the pharmacological field in general. Many different methods for delivery of drugs or gene therapies to the brain have been proposed, all of which could potentially be used to deliver PKCα inhibiting factors.

More generally, the work presented in this thesis highlights the benefits of combining unbiased, large-scale screens with hypothesis-driven biochemistry. Both Chapters 2-3, which concern PKCα signaling in Alzheimer's disease, and Chapter 4, which concerns how the C2 domain regulates PKCα signaling through autoinhibition and tyrosine phosphorylation, started with large-scale GWAS or phosphoproteomics observations, respectively. We then followed up on and corroborated these unbiased

approaches with in-depth biochemistry. This combination of tactics will be necessary in order to identify PKC-dependent pathways that are deregulated in neuropathologies, which in turn will pave the road for new therapeutic strategies for the treatment of neurodegenerative diseases.

FIGURES AND TABLES

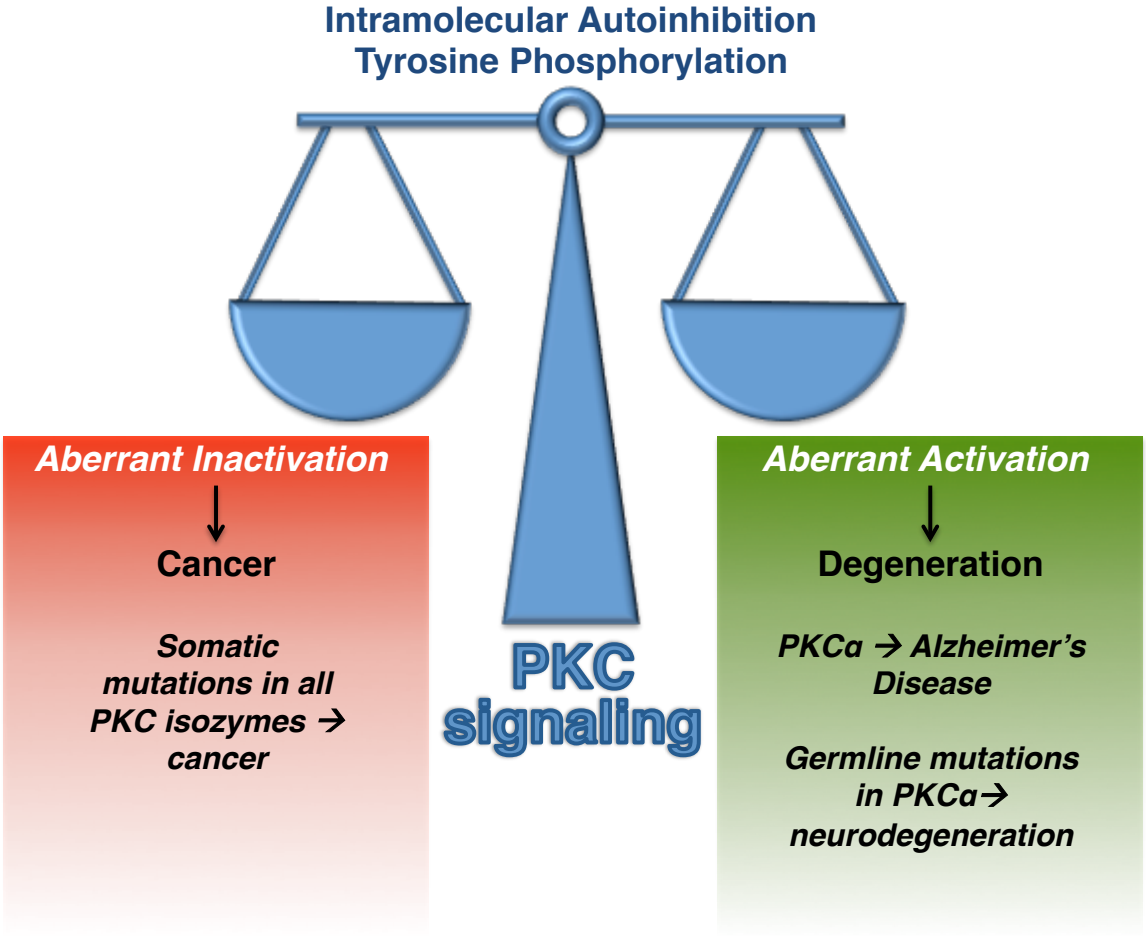

Figure 5.1: The balance of PKCα activity signaling. In this thesis, we show that PKCα activity is precisely regulated by its C2 domain via intramolecular autoinhibition and tyrosine phosphorylation. Deregulation of this balance has pathological consequences: too little PKC activity promotes proliferative phenotypes such as cancer (11, 180), while aberrant PKC activity contributes to degeneration and Alzheimer's disease (121, 242).

REFERENCES

1. Inoue M, Kishimoto A, Takai Y, & Nishizuka Y (1977) Studies on a Cyclic Nucleotide-Independent Protein Kinase and Its Proenzyme in Mammalian Tissues. *J. Biol. Chem.* 252:7610-7616.

2. Takai Y, Kishimoto A, Inoue M, & Nishizuka Y (1977) Studies on a Cyclic Nucleotide-independent Protein Kinase and Its Proenzyme in Mammalian Tissues. *J. Biol. Chem.* 252:7603-7609.

3. Takai Y, Kishimoto A, Iwasa Y, Kawahara Y, Mori T, & Nishizuka Y (1979) Calcium-dependent Activation of a Multifunctional Protein Kinase by Membrane Phospholipids. *J. Biol. Chem.* 254:3692-3695.

4. Takai Y, Kishimoto A, Kikkawa U, Mori T, & Nishizuka Y (1979) Unsaturated Diacylglycerol as a Possible Messenger for the Activation of Calcium-activated, Phospholipid-dependent Protein Kinase System. *Biochem. Biophys. Res. Comm.* 91:1218-1224.

5. Hokin MR & Hokin LE (1953) Enzyme Secretion and the Incorporation of P32 into Phospholipids of Pancreas Slices. *J. Biol. Chem.* 203:967-977.

6. Castagna M, Takai Y, Kaibuchi K, Sano K, Kikkawa U, & Nishizuka Y (1982) Direct Activation of Calcium-activated, Phospholipid-dependent Protein Kinase by Tumor-promoting Phorbol Esters. *J. Biol. Chem.* 257:7847-7851.

7. Driedger PE & Blumberg PM (1980) Specific Binding of Phorbol Ester Tumor Promoters. *Proc. Natl. Acad. Sci. U. S. A.* 77:567-571.

8. Griner EM & Kazanietz MG (2007) Protein kinase C and other diacylglycerol effectors in cancer. *Nature reviews. Cancer* 7(4):281-294.

9. Mochly-Rosen D, Das K, & Grimes KV (2012) Protein kinase C, an elusive therapeutic target? *Nature reviews. Drug discovery* 11(12):937-957.

10. Zhang LL, Cao FF, Wang Y, Meng FL, Zhang Y, Zhong DS, & Zhou QH (2015) The protein kinase C (PKC) inhibitors combined with chemotherapy in the

treatment of advanced non-small cell lung cancer: meta-analysis of randomized controlled trials. *Clinical & translational oncology : official publication of the Federation of Spanish Oncology Societies and of the National Cancer Institute of Mexico* 17(5):371-377.

11. Antal CE, Hudson AM, Kang E, Zanca C, Wirth C, Stephenson NL, Trotter EW, Gallegos LL, Miller CJ, Furnari FB, Hunter T, Brognard J, & Newton AC (2015) Cancer-associated protein kinase C mutations reveal kinase's role as tumor suppressor. *Cell* 160(3):489-502.

12. Bivona TG, Quatela SE, Bodemann BO, Ahearn IM, Soskis MJ, Mor A, Miura J, Wiener HH, Wright L, Saba SG, Yim D, Fein A, Perez de Castro I, Li C, Thompson CB, Cox AD, & Philips MR (2006) PKC regulates a farnesyl-electrostatic switch on K-Ras that promotes its association with Bcl-XL on mitochondria and induces apoptosis. *Molecular cell* 21(4):481-493.

13. Wang MT, Holderfield M, Galeas J, Delrosario R, To MD, Balmain A, & McCormick F (2015) K-Ras Promotes Tumorigenicity through Suppression of Non-canonical Wnt Signaling. *Cell* 163(5):1237-1251.

14. Santiskulvong C & Rozengurt E (2007) Protein kinase Calpha mediates feedback inhibition of EGF receptor transactivation induced by Gq-coupled receptor agonists. *Cell Signal* 19(6):1348-1357.

15. Hunter T, Ling N, & Cooper JA (1984) Protein Kinase C Phosphorylation of the EGF Receptor at a Threonine Residue Close to the Cytoplasmic Face of the Plasma Membrane. *Nature* 311:480-483.

16. Cochet C, Gill GN, Meisenhelder J, Cooper JA, & T. H (1984) C-kinase phosphorylates the epidermal growth factor receptor and reduces its epidermal growth factor-stimulated tyrosine protein kinase activity. *The Journal of biological chemistry* 259(4):2553-2558.

17. Sipeki S, Bander E, Parker PJ, & Farago A (2006) PKCalpha reduces the lipid kinase activity of the p110alpha/p85alpha PI3K through the phosphorylation of the catalytic subunit. *Biochemical and biophysical research communications* 339(1):122-125.

18. Lee JY, Chiu YH, Asara J, & Cantley LC (2011) Inhibition of PI3K binding to activators by serine phosphorylation of PI3K regulatory subunit p85alpha Src homology-2 domains. *Proceedings of the National Academy of Sciences of the United States of America* 108(34):14157-14162.

19. Hoshino D, Jourquin J, Emmons SW, Miller T, Goldgof M, Costello K, Tyson DR, Brown B, Lu Y, Prasad NK, Zhang B, Mills GB, Yarbrough WG, Quaranta V, Seiki M, & Weaver AM (2012) Network analysis of the focal adhesion to invadopodia transition identifies a PI3K-PKCalpha invasive signaling axis. *Science signaling* 5(241):ra66.

20. Parker PJ & Murray-Rust J (2004) PKC at a glance. *Journal of cell science* 117(Pt 2):131-132.

21. Newton AC (2010) Protein kinase C: poised to signal. *American journal of physiology. Endocrinology and metabolism* 298(3):E395-402.

22. Hernandez AI, Blace N, Crary JF, Serrano PA, Leitges M, Libien JM, Weinstein G, Tcherapanov A, & Sacktor TC (2003) Protein kinase M zeta synthesis from a brain mRNA encoding an independent protein kinase C zeta catalytic domain. Implications for the molecular mechanism of memory. *The Journal of biological chemistry* 278(41):40305-40316.

23. Kikkawa U, Takai Y, Minakuchi R, Inohara S, & Nishizuka Y (1982) Calcium-activated, Phospholipid-dependent Protein Kinase from Rat Brain. *J. Biol. Chem.* 257:13341-13348.

24. Saito N, Kikkawa U, Nishizuka Y, & Tanaka C (1988) Distribution of Protein Kinase C-like Immunoreactive Neurons in Rat Brain. 8:369-382.

25. Go M, Nomura H, Kitano T, Koumoto J, Kikkawa U, Saito N, Tanaka C, & Nishizuka Y (1989) The protein kinase C family in the brain: heterogeneity and its implications. *Annals of the New York Academy of Sciences* 568(181):181-186.

26. Kikkawa U, Kitano T, Saito N, Fujiwara H, Nakanishi H, Kishimoto A, Taniyama K, Tanaka C, & Nishizuka Y (1991) Protein kinase C family and nervous function. *Prog Brain Res* 89(125):125-141.

27. Mochly-Rosen D, Basbaum AI, & Koshland DE, Jr. (1987) Distinct Cellular and Regional Localization of Immunoreactive Protein Kinase C in Rat Brain. *Proc. Natl. Acad. Sci. U. S. A.* 84:4660-4664.

28. Uhlen M, Fagerberg L, Hallstrom BM, Lindskog C, Oksvold P, Mardinoglu A, Sivertsson A, Kampf C, Sjostedt E, Asplund A, Olsson I, Edlund K, Lundberg E, Navani S, Szigyarto CA, Odeberg J, Djureinovic D, Takanen JO, Hober S, Alm T, Edqvist PH, Berling H, Tegel H, Mulder J, Rockberg J, Nilsson P, Schwenk JM, Hamsten M, von Feilitzen K, Forsberg M, Persson L, Johansson F, Zwahlen M, von Heijne G, Nielsen J, & Ponten F (2015) Proteomics. Tissue-based map of the human proteome. *Science (New York, N.Y.)* 347(6220):1260419.

29. Ding YQ, Xiang CX, & Chen ZF (2005) Generation and characterization of the PKC gamma-Cre mouse line. *Genesis* 43(1):28-33.

30. Antal CE & Newton AC (2014) Tuning the signalling output of protein kinase C. *Biochemical Society transactions* 42(6):1477-1483.

31. Antal CE, Violin JD, Kunkel MT, Skovso S, & Newton AC (2014) Intramolecular conformational changes optimize protein kinase C signaling. *Chemistry & biology* 21(4):459-469.

32. Antal CE, Callender JA, Kornov AP, Taylor SS, & Newton AC (2015) Intramolecular C2 Domain-Mediated Autoinhibition of Protein Kinase CbII. *Cell reports* 10.1016/j.celrep.2015.07.039.

33. Staudinger J, Lu J, & Olson EN (1997) Specific interaction of the PDZ domain protein PICK1 with the COOH terminus of protein kinase C-alpha. *The Journal of biological chemistry* 272(51):32019-32024.

34. O'Neill AK, Gallegos LL, Justilien V, Garcia EL, Leitges M, Fields AP, Hall RA, & Newton AC (2011) Protein kinase Calpha promotes cell migration through a PDZ-dependent interaction with its novel substrate discs large homolog 1 (DLG1). *The Journal of biological chemistry* 286(50):43559-43568.

35. Wu-Zhang AX & Newton AC (2013) Protein kinase C pharmacology: refining the toolbox. *The Biochemical journal* 452(2):195-209.

36. Rosse C, Linch M, Kermorgant S, Cameron AJ, Boeckeler K, & Parker PJ (2010) PKC and the control of localized signal dynamics. *Nature reviews. Molecular cell biology* 11(2):103-112.

37. Battaini F & Mochly-Rosen D (2007) Happy birthday protein kinase C: past, present and future of a superfamily. *Pharmacological research* 55(6):461-466.

38. Antal CE, Callender JA, Kornev AP, Taylor SS, & Newton AC (2015) Intramolecular C2 Domain-Mediated Autoinhibition of Protein Kinase C betaII. *Cell reports* 12(8):1252-1260.

39. Nishizuka Y (1984) Turnover of Inositol Phospholipids and Signal Transduction. *Science* 225:1365-1370.

40. Berridge MJ & Irvine RF (1984) Inositol trisphosphate, a novel second messenger in cellular signal transduction. *Nature* 312(5992):315-321.

41. Kruse M, Vivas O, Traynor-Kaplan A, & Hille B (2016) Dynamics of Phosphoinositide-Dependent Signaling in Sympathetic Neurons. *The Journal of neuroscience : the official journal of the Society for Neuroscience* 36(4):1386-1400.

42. Kraft AS, Anderson WB, Cooper HL, & Sando JJ (1982) Decrease in Cytosolic Calcium/Phospholipid-dependent Protein Kinase Activity Following Phorbol Ester Treatment of EL4 Thymoma Cells. *J. Biol. Chem.* 257:13193-13196.

43. Sakai N, Sasaki K, Ikegaki N, Shirai Y, Ono Y, & Saito N (1997) Direct visualization of the translocation of the gamma-subspecies of protein kinase C in living cells using fusion proteins with green fluorescent protein. *The Journal of cell biology* 139(6):1465-1476.

44. Mochly-Rosen D, Khaner H, & Lopez J (1991) Identification of intracellular receptor proteins for activated protein kinase C. *Proceedings of the National Academy of Sciences of the United States of America* 88(9):3997-4000.

45. Schechtman D & Mochly-Rosen D (2001) Adaptor proteins in protein kinase C-mediated signal transduction. *Oncogene* 20(44):6339-6347.

46. Dutil EM, Keranen LM, DePaoli-Roach AA, & Newton AC (1994) In vivo regulation of protein kinase C by trans-phosphorylation followed by autophosphorylation. *The Journal of biological chemistry* 269(47):29359-29362.

47. Hansra G, Garcia-Paramio P, Prevostel C, Whelan RD, Bornancin F, & Parker PJ (1999) Multisite dephosphorylation and desensitization of conventional protein kinase C isotypes. *The Biochemical journal* 342 (Pt 2):337-344.

48. Baffi TR, Van AN, Zhao W, Mills GB, & Newton AC (2019) Protein Kinase C Quality Control by Phosphatase PHLPP1 Unveils Loss-of-Function Mechanism in Cancer. *Molecular cell* 74(2):378-392.e375.

49. Szallasi Z, Smith CB, Pettit GR, & Blumberg PM (1994) Differential Regulation of Protein Kinase C Isozymes by Bryostatin 1 and Phorbol 12-Myristate 13-Acetate in NIH 3T3 Fibroblasts. *J. Biol. Chem.* 269:2118-2124.

50. Grodsky N, Li Y, Bouzida D, Love R, Jensen J, Nodes B, Nonomiya J, & Grant S (2006) Structure of the catalytic domain of human protein kinase C beta II complexed with a bisindolylmaleimide inhibitor. *Biochemistry* 45(47):13970-13981.

51. Messerschmidt A, Macieira S, Velarde M, Badeker M, Benda C, Jestel A, Brandstetter H, Neuefeind T, & Blaesse M (2005) Crystal structure of the catalytic domain of human atypical protein kinase C-iota reveals interaction mode of phosphorylation site in turn motif. *Journal of molecular biology* 352(4):918-931.

52. Takimura T, Kamata K, Fukasawa K, Ohsawa H, Komatani H, Yoshizumi T, Takahashi I, Kotani H, & Iwasawa Y (2010) Structures of the PKC-iota kinase domain in its ATP-bound and apo forms reveal defined structures of residues 533-551 in the C-terminal tail and their roles in ATP binding. *Acta crystallographica. Section D, Biological crystallography* 66(Pt 5):577-583.

53. Xu ZB, Chaudhary D, Olland S, Wolfrom S, Czerwinski R, Malakian K, Lin L, Stahl ML, Joseph-McCarthy D, Benander C, Fitz L, Greco R, Somers WS, & Mosyak L (2004) Catalytic domain crystal structure of protein kinase C-theta (PKCtheta). *J Biol Chem* 279(48):50401-50409.

54. Wagner J, von Matt P, Sedrani R, Albert R, Cooke N, Ehrhardt C, Geiser M, Rummel G, Stark W, Strauss A, Cowan-Jacob SW, Beerli C, Weckbecker G, Evenou JP, Zenke G, & Cottens S (2009) Discovery of 3-(1H-indol-3-yl)-4-[2-(4-methylpiperazin-1-yl)quinazolin-4-yl]pyrrole-2,5-dione (AEB071), a potent and selective inhibitor of protein kinase C isotypes. *Journal of medicinal chemistry* 52(20):6193-6196.

55. Guerrero-Valero M, Ferrer-Orta C, Querol-Audi J, Marin-Vicente C, Fita I, Gomez-Fernandez JC, Verdaguer N, & Corbalan-Garcia S (2009) Structural and mechanistic insights into the association of PKCalpha-C2 domain to PtdIns(4,5)P2. *Proceedings of the National Academy of Sciences of the United States of America* 106(16):6603-6607.

56. Littler DR, Walker JR, She YM, Finerty PJ, Jr., Newman EM, & Dhe-Paganon S (2006) Structure of human protein kinase C eta (PKCeta) C2 domain and identification of phosphorylation sites. *Biochemical and biophysical research communications* 349(4):1182-1189.

57. Ochoa WF, Garcia-Garcia J, Fita I, Corbalan-Garcia S, Verdaguer N, & Gomez-Fernandez JC (2001) Structure of the C2 domain from novel protein kinase Cepsilon. A membrane binding model for Ca(2+)-independent C2 domains. *Journal of molecular biology* 311(4):837-849.

58. Pappa H, Murray-Rust J, Dekker LV, Parker PJ, & McDonald NQ (1998) Crystal structure of the C2 domain from protein kinase C-delta. *Structure (London, England : 1993)* 6(7):885-894.

59. Sutton RB & Sprang SR (1998) Structure of the protein kinase Cbeta phospholipid-binding C2 domain complexed with Ca2+. *Structure (London, England : 1993)* 6(11):1395-1405.

60. Verdaguer N, Corbalan-Garcia S, Ochoa WF, Fita I, & Gomez-Fernandez JC (1999) Ca(2+) bridges the C2 membrane-binding domain of protein kinase Calpha directly to phosphatidylserine. *The EMBO journal* 18(22):6329-6338.

61. Hommel U, Zurini M, & Luyten M (1994) Solution structure of a cysteine rich domain of rat protein kinase C. *Nature structural biology* 1(6):383-387.

62. Xu RX, Pawelczyk T, Xia TH, & Brown SC (1997) NMR structure of a protein kinase C-gamma phorbol-binding domain and study of protein-lipid micelle interactions. *Biochemistry* 36(35):10709-10717.

63. Zhang G, Kazanietz MG, Blumberg PM, & Hurley JH (1995) Crystal structure of the cys2 activator-binding domain of protein kinase C delta in complex with phorbol ester. *Cell* 81(6):917-924.

64. Leonard TA, Rozycki B, Saidi LF, Hummer G, & Hurley JH (2011) Crystal structure and allosteric activation of protein kinase C betaII. *Cell* 144(1):55-66.

65. Yang Y, Shu C, Li P, & Igumenova TI (2018) Structural Basis of Protein Kinase Calpha Regulation by the C-Terminal Tail. *Biophysical journal* 114(7):1590-1603.

66. Wu WC, Walaas SI, Nairn AC, & Greengard P (1982) Calcium/phospholipid regulates phosphorylation of a Mr "87k" substrate protein in brain synaptosomes. *Proceedings of the National Academy of Sciences of the United States of America* 79(17):5249-5253.

67. Stumpo DJ, Graff JM, Albert KA, Greengard P, & Blackshear PJ (1989) Molecular cloning, characterization, and expression of a cDNA encoding the "80- to 87-kDa" myristoylated alanine-rich C kinase substrate: a major cellular substrate for protein kinase C. *Proceedings of the National Academy of Sciences of the United States of America* 86(11):4012-4016.

68. Brudvig JJ & Weimer JM (2015) X MARCKS the spot: myristoylated alanine-rich C kinase substrate in neuronal function and disease. *Frontiers in cellular neuroscience* 9:407.

69. Stumpo DJ, Bock CB, Tuttle JS, & Blackshear PJ (1995) MARCKS deficiency in mice leads to abnormal brain development and perinatal death. *Proceedings of the National Academy of Sciences of the United States of America* 92(4):944-948.

70. McLaughlin S & Aderem A (1995) The myristoyl-electrostatic switch: a modulator of reversible protein-membrane interactions. *Trends in biochemical sciences* 20:272-276.

71. Yarmola EG, Edison AS, Lenox RH, & Bubb MR (2001) Actin filament cross-linking by MARCKS: characterization of two actin-binding sites within the phosphorylation site domain. *The Journal of biological chemistry* 276(25):22351-22358.

72. Aderem A (1995) The MARCKS family of protein kinase-C substrates. *Biochemical Society transactions* 23(3):587-591.

73. Kim J, Blackshear PJ, Johnson JD, & McLaughlin S (1994) Phosphorylation Reverses the Membrane Association of Peptides that Correspond to the Basic Domains of MARCKS and Neuromodulin. *Biophys. J.* 67:227-237.

74. Thelen M, Rosen A, Nairn AC, & Aderem A (1991) Regulation by Phosphorylation of Reversible Association of a Myristoylated Protein Kinase C Substrate with the Plasma Membrane. *Nature* 351:320-322.

75. Hartwig JH, Thelen M, Rosen A, Janmey PA, Nairn AC, & Aderem A (1992) MARCKS is an actin filament crosslinking protein regulated by protein kinase C and calcium-calmodulin. *Nature* 356(6370):618-622.

76. Wohnsland F, Schmitz AA, Steinmetz MO, Aebi U, & Vergeres G (2000) Interaction between actin and the effector peptide of MARCKS-related protein. Identification of functional amino acid segments. *J Biol Chem* 275(27):20873-20879.

77. Benowitz LI & Routtenberg A (1997) GAP-43: an intrinsic determinant of neuronal development and plasticity. *Trends Neurosci* 20(2):84-91.

78. Tejero-Diez P, Rodriguez-Sanchez P, Martin-Cofreces NB, & Diez-Guerra FJ (2000) bFGF stimulates GAP-43 phosphorylation at ser41 and modifies its intracellular localization in cultured hippocampal neurons. *Molecular and cellular neurosciences* 16(6):766-780.

79. He Q, Dent EW, & Meiri KF (1997) Modulation of actin filament behavior by GAP-43 (neuromodulin) is dependent on the phosphorylation status of serine 41, the protein kinase C site. *The Journal of neuroscience : the official journal of the Society for Neuroscience* 17(10):3515-3524.

80. Alexander KA, Cimler BM, Meier KE, & Storm DR (1987) Regulation of calmodulin binding to P-57. A neurospecific calmodulin binding protein. *The Journal of biological chemistry* 262(13):6108-6113.

81. Coggins PJ & Zwiers H (1991) B-50 (GAP-43): biochemistry and functional neurochemistry of a neuron-specific phosphoprotein. *Journal of neurochemistry* 56(4):1095-1106.

82. Laux T, Fukami K, Thelen M, Golub T, Frey D, & Caroni P (2000) GAP43, MARCKS, and CAP23 modulate PI(4,5)P(2) at plasmalemmal rafts, and regulate cell cortex actin dynamics through a common mechanism. *The Journal of cell biology* 149(7):1455-1472.

83. Ziemba BP, Burke JE, Masson G, Williams RL, & Falke JJ (2016) Regulation of PI3K by PKC and MARCKS: Single-Molecule Analysis of a Reconstituted Signaling Pathway. *Biophys J* 110(8):1811-1825.

84. Wang Y & Mandelkow E (2016) Tau in physiology and pathology. *Nat Rev Neurosci* 17(1):5-21.

85. Kumar P, Jha NK, Jha SK, Ramani K, & Ambasta RK (2015) Tau phosphorylation, molecular chaperones, and ubiquitin E3 ligase: clinical relevance in Alzheimer's disease. *Journal of Alzheimer's disease : JAD* 43(2):341-361.

86. Correas I, Diaz-Nido J, & Avila J (1992) Microtubule-associated protein tau is phosphorylated by protein kinase C on its tubulin binding domain. *The Journal of biological chemistry* 267(22):15721-15728.

87. Isagawa T, Mukai H, Oishi K, Taniguchi T, Hasegawa H, Kawamata T, Tanaka C, & Ono Y (2000) Dual effects of PKNalpha and protein kinase C on phosphorylation of tau protein by glycogen synthase kinase-3beta. *Biochemical and biophysical research communications* 273(1):209-212.

88. De Montigny A, Elhiri I, Allyson J, Cyr M, & Massicotte G (2013) NMDA reduces Tau phosphorylation in rat hippocampal slices by targeting NR2A receptors, GSK3beta, and PKC activities. *Neural plasticity* 2013:261593.

89. Lee D, Kim E, & Tanaka-Yamamoto K (2016) Diacylglycerol Kinases in the Coordination of Synaptic Plasticity. *Frontiers in cell and developmental biology* 4:92.

90. Maren S (2005) Synaptic mechanisms of associative memory in the amygdala. *Neuron* 47(6):783-786.

91. Malenka RC & Bear MF (2004) LTP and LTD: an embarrassment of riches. *Neuron* 44(1):5-21.

92. Anggono V & Huganir RL (2012) Regulation of AMPA receptor trafficking and synaptic plasticity. *Current opinion in neurobiology* 22(3):461-469.

93. Malinow R, Madison DV, & Tsien RW (1988) Persistent protein kinase activity underlying long-term potentiation. *Nature* 335(6193):820-824.

94. Foster JD & Vaughan RA (2016) Phosphorylation Mechanisms in Dopamine Transporter Regulation. *Journal of chemical neuroanatomy*.

95. Bright DP & Smart TG (2013) Protein kinase C regulates tonic GABA(A) receptor-mediated inhibition in the hippocampus and thalamus. *The European journal of neuroscience* 38(10):3408-3423.

96. Illing S, Mann A, & Schulz S (2014) Heterologous regulation of agonist-independent mu-opioid receptor phosphorylation by protein kinase C. *British journal of pharmacology* 171(5):1330-1340.

97. Kim CH, Braud S, Isaac JT, & Roche KW (2005) Protein kinase C phosphorylation of the metabotropic glutamate receptor mGluR5 on Serine 839 regulates Ca2+ oscillations. *The Journal of biological chemistry* 280(27):25409-25415.

98. Boehm J, Kang MG, Johnson RC, Esteban J, Huganir RL, & Malinow R (2006) Synaptic incorporation of AMPA receptors during LTP is controlled by a PKC phosphorylation site on GluR1. *Neuron* 51(2):213-225.

99. Chung HJ, Xia J, Scannevin RH, Zhang X, & Huganir RL (2000) Phosphorylation of the AMPA receptor subunit GluR2 differentially regulates its interaction with PDZ domain-containing proteins. *The Journal of neuroscience : the official journal of the Society for Neuroscience* 20(19):7258-7267.

100. Perez JL, Khatri L, Chang C, Srivastava S, Osten P, & Ziff EB (2001) PICK1 targets activated protein kinase Calpha to AMPA receptor clusters in spines of hippocampal neurons and reduces surface levels of the AMPA-type glutamate receptor subunit 2. *The Journal of neuroscience : the official journal of the Society for Neuroscience* 21(15):5417-5428.

101. Hodge CW, Mehmert KK, Kelley SP, McMahon T, Haywood A, Olive MF, Wang D, Sanchez-Perez AM, & Messing RO (1999) Supersensitivity to allosteric GABA(A) receptor modulators and alcohol in mice lacking PKCepsilon. *Nature neuroscience* 2(11):997-1002.

102. Bright R & Mochly-Rosen D (2005) The role of protein kinase C in cerebral ischemic and reperfusion injury. *Stroke* 36(12):2781-2790.

103. Lee AM & Messing RO (2008) Protein kinases and addiction. *Annals of the New York Academy of Sciences* 1141:22-57.

104. Bernard C, Anderson A, Becker A, Poolos NP, Beck H, & Johnston D (2004) Acquired dendritic channelopathy in temporal lobe epilepsy. *Science (New York, N.Y.)* 305(5683):532-535.

105. Parker PJ, Justilien V, Riou P, Linch M, & Fields AP (2014) Atypical protein kinase Ciota as a human oncogene and therapeutic target. *Biochemical pharmacology* 88(1):1-11.

106. Van Cauwenberghe C, Van Broeckhoven C, & Sleegers K (2016) The genetic landscape of Alzheimer disease: clinical implications and perspectives. *Genetics in medicine : official journal of the American College of Medical Genetics* 18(5):421-430.

107. Sutovsky S, Blaho A, Kollar B, Siarnik P, Csefalvay Z, Dragasek J, & Turcani P (2014) Clinical accuracy of the distinction between Alzheimer's disease and frontotemporal lobar degeneration. *Bratislavske lekarske listy* 115(3):161-167.

108. Tanzi RE, Moir RD, & Wagner SL (2004) Clearance of Alzheimer's Abeta peptide: the many roads to perdition. *Neuron* 43(5):605-608.

109. Tagawa K, Homma H, Saito A, Fujita K, Chen X, Imoto S, Oka T, Ito H, Motoki K, Yoshida C, Hatsuta H, Murayama S, Iwatsubo T, Miyano S, & Okazawa H (2015) Comprehensive phosphoproteome analysis unravels the core signaling network that initiates the earliest synapse pathology in preclinical Alzheimer's disease brain. *Human molecular genetics* 24(2):540-558.

110. Masliah E, Cole GM, Hansen LA, Mallory M, Albright T, Terry RD, & Saitoh T (1991) Protein kinase C alteration is an early biochemical marker in Alzheimer's disease. *The Journal of neuroscience : the official journal of the Society for Neuroscience* 11(9):2759-2767.

111. Clark EA, Leach KL, Trojanowski JQ, & Lee VM (1991) Characterization and differential distribution of the three major human protein kinase C isozymes (PKC alpha, PKC beta, and PKC gamma) of the central nervous system in normal and Alzheimer's disease brains. *Laboratory investigation; a journal of technical methods and pathology* 64(1):35-44.

112. Kim T, Hinton DJ, & Choi DS (2011) Protein kinase C-regulated abeta production and clearance. *International journal of Alzheimer's disease* 2011:857368.

113. Fu H, Dou J, Li W, Cui W, Mak S, Hu Q, Luo J, Lam CS, Pang Y, Youdim MB, & Han Y (2009) Promising multifunctional anti-Alzheimer's dimer bis(7)-Cognitin acting as an activator of protein kinase C regulates activities of alpha-secretase and BACE-1 concurrently. *European journal of pharmacology* 623(1-3):14-21.

114. Savage MJ, Trusko SP, Howland DS, Pinsker LR, Mistretta S, Reaume AG, Greenberg BD, Siman R, & Scott RW (1998) Turnover of amyloid beta-protein in mouse brain and acute reduction of its level by phorbol ester. *The Journal of neuroscience : the official journal of the Society for Neuroscience* 18(5):1743-1752.

115. Ehehalt R, Keller P, Haass C, Thiele C, & Simons K (2003) Amyloidogenic processing of the Alzheimer beta-amyloid precursor protein depends on lipid rafts. *The Journal of cell biology* 160(1):113-123.

116. Zhu G, Wang D, Lin YH, McMahon T, Koo EH, & Messing RO (2001) Protein kinase C epsilon suppresses Abeta production and promotes activation of alpha-secretase. *Biochemical and biophysical research communications* 285(4):997-1006.

117. Cataldo AM, Peterhoff CM, Troncoso JC, Gomez-Isla T, Hyman BT, & Nixon RA (2000) Endocytic pathway abnormalities precede amyloid beta deposition in sporadic Alzheimer's disease and Down syndrome: differential effects of APOE genotype and presenilin mutations. *The American journal of pathology* 157(1):277-286.

118. Cataldo AM, Barnett JL, Pieroni C, & Nixon RA (1997) Increased neuronal endocytosis and protease delivery to early endosomes in sporadic Alzheimer's disease: neuropathologic evidence for a mechanism of increased beta-amyloidogenesis. *The Journal of neuroscience : the official journal of the Society for Neuroscience* 17(16):6142-6151.

119. Xu W, Weissmiller AM, White JA, 2nd, Fang F, Wang X, Wu Y, Pearn ML, Zhao X, Sawa M, Chen S, Gunawardena S, Ding J, Mobley WC, & Wu C (2016) Amyloid precursor protein-mediated endocytic pathway disruption induces axonal dysfunction and neurodegeneration. *The Journal of clinical investigation* 126(5):1815-1833.

120. Su R, Han ZY, Fan JP, & Zhang YL (2010) A possible role of myristoylated alanine-rich C kinase substrate in endocytic pathway of Alzheimer's disease. *Neuroscience bulletin* 26(4):338-344.

121. Alfonso SI, Callender JA, Hooli B, Antal CE, Mullin K, Sherman MA, Lesne SE, Leitges M, Newton AC, Tanzi RE, & Malinow R (2016) Gain-of-function mutations in protein kinase Calpha (PKCalpha) may promote synaptic defects in Alzheimer's disease. *Science signaling* 9(427):ra47.

122. Hoshi N, Langeberg LK, Gould CM, Newton AC, & Scott JD (2010) Interaction with AKAP79 modifies the cellular pharmacology of PKC. *Molecular cell* 37(4):541-550.

123. Hsieh H, Boehm J, Sato C, Iwatsubo T, Tomita T, Sisodia S, & Malinow R (2006) AMPAR removal underlies Abeta-induced synaptic depression and dendritic spine loss. *Neuron* 52(5):831-843.

124. Alfonso S, Kessels HW, Banos CC, Chan TR, Lin ET, Kumaravel G, Scannevin RH, Rhodes KJ, Huganir R, Guckian KM, Dunah AW, & Malinow R (2014) Synapto-depressive effects of amyloid beta require PICK1. *The European journal of neuroscience* 39(7):1225-1233.

125. Leitges M, Kovac J, Plomann M, & Linden DJ (2004) A unique PDZ ligand in PKCalpha confers induction of cerebellar long-term synaptic depression. *Neuron* 44(4):585-594.

126. Verbeek DS, Goedhart J, Bruinsma L, Sinke RJ, & Reits EA (2008) PKC gamma mutations in spinocerebellar ataxia type 14 affect C1 domain accessibility and kinase activity leading to aberrant MAPK signaling. *Journal of cell science* 121(Pt 14):2339-2349.

127. Yamamoto K, Seki T, Adachi N, Takahashi T, Tanaka S, Hide I, Saito N, & Sakai N (2010) Mutant protein kinase C gamma that causes spinocerebellar ataxia type 14 (SCA14) is selectively degraded by autophagy. *Genes Cells* 15(5):425-438.

128. Adachi N, Kobayashi T, Takahashi H, Kawasaki T, Shirai Y, Ueyama T, Matsuda T, Seki T, Sakai N, & Saito N (2008) Enzymological analysis of mutant protein kinase Cgamma causing spinocerebellar ataxia type 14 and dysfunction in Ca2+ homeostasis. *The Journal of biological chemistry* 283(28):19854-19863.

129. Aramillo Irizar P, Schauble S, Esser D, Groth M, Frahm C, Priebe S, Baumgart M, Hartmann N, Marthandan S, Menzel U, Muller J, Schmidt S, Ast V, Caliebe A, Konig R, Krawczak M, Ristow M, Schuster S, Cellerino A, Diekmann S, Englert C, Hemmerich P, Suhnel J, Guthke R, Witte OW, Platzer M, Ruppin E, & Kaleta C (2018) Transcriptomic alterations during ageing reflect the shift from cancer to degenerative diseases in the elderly. *Nature communications* 9(1):327.

130. Roe CM & Behrens MI (2013) AD and cancer: epidemiology makes for strange bedfellows. *Neurology* 81(4):310-311.

131. Roe CM, Behrens MI, Xiong C, Miller JP, & Morris JC (2005) Alzheimer disease and cancer. *Neurology* 64(5):895-898.

132. Shi HB, Tang B, Liu YW, Wang XF, & Chen GJ (2015) Alzheimer disease and cancer risk: a meta-analysis. *Journal of cancer research and clinical oncology* 141(3):485-494.

133. Terry RD, Masliah E, Salmon DP, Butters N, DeTeresa R, Hill R, Hansen LA, & Katzman R (1991) Physical basis of cognitive alterations in Alzheimer's disease: synapse loss is the major correlate of cognitive impairment. *Ann Neurol* 30(4):572-580.

134. Selkoe DJ (2002) Alzheimer's disease is a synaptic failure. *Science* 298(5594):789-791.

135. Hsia AY, Masliah E, McConlogue L, Yu GQ, Tatsuno G, Hu K, Kholodenko D, Malenka RC, Nicoll RA, & Mucke L (1999) Plaque-independent disruption of neural circuits in Alzheimer's disease mouse models. *Proc Natl Acad Sci U S A* 96(6):3228-3233.

136. Mucke L, Masliah E, Yu GQ, Mallory M, Rockenstein EM, Tatsuno G, Hu K, Kholodenko D, Johnson-Wood K, & McConlogue L (2000) High-level neuronal expression of abeta 1-42 in wild-type human amyloid protein precursor transgenic mice: synaptotoxicity without plaque formation. *J Neurosci* 20(11):4050-4058.

137. Oddo S, Caccamo A, Shepherd JD, Murphy MP, Golde TE, Kayed R, Metherate R, Mattson MP, Akbari Y, & LaFerla FM (2003) Triple-transgenic model of Alzheimer's disease with plaques and tangles: intracellular Abeta and synaptic dysfunction. *Neuron* 39(3):409-421.

138. Kamenetz F, Tomita T, Hsieh H, Seabrook G, Borchelt D, Iwatsubo T, Sisodia S, & Malinow R (2003) APP processing and synaptic function. *Neuron* 37(6):925-937.

139. Wilcox KC, Lacor PN, Pitt J, & Klein WL (2011) Abeta oligomer-induced synapse degeneration in Alzheimer's disease. *Cellular and molecular neurobiology* 31(6):939-948.

140. Holtzman DM, Mandelkow E, & Selkoe DJ (2012) Alzheimer disease in 2020. *Cold Spring Harbor perspectives in medicine* 2(11).

141. Corder EH, Saunders AM, Strittmatter WJ, Schmechel DE, Gaskell PC, Small GW, Roses AD, Haines JL, & Pericak-Vance MA (1993) Gene dose of apolipoprotein E type 4 allele and the risk of Alzheimer's disease in late onset families. *Science* 261(5123):921-923.

142. Pimplikar SW, Nixon RA, Robakis NK, Shen J, & Tsai LH (2010) Amyloid-independent mechanisms in Alzheimer's disease pathogenesis. *J Neurosci* 30(45):14946-14954.

143. Shen J (2014) Function and dysfunction of presenilin. *Neuro-degenerative diseases* 13(2-3):61-63.

144. Woodruff G, Reyna SM, Dunlap M, Van Der Kant R, Callender JA, Young JE, Roberts EA, & Goldstein LS (2016) Defective Transcytosis of APP and Lipoproteins in Human iPSC-Derived Neurons with Familial Alzheimer's Disease Mutations. *Cell reports* 17(3):759-773.

145. Wei W, Nguyen LN, Kessels HW, Hagiwara H, Sisodia S, & Malinow R (2010) Amyloid beta from axons and dendrites reduces local spine number and plasticity. *Nat Neurosci* 13(2):190-196.

146. Haass C, Kaether C, Thinakaran G, & Sisodia S (2012) Trafficking and proteolytic processing of APP. *Cold Spring Harbor perspectives in medicine* 2(5):a006270.

147. Violin JD, Zhang J, Tsien RY, & Newton AC (2003) A genetically encoded fluorescent reporter reveals oscillatory phosphorylation by protein kinase C. *The Journal of cell biology* 161(5):899-909.

148. Leitges M, Plomann M, Standaert ML, Bandyopadhyay G, Sajan MP, Kanoh Y, & Farese RV (2002) Knockout of PKC alpha enhances insulin signaling through PI3K. *Molecular endocrinology* 16(4):847-858.

149. Kessels HW, Nabavi S, & Malinow R (2013) Metabotropic NMDA receptor function is required for beta-amyloid-induced synaptic depression. *Proc Natl Acad Sci U S A* 110(10):4033-4038.

150. Antal CE, Callender JA, Kornev AP, Taylor SS, & Newton AC (2015) Intramolecular C2 Domain-Mediated Autoinhibition of Protein Kinase C βII. *Cell reports* 12(8):1252-1260.

151. Keranen LM, Dutil EM, & Newton AC (1995) Protein kinase C is regulated in vivo by three functionally distinct phosphorylations. *Curr Biol* 5(12):1394-1403.

152. Dutil EM, Keranen LM, DePaoli-Roach AA, & Newton AC (1994) In vivo regulation of protein kinase C by trans-phosphorylation followed by autophosphorylation. *J Biol Chem* 269(47):29359-29362.

153. Kawahara M, Negishi-Kato M, & Sadakane Y (2009) Calcium dyshomeostasis and neurotoxicity of Alzheimer's beta-amyloid protein. *Expert review of neurotherapeutics* 9(5):681-693.

154. Agostini M & Fasolato C (2016) When, where and how? Focus on neuronal calcium dysfunctions in Alzheimer's Disease. *Cell calcium* 60(5):289-298.

155. Oseki KT, Monteforte PT, Pereira GJ, Hirata H, Ureshino RP, Bincoletto C, Hsu YT, & Smaili SS (2014) Apoptosis induced by Abeta25-35 peptide is Ca(2+) -IP3 signaling-dependent in murine astrocytes. *The European journal of neuroscience* 40(3):2471-2478.

156. Guerreiro R, Wojtas A, Bras J, Carrasquillo M, Rogaeva E, Majounie E, Cruchaga C, Sassi C, Kauwe JS, Younkin S, Hazrati L, Collinge J, Pocock J, Lashley T, Williams J, Lambert JC, Amouyel P, Goate A, Rademakers R, Morgan K, Powell J, St George-Hyslop P, Singleton A, Hardy J, & Alzheimer Genetic Analysis G (2013) TREM2 variants in Alzheimer's disease. *N Engl J Med* 368(2):117-127.

157. Cruchaga C, Karch CM, Jin SC, Benitez BA, Cai Y, Guerreiro R, Harari O, Norton J, Budde J, Bertelsen S, Jeng AT, Cooper B, Skorupa T, Carrell D, Levitch D, Hsu S, Choi J, Ryten M, Consortium UKBE, Hardy J, Ryten M, Trabzuni D, Weale ME, Ramasamy A, Smith C, Sassi C, Bras J, Gibbs JR, Hernandez DG, Lupton MK, Powell J, Forabosco P, Ridge PG, Corcoran CD, Tschanz JT, Norton MC, Munger RG, Schmutz C, Leary M, Demirci FY, Bamne MN, Wang X, Lopez OL, Ganguli M, Medway C, Turton J, Lord J, Braae A, Barber I, Brown K, Alzheimer's Research UKC, Passmore P, Craig D, Johnston J, McGuinness B, Todd S, Heun R, Kolsch H, Kehoe PG, Hooper NM, Vardy ER,

Mann DM, Pickering-Brown S, Brown K, Kalsheker N, Lowe J, Morgan K, David Smith A, Wilcock G, Warden D, Holmes C, Pastor P, Lorenzo-Betancor O, Brkanac Z, Scott E, Topol E, Morgan K, Rogaeva E, Singleton AB, Hardy J, Kamboh MI, St George-Hyslop P, Cairns N, Morris JC, Kauwe JS, & Goate AM (2014) Rare coding variants in the phospholipase D3 gene confer risk for Alzheimer's disease. *Nature* 505(7484):550-554.

158. Mucke L & Selkoe DJ (2012) Neurotoxicity of amyloid beta-protein: synaptic and network dysfunction. *Cold Spring Harbor perspectives in medicine* 2(7):a006338.

159. Querfurth HW & LaFerla FM (2010) Alzheimer's disease. *N Engl J Med* 362(4):329-344.

160. da Cruz e Silva OA, Rebelo S, Vieira SI, Gandy S, da Cruz e Silva EF, & Greengard P (2009) Enhanced generation of Alzheimer's amyloid-beta following chronic exposure to phorbol ester correlates with differential effects on alpha and epsilon isozymes of protein kinase C. *Journal of neurochemistry* 108(2):319-330.

161. Lane RF, Gatson JW, Small SA, Ehrlich ME, & Gandy S (2010) Protein kinase C and rho activated coiled coil protein kinase 2 (ROCK2) modulate Alzheimer's APP metabolism and phosphorylation of the Vps10-domain protein, SorL1. *Molecular neurodegeneration* 5:62.

162. Kinouchi T, Sorimachi H, Maruyama K, Mizuno K, Ohno S, Ishiura S, & Suzuki K (1995) Conventional protein kinase C (PKC)-alpha and novel PKC epsilon, but not -delta, increase the secretion of an N-terminal fragment of Alzheimer's disease amyloid precursor protein from PKC cDNA transfected 3Y1 fibroblasts. *FEBS letters* 364(2):203-206.

163. Magi S, Castaldo P, Macri ML, Maiolino M, Matteucci A, Bastioli G, Gratteri S, Amoroso S, & Lariccia V (2016) Intracellular Calcium Dysregulation: Implications for Alzheimer's Disease. *BioMed research international* 2016:6701324.

164. Smith IF, Green KN, & LaFerla FM (2005) Calcium dysregulation in Alzheimer's disease: recent advances gained from genetically modified animals. *Cell calcium* 38(3-4):427-437.

165. Driver JA, Beiser A, Au R, Kreger BE, Splansky GL, Kurth T, Kiel DP, Lu KP, Seshadri S, & Wolf PA (2012) Inverse association between cancer and Alzheimer's disease: results from the Framingham Heart Study. *BMJ (Clinical research ed.)* 344:e1442.

166. Stoppini L, Buchs PA, & Muller D (1991) A simple method for organotypic cultures of nervous tissue. *J Neurosci Methods* 37(2):173-182.

167. Efron B (1979) 1977 Rietz Lecture - Bootstrap Methods - Another Look at the Jackknife. *Ann Stat* 7(1):1-26.

168. Dutil EM, Toker A, & Newton AC (1998) Regulation of conventional protein kinase C isozymes by phosphoinositide-dependent kinase 1 (PDK-1). *Current biology : CB* 8(25):1366-1375.

169. Dusaban SS, Chun J, Rosen H, Purcell NH, & Brown JH (2017) Sphingosine 1-phosphate receptor 3 and RhoA signaling mediate inflammatory gene expression in astrocytes. *Journal of neuroinflammation* 14(1):111.

170. Gallegos LL, Kunkel MT, & Newton AC (2006) Targeting protein kinase C activity reporter to discrete intracellular regions reveals spatiotemporal differences in agonist-dependent signaling. *The Journal of biological chemistry* 281(41):30947-30956.

171. Blacker D, Bertram L, Saunders AJ, Moscarillo TJ, Albert MS, Wiener H, Perry RT, Collins JS, Harrell LE, Go RC, Mahoney A, Beaty T, Fallin MD, Avramopoulos D, Chase GA, Folstein MF, McInnis MG, Bassett SS, Doheny KJ, Pugh EW, Tanzi RE, & Group NGIAsDS (2003) Results of a high-resolution genome screen of 437 Alzheimer's disease families. *Hum Mol Genet* 12(1):23-32.

172. McKenna A, Hanna M, Banks E, Sivachenko A, Cibulskis K, Kernytsky A, Garimella K, Altshuler D, Gabriel S, Daly M, & DePristo MA (2010) The Genome Analysis Toolkit: a MapReduce framework for analyzing next-generation DNA sequencing data. *Genome research* 20(9):1297-1303.

173. Paila U, Chapman BA, Kirchner R, & Quinlan AR (2013) GEMINI: integrative exploration of genetic variation and genome annotations. *PLoS computational biology* 9(7):e1003153.

174. Nishizuka Y (1995) Protein kinase C and lipid signaling for sustained cellular responses. *FASEB journal : official publication of the Federation of American Societies for Experimental Biology* 9(7):484-496.

175. Pysz MA, Leontieva OV, Bateman NW, Uronis JM, Curry KJ, Threadgill DW, Janssen KP, Robine S, Velcich A, Augenlicht LH, Black AR, & Black JD (2009) PKCalpha tumor suppression in the intestine is associated with transcriptional and translational inhibition of cyclin D1. *Experimental cell research* 315(8):1415-1428.

176. Saxon ML, Zhao X, & Black JD (1994) Activation of protein kinase C isozymes is associated with post-mitotic events in intestinal epithelial cells in situ. *The Journal of cell biology* 126(3):747-763.

177. Frey MR, Saxon ML, Zhao X, Rollins A, Evans SS, & Black JD (1997) Protein kinase C isozyme-mediated cell cycle arrest involves induction of p21(waf1/cip1) and p27(kip1) and hypophosphorylation of the retinoblastoma protein in intestinal epithelial cells. *The Journal of biological chemistry* 272(14):9424-9435.

178. Black JD ed (2010) *PKC and Control of the Cell Cycle* (Humana Press, Totowa, NJ), pp 155-188.

179. Jerome-Morais A, Rahn HR, Tibudan SS, & Denning MF (2009) Role for protein kinase C-alpha in keratinocyte growth arrest. *J Invest Dermatol* 129(10):2365-2375.

180. Newton AC & Brognard J (2017) Reversing the Paradigm: Protein Kinase C as a Tumor Suppressor. *Trends in pharmacological sciences* 38(5):438-447.

181. Oster H & Leitges M (2006) Protein kinase C alpha but not PKCzeta suppresses intestinal tumor formation in ApcMin/+ mice. *Cancer research* 66(14):6955-6963.

182. Suga K, Sugimoto I, Ito H, & Hashimoto E (1998) Down-regulation of protein kinase C-alpha detected in human colorectal cancer. *Biochemistry and molecular biology international* 44(3):523-528.

183. Prevostel C, Alvaro V, de Boisvilliers F, Martin A, Jaffiol C, & Joubert D (1995) The natural protein kinase C alpha mutant is present in human thyroid neoplasms. *Oncogene* 11(4):669-674.

184. Alvaro V, Prevostel C, Joubert D, Slosberg E, & Weinstein BI (1997) Ectopic expression of a mutant form of PKCalpha originally found in human tumors: aberrant subcellular translocation and effects on growth control. *Oncogene* 14(6):677-685.

185. Vallentin A, Lo TC, & Joubert D (2001) A single point mutation in the V3 region affects protein kinase Calpha targeting and accumulation at cell-cell contacts. *Molecular and cellular biology* 21(10):3351-3363.

186. Kataoka K, Nagata Y, Kitanaka A, Shiraishi Y, Shimamura T, Yasunaga J, Totoki Y, Chiba K, Sato-Otsubo A, Nagae G, Ishii R, Muto S, Kotani S, Watatani Y, Takeda J, Sanada M, Tanaka H, Suzuki H, Sato Y, Shiozawa Y, Yoshizato T, Yoshida K, Makishima H, Iwanaga M, Ma G, Nosaka K, Hishizawa M, Itonaga H, Imaizumi Y, Munakata W, Ogasawara H, Sato T, Sasai K, Muramoto K, Penova M, Kawaguchi T, Nakamura H, Hama N, Shide K, Kubuki Y, Hidaka T, Kameda T, Nakamaki T, Ishiyama K, Miyawaki S, Yoon SS, Tobinai K, Miyazaki Y, Takaori-Kondo A, Matsuda F, Takeuchi K, Nureki O, Aburatani H, Watanabe T, Shibata T, Matsuoka M, Miyano S, Shimoda K, & Ogawa S (2015) Integrated molecular analysis of adult T cell leukemia/lymphoma. *Nature genetics* 47(11):1304-1315.

187. Gallegos LL & Newton AC (2008) Spatiotemporal dynamics of lipid signaling: protein kinase C as a paradigm. *IUBMB Life* 60(12):782-789.

188. Kraft AS, Anderson WB, Cooper HL, & Sando JJ (1982) Decrease in cytosolic calcium/phospholipid-dependent protein kinase activity following phorbol ester treatment of EL4 thymoma cells. *The Journal of biological chemistry* 257(22):13193-13196.

189. Szallasi Z, Smith CB, Pettit GR, & Blumberg PM (1994) Differential regulation of protein kinase C isozymes by bryostatin 1 and phorbol 12-myristate 13-acetate in NIH 3T3 fibroblasts. *The Journal of biological chemistry* 269(3):2118-2124.

190. Kornev AP & Taylor SS (2015) Dynamics-Driven Allostery in Protein Kinases. *Trends in biochemical sciences* 40(11):628-647.

191. Violin JD & Newton AC (2003) Pathway illuminated: visualizing protein kinase C signaling. *IUBMB Life* 55(12):653-660.

192. Hannun YA, Loomis CR, & Bell RM (1985) Activation of Protein Kinase C by Triton X-100 Mixed Micelles Containing Diacylglycerol and Phosphatidylserine. *J. Biol. Chem.* 260:10039-10043.

193. Orr JW & Newton AC (1992) Interaction of protein kinase C with phosphatidylserine. 1. Cooperativity in lipid binding. *Biochemistry* 31(19):4661-4667.

194. Orr JW & Newton AC (1992) Interaction of protein kinase C with phosphatidylserine. 2. Specificity and regulation. *Biochemistry* 31(19):4667-4673.

195. Greenwald EC, Redden JM, Dodge-Kafka KL, & Saucerman JJ (2014) Scaffold state switching amplifies, accelerates, and insulates protein kinase C signaling. *The Journal of biological chemistry* 289(4):2353-2360.

196. Eisenmesser EZ, Millet O, Labeikovsky W, Korzhnev DM, Wolf-Watz M, Bosco DA, Skalicky JJ, Kay LE, & Kern D (2005) Intrinsic dynamics of an enzyme underlies catalysis. *Nature* 438(7064):117-121.

197. Holliday MJ, Camilloni C, Armstrong GS, Vendruscolo M, & Eisenmesser EZ (2017) Networks of Dynamic Allostery Regulate Enzyme Function. *Structure (London, England : 1993)* 25(2):276-286.

198. Joseph RE, Kleino I, Wales TE, Xie Q, Fulton DB, Engen JR, Berg LJ, & Andreotti AH (2013) Activation loop dynamics determine the different catalytic efficiencies of B cell- and T cell-specific tec kinases. *Science signaling* 6(290):ra76.

199. Kornev AP, Haste NM, Taylor SS, & Eyck LF (2006) Surface comparison of active and inactive protein kinases identifies a conserved activation mechanism. *Proceedings of the National Academy of Sciences of the United States of America* 103(47):17783-17788.

200. Zhou J & Adams JA (1997) Participation of ADP dissociation in the rate-determining step in cAMP-dependent protein kinase. *Biochemistry* 36(50):15733-15738.

201. Bar-Even A, Noor E, Savir Y, Liebermeister W, Davidi D, Tawfik DS, & Milo R (2011) The moderately efficient enzyme: evolutionary and physicochemical trends shaping enzyme parameters. *Biochemistry* 50(21):4402-4410.

202. Levinson NM, Seeliger MA, Cole PA, & Kuriyan J (2008) Structural basis for the recognition of c-Src by its inactivator Csk. *Cell* 134(1):124-134.

203. Newton AC (2017) Protein kinase C as a tumor suppressor. *Seminars in cancer biology*.

204. McSkimming DI, Dastgheib S, Baffi TR, Byrne DP, Ferries S, Scott ST, Newton AC, Eyers CE, Kochut KJ, Eyers PA, & Kannan N (2016) KinView: a visual comparative sequence analysis tool for integrated kinome research. *Molecular bioSystems* 12(12):3651-3665.

205. Marshall JL, Bangalore N, El-Ashry D, Fuxman Y, Johnson M, Norris B, Oberst M, Ness E, Wojtowicz-Praga S, Bhargava P, Rizvi N, Baidas S, & Hawkins MJ (2002) Phase I study of prolonged infusion Bryostatin-1 in patients with advanced malignancies. *Cancer biology & therapy* 1(4):409-416.

206. Tobias IS, Kaulich M, Kim PK, Simon N, Jacinto E, Dowdy SF, King CC, & Newton AC (2016) Protein kinase Czeta exhibits constitutive phosphorylation and phosphatidylinositol-3,4,5-triphosphate-independent regulation. *The Biochemical journal* 473(4):509-523.

207. Keranen LM & Newton AC (1997) Ca2+ differentially regulates conventional protein kinase Cs' membrane interaction and activation. *The Journal of biological chemistry* 272(41):25959-25967.

208. Newton AC & Koshland DE, Jr. (1989) High cooperativity, specificity, and multiplicity in the protein kinase C-lipid interaction. *The Journal of biological chemistry* 264(25):14909-14915.

209. Schoenmakers TJ, Visser GJ, Flik G, & Theuvenet AP (1992) CHELATOR: an improved method for computing metal ion concentrations in physiological solutions. *BioTechniques* 12(6):870-874, 876-879.

210. Essmann U, Perera L, Berkowitz ML, Darden T, Lee H, & Pedersen LG (1995) A Smooth Particle Mesh Ewald Method. *J Chem Phys* 103(19):8577-8593.

211. Berendsen HJC, Postma JPM, Vangunsteren WF, Dinola A, & Haak JR (1984) Molecular-Dynamics with Coupling to an External Bath. *J Chem Phys* 81(8):3684-3690.

212. Nose S (1984) A Unified Formulation of the Constant Temperature Molecular-Dynamics Methods. *J Chem Phys* 81(1):511-519.

213. Parrinello M & Rahman A (1981) Polymorphic Transitions in Single-Crystals - a New Molecular-Dynamics Method. *J Appl Phys* 52(12):7182-7190.

214. Newton AC (2018) Protein kinase C: perfectly balanced. *Critical reviews in biochemistry and molecular biology* 53(2):208-230.

215. Newton AC (2003) Regulation of the ABC kinases by phosphorylation: protein kinase C as a paradigm. *The Biochemical journal* 370(Pt 2):361-371.

216. Blumberg PM, Kedei N, Lewin NE, Yang D, Czifra G, Pu Y, Peach ML, & Marquez VE (2008) Wealth of opportunity - the C1 domain as a target for drug development. *Current drug targets* 9(8):641-652.

217. Corbalan-Garcia S, Guerrero-Valero M, Marin-Vicente C, & Gomez-Fernandez JC (2007) The C2 domains of classical/conventional PKCs are specific PtdIns(4,5)P(2)-sensing domains. *Biochemical Society transactions* 35(Pt 5):1046-1048.

218. Cho W & Stahelin RV (2006) Membrane binding and subcellular targeting of C2 domains. *Biochimica et biophysica acta* 1761(8):838-849.

219. Johnson JE, Giorgione J, & Newton AC (2000) The C1 and C2 domains of protein kinase C are independent membrane targeting modules, with specificity for phosphatidylserine conferred by the C1 domain. *Biochemistry* 39(37):11360-11369.

220. Medkova M & Cho W (1999) Interplay of C1 and C2 domains of protein kinase C-alpha in its membrane binding and activation. *The Journal of biological chemistry* 274(28):19852-19861.

221. Borner C, Filipuzzi I, Wartmann M, Eppenberger U, & Fabbro D (1989) Biosynthesis and posttranslational modifications of protein kinase C in human breast cancer cells. *J Biol Chem* 264(23):13902-13909.

222. Newton AC (2001) Protein kinase C: structural and spatial regulation by phosphorylation, cofactors, and macromolecular interactions. *Chemical reviews* 101(8):2353-2364.

223. Gschwendt M, Kielbassa K, Kittstein W, & Marks F (1994) Tyrosine phosphorylation and stimulation of protein kinase C delta from porcine spleen by src in vitro. Dependence on the activated state of protein kinase C delta. *FEBS letters* 347(1):85-89.

224. Li W, Mischak H, Yu JC, Wang LM, Mushinski JF, Heidaran MA, & Pierce JH (1994) Tyrosine phosphorylation of protein kinase C-delta in response to its activation. *The Journal of biological chemistry* 269(4):2349-2352.

225. Liu F & Roth RA (1994) Insulin-stimulated tyrosine phosphorylation of protein kinase C alpha: evidence for direct interaction of the insulin receptor and protein kinase C in cells. *Biochemical and biophysical research communications* 200(3):1570-1577.

226. Konishi H, Tanaka M, Takemura Y, Matsuzaki H, Ono Y, Kikkawa U, & Nishizuka Y (1997) Activation of protein kinase C by tyrosine phosphorylation in response to H2O2. *Proceedings of the National Academy of Sciences of the United States of America* 94(21):11233-11237.

227. Hornbeck PV, Zhang B, Murray B, Kornhauser JM, Latham V, & Skrzypek E (2015) PhosphoSitePlus, 2014: mutations, PTMs and recalibrations. *Nucleic acids research* 43(Database issue):D512-520.

228. Oancea E & Meyer T (1998) Protein kinase C as a molecular machine for decoding calcium and diacylglycerol signals. *Cell* 95(3):307-318.

229. Stensman H, Raghunath A, & Larsson C (2004) Autophosphorylation suppresses whereas kinase inhibition augments the translocation of protein kinase Cα in response to diacylglycerol. *J. Biol. Chem.* 279(39):40576-40583.

230. Antal CE, Violin JD, Kunkel MT, Skovso S, & Newton AC (2014) Intramolecular Conformational Changes Optimize Protein Kinase C Signaling. *Chem. Biol.* 21(4):459-469.

231. Antal CE, Callender JA, Kornev AP, Taylor SS, & Newton AC (2015) Intramolecular C2 domain-mediated autoinhibition of protein kinase C βII. *Cell reports* 12(8):1252-1260.

232. Manna D, Bhardwaj N, Vora MS, Stahelin RV, Lu H, & Cho WH (2008) Differential roles of phosphatidylserine, PtdIns(4,5)P-2, and PtdIns(3,4,5)P-3 in plasma membrane targeting of C2 domains - Molecular dynamics simulation, membrane binding, and cell translocation studies of the PKC alpha C2 domain. *J. Biol. Chem.* 283(38):26047-26058.

233. Gao J, Aksoy BA, Dogrusoz U, Dresdner G, Gross B, Sumer SO, Sun Y, Jacobsen A, Sinha R, Larsson E, Cerami E, Sander C, & Schultz N (2013) Integrative analysis of complex cancer genomics and clinical profiles using the cBioPortal. *Science signaling* 6(269):pl1.

234. Cerami E, Gao J, Dogrusoz U, Gross BE, Sumer SO, Aksoy BA, Jacobsen A, Byrne CJ, Heuer ML, Larsson E, Antipin Y, Reva B, Goldberg AP, Sander C, & Schultz N (2012) The cBio cancer genomics portal: an open platform for exploring multidimensional cancer genomics data. *Cancer discovery* 2(5):401-404.

235. Scott AM, Antal CE, & Newton AC (2013) Electrostatic and hydrophobic interactions differentially tune membrane binding kinetics of the C2 domain of protein kinase Calpha. *The Journal of biological chemistry* 288(23):16905-16915.

236. Stensman H & Larsson C (2007) Identification of acidic amino acid residues in the protein kinase C alpha V5 domain that contribute to its insensitivity to diacylglycerol. *J. Biol. Chem.* 282(39):28627-28638.

237. Slater SJ, Seiz JL, Cook AC, Buzas CJ, Malinowski SA, Kershner JL, Stagliano BA, & Stubbs CD (2002) Regulation of PKC alpha activity by C1-C2 domain interactions. *J. Biol. Chem.* 277(18):15277-15285.

238. Stahelin RV, Wang JY, Blatner NR, Raftner JD, Murray D, & Cho WH (2005) The origin of C1A-C2 interdomain interactions in protein kinase C alpha. *J. Biol. Chem.* 280(43):36452-36463.

239. Keranen LM & Newton AC (1997) Ca2+ differentially regulates conventional protein kinase Cs' membrane interaction and activation. *J. Biol. Chem.* 272(41):25959-25967.

240. Violin JD, Zhang J, Tsien RY, & Newton AC (2003) A genetically encoded fluorescent reporter reveals oscillatory phosphorylation by protein kinase C. *The Journal of cell biology* 161(5):899-909.

241. Gallegos LL, Kunkel MT, & Newton AC (2006) Targeting protein kinase C activity reporter to discrete intracellular regions reveals spatiotemporal differences in agonist-dependent signaling. *J. Biol. Chem.* 281(41):30947-30956.

242. Callender JA, Yang Y, Lorden G, Stephenson NL, Jones AC, Brognard J, & Newton AC (2018) Protein kinase Calpha gain-of-function variant in Alzheimer's disease displays enhanced catalysis by a mechanism that evades down-regulation. *Proceedings of the National Academy of Sciences of the United States of America* 115(24):E5497-e5505.

243. Farlow MR, Thompson RE, Wei LJ, Tuchman AJ, Grenier E, Crockford D, Wilke S, Benison J, & Alkon DL (2019) A Randomized, Double-Blind, Placebo-Controlled, Phase II Study Assessing Safety, Tolerability, and Efficacy of

Bryostatin in the Treatment of Moderately Severe to Severe Alzheimer's Disease. *Journal of Alzheimer's disease : JAD* 67(2):555-570.